

**MEASURING  
PHARMACODYNAMICS  
IN EARLY CLINICAL DRUG  
STUDIES IN MULTIPLE  
SCLEROSIS**

**KAWITA KANHAI**

SEE INSIDE FOR COLOR  
ILLUSTRATIONS OF  
CHAPTER 5 AND 6



TO MY PARENTS – MONIQUE AND SURIN – AND MY GRANDPARENTS

**MEASURING  
PHARMACODYNAMICS  
IN EARLY CLINICAL DRUG  
STUDIES IN MULTIPLE  
SCLEROSIS**

**PROEFSCHRIFT**

ter verkrijging van  
de graad doctor aan de universiteit Leiden,  
op gezag van Rector Magnificus prof.mr.C.J.J.M. Stolker,  
volgens besluit van het College voor Promoties  
te verdedigen op donderdag 10 oktober 2019  
klokke 11:15 uur

**DOOR**

Kawita Monique Samriti Kanhai  
geboren te Leiden  
in 1984

**PROMOTOR**

Prof. dr. A.F. Cohen

**CO-PROMOTOR**

Dr. G.J. Groeneveld

**LEDEN PROMOTIECOMMISSIE**

Prof. dr. J. Burggraaf

Prof. dr. E.C.M. de Lange (*Faculty of Science, Leiden*)

Prof. dr. J. Killestein (*Amsterdam UMC, location VUmc, Amsterdam*)

**DESIGN**

Caroline de Lint, Voorburg (caro@delint.nl)

**COVER IMAGES**

*Poetry*, Elizabeth Jameson – An embroidery of the sagittal view of the artist's DTI (*front cover*)

*In Motion*, Elizabeth Jameson (*back cover*)

The publication of this thesis was financially supported by the foundation  
Centre for Human Drug Research in Leiden, the Netherlands

<b>8</b>	<b>CHAPTER I</b> Introduction
<b>21</b>	<b>CHAPTER II</b> Effects on spasticity and neuropathic pain of an oral formulation of $\Delta$ 9-tetrahydrocannabinol in patients with progressive multiple sclerosis
<b>41</b>	<b>CHAPTER III</b> Glutathione PEGylated liposomal methylprednisolone in comparison to free methylprednisolone: slow release characteristics and prolonged lymphocyte depression in a first in human study
<b>55</b>	<b>CHAPTER IV</b> A first-in-human study in healthy subjects of CNM-AU8, gold nanoparticles with remyelinating properties
<b>69</b>	<b>CHAPTER V</b> Quantifying beta-galactosylceramide kinetics in cerebrospinal fluid of healthy subjects using deuterium labeling
<b>85</b>	<b>CHAPTER VI</b> Kinetics of myelin breakdown products: a labeling study in patients with progressive multiple sclerosis
<b>101</b>	<b>CHAPTER VII</b> Treatment of internuclear ophthalmoparesis in multiple sclerosis with fampridine: a randomized, double-blind, placebo-controlled, crossover trial
<b>117</b>	<b>CHAPTER VIII</b> Summary and general discussion
<b>129</b>	<b>CHAPTER IX</b> Nederlandse samenvatting
<b>133</b>	List of publications
<b>135</b>	Curriculum Vitae

# I

## INTRODUCTION



Multiple sclerosis (MS) is the most common autoimmune disorder of the central nervous system, estimated to affect 2-3 million individuals worldwide<sup>1,2</sup>. It is primarily an inflammatory disorder of the brain and spinal cord in which focal lymphocytic infiltration leads to damage of myelin (demyelination) and axons<sup>3</sup>. Direct binding of T lymphocytes to myelin epitopes can lead to activation of macrophages and a subsequent attack of the myelin sheath leading to its phagocytosis<sup>4</sup>. This damage impairs the conduction of signals in the affected nerves. In turn, the reduction in conduction ability causes deficiency in sensation, movement, cognition, or other functions depending on which nerves are involved<sup>5</sup>. Several phenotypes (commonly named types), or patterns of progression, of MS have been described. These phenotypes use the past course of the disease in an attempt to predict the future course. Subtypes that describe the majority of the patients are relapsing-remitting (RRMS), secondary progressive (SPMS), primary progressive (PPMS) and progressive relapsing (PRMS)<sup>6</sup>.

**DEMYELINATION** In demyelination the myelin sheath of neurons is damaged. Demyelinated axons cannot transmit fast trains of impulse, explaining symptoms resulting from physiological fatigue. Depolarisation might traverse the lesion but at reduced velocity, accounting for the characteristic delay of evoked potentials<sup>3</sup>. Partially demyelinated axons can discharge spontaneously, producing unpleasant distortions of sensation. Symptom recovery might suggest resolution of conduction block in structurally intact nerve fibres as the episode of inflammation wanes<sup>7</sup>. When structural damage has occurred, sodium channels are redistributed across the demyelinated axonal membrane<sup>8</sup>. Electrical activity is restored, but alterations in sodium and calcium exchange can prove hazardous until normal nodal arrangements are re-established by remyelination<sup>9</sup>. There are many possible biochemical and cellular mechanisms whereby activated immune cells may destroy myelin and oligodendrocytes (table 1)<sup>4</sup>.

**REMYELINATION** Following acute inflammatory episodes, the resolution of the inflammatory process is probably an important factor contributing to the neurological recovery often observed after clinical relapses. Remyelination can occur to a significant extent in lesion areas, and this probably also contributes to functional recovery. Up to 40% of sclerotic plaques show signs of remyelination<sup>4,10</sup>, and it is unknown what determines the fate of a given lesion<sup>11</sup>. However, remyelination is generally incomplete, and the myelin is of lower quality, which might be the reason why the original conduction properties are not fully restored<sup>12</sup>. Although remyelination is most active during the acute inflammatory process, it also occurs in the progressive phase of MS<sup>3,13</sup>.

**AXONAL LOSS** In addition to damage to myelin and oligodendrocytes, axonal loss and injury are characteristic features of sclerotic plaques. In end-state multiple sclerosis, up to 60% of the axons present in sclerotic plaques may have disappeared<sup>14,15</sup>. As with loss of myelin, neuronal axonal damage is likely to be a multifactorial process. A number of cellular and humoral mediators of the immune response have been shown to be capable of damaging axons, including T lymphocyte, macrophages, antibodies, nitric oxide, glutamate and matrix metalloproteases<sup>4,16,17</sup>.

## PHARMACOLOGICAL TREATMENT OF MS

Current treatment of MS can be divided into disease-modifying treatments and symptomatic treatments. The most common symptoms in MS, such as fatigue, sleep disorders, pain, vestibular symptoms, speech and swallowing, tremors and ataxia, weakness, spasticity, gait, bladder and bowel dysfunction and psychiatric symptoms, are often treated symptomatically with pharmaceutical compounds, physiotherapy and/or psychological help<sup>18</sup>. A new symptomatic treatment is discussed in **chapter 2**, where the effects of a new oral formulation of  $\Delta 9$ -tetrahydrocannabinol ( $\Delta 9$ -THC) on spasticity and pain in 24 patients with progressive MS is described.

Most registered disease-modifying drugs (DMDS) target the immune system, preventing it from destructing myelin. However, with increasing efficacy and discovery of these compounds over the years<sup>2</sup>, burden due to side effect of these compounds also increases. Figure 1 shows the different DMDS, of first line treatment (interferons, glatiramer acetate, teriflunomide, dimethylfumarate), second line treatment (natalizumab, fingolimod) and third line treatment (alemtuzumab, mitoxantrone)<sup>3,19</sup>. A short description of the different pharmacological treatments is listed in table 2.

**INTERFERONS** Interferons belong to the large class of proteins known as cytokines, molecules used for communication between cells to trigger the protective defences of the immune system that help eradicate pathogens and are divided into type 1 ( $\alpha$  and  $\beta$  interferons) and type 2 ( $\gamma$  or immune interferon)<sup>20</sup>. Studies show administration of interferon  $\gamma$  increases the exacerbation rate and interferon  $\gamma$  may be involved in the pathogenesis of MS lesions. In contrast, interferon  $\beta$  tends to inhibit the activity of interferon  $\gamma$  and appears to prevent disease activity. Interferon  $\beta$ -1a and interferon  $\beta$ -1b are currently used to treat and control the autoimmune process in MS. The efficacy of subcutaneous interferon  $\beta$ -1b was demonstrated in a double-blind, placebo-controlled trial of 372 patients with RRMS who were randomly assigned to treatment with either interferon  $\beta$ -1b 50 mcg every other day, interferon  $\beta$ -1b 250 mcg every other day, or placebo<sup>21,22</sup>. A study in which safety and efficacy of PEGylated interferon  $\beta$ -1a in 1512 patients with RRMS assessed reported PEG interferon  $\beta$ -1a significantly reduced relapse rate compared with placebo<sup>23</sup>. Injection site reactions are common with IFN- $\beta$  therapy and can include injection site necrosis<sup>24</sup>. There is a high prevalence of mainly asymptomatic liver dysfunction associated with IFN- $\beta$  therapy. However, serious hepatotoxicity associated with IFN- $\beta$  is rare<sup>25</sup>.

**GLATIRAMER ACETATE** Glatiramer acetate (copolymer 1) is a mixture of random polymers of four amino acids. The mixture is antigenically similar to myelin basic protein, a component of the myelin sheath of nerves. In experimental models, the immunomodulatory mechanism of action for glatiramer involves binding to major histocompatibility complex molecules and consequent competition with various myelin antigens for their presentation to the T lymphocyte. In addition, glatiramer is a potent inducer of specific T helper 2 type suppressor cells that migrate to the brain and lead to bystander suppression; these cells also express anti-inflammatory cytokines<sup>26</sup>. In 1995 a double-blind trial with

glatiramer acetate in 251 patients with RRMS was published. Patients treated with glatiramer acetate (20 mg subcutaneously daily) had a significantly lower relapse rate than those receiving placebo (1.19 versus 1.68)<sup>27</sup>. Furthermore, over 140 weeks, a significantly larger proportion of patients in the placebo group experienced increased disability by  $\geq 1.5$  steps on the Expanded Disability Status Scale (EDSS) compared with the treatment group (41 versus 22 percent)<sup>28</sup>. In the clinical trials for glatiramer, the most common adverse reactions reported by those taking glatiramer were skin problems at the injection site (redness, pain, swelling and itching), flushing (vasodilation), rash, shortness of breath and chest pain<sup>29</sup>.

**TERIFLUNOMIDE** The immunomodulator teriflunomide is the active metabolite of leflunomide that inhibits pyrimidine biosynthesis what leads to impaired proliferation of T lymphocyte<sup>30</sup>. The effectiveness of teriflunomide for the treatment of RRMS was demonstrated in several randomized controlled trials. A trial with 1088 adults with relapsing MS found that teriflunomide significantly reduced the relapse rate by approximately 31 percent compared with placebo<sup>31</sup>. In 2014 a phase 3 trial with over 1100 adults with relapsing forms of MS, showed teriflunomide was superior to placebo for reducing the relapse rate<sup>32</sup>. The most common adverse effects of teriflunomide were diarrhoea, nausea, hair thinning, and elevated alanine aminotransferase (ALT) levels<sup>31</sup>.

**DIMETHYL FUMARATE** Dimethyl fumarate and its primary metabolite, monomethyl fumarate, are cytoprotective of neurons and astrocytes against oxidative stress-induced cellular injury and loss, potentially by up-regulation of a Nrf2-dependent antioxidant response<sup>33</sup>. The Nrf2-mediated oxidative stress response mechanisms previously implicated as important for protection of the Central Nervous System (CNS) in a variety of pathological conditions, which can be beneficial for MS patients<sup>34</sup>. Two phase 3 studies reported in 2012 significantly reduced relapse rates and the less development of new brain lesions on MRI in patients with active MS, what suggests it might reduce the rate of disability progression. A first study enrolled 1234 patients and compared dimethyl fumarate to placebo<sup>35</sup>. A second study enrolled 1430 patients and also included glatiramer as treatment<sup>36</sup>. The most common side effects of dimethyl fumarate are flushing and gastrointestinal symptoms, including diarrhoea, nausea, and abdominal pain. Treatment with dimethyl fumarate may decrease lymphocyte counts, so patients should have a complete blood count checked frequently during treatment and discontinue if lymphocytopenia develops<sup>35,36</sup>.

**NATALIZUMAB** Natalizumab is a recombinant monoclonal antibody directed against alpha-4 integrins. Alpha-4 integrin is expressed on the surface of inflammatory lymphocytes and monocytes and may play a critical role in their adhesion to the vascular endothelium and the migration of these cells to the brain<sup>37</sup>. A decrease in migration of immune cells to the brain will leave less immune cells in the brain to destruct myelin. In 2011 a systematic review of trials evaluating natalizumab for RRMS, pooled efficacy data from two randomized controlled trials, and showed that natalizumab significantly reduced the risk for a relapse during two years of treatment. In addition, natalizumab significantly reduced the risk for experiencing progression at two years<sup>38-40</sup>. The JC viral titre is used in the risk

assessment in patients using natalizumab. Natalizumab is one of the most effective treatments for MS currently available<sup>41</sup>. However, progressive multifocal leukoencephalopathy (PML) emerged as a rare adverse event from its treatment, generally occurring late (> 24 months) after initiating treatment<sup>42</sup>. PML is caused by reactivation of a latent JC virus in immunocompromised individuals and leads to a debilitating encephalopathy that is fatal in up to 20-50%<sup>43</sup>. Determining a JC viral titre is indicated when patients use immunosuppressive medication or use natalizumab for a period of more than 2 years. However, while 50% of MS patients<sup>44,45</sup> are JCv Ab seropositive, less than 1% will develop PML<sup>46</sup>, emphasizing the limitations of this biomarker. The risk in sero-negative patients is 6-18 times lower (chances in sero-positive patients increases after two years)<sup>47</sup>. Also, seroconversion rate was reported to be 26.67%<sup>44</sup>.

**FINGOLIMOD** Fingolimod is sphingosine analogue that modulates the sphingosine-1-phosphate (S1P) receptor, causing internalization of S1P receptors, which sequesters lymphocytes in lymph nodes, preventing them from moving to the central nervous system and cause a relapse in multiple sclerosis.<sup>48</sup>. A 2016 review combined 6 RCTs with a total of 5152 patients, and concluded treatment with fingolimod compared to placebo in RRMS patients is effective in reducing inflammatory disease activity, but it may lead to little or no difference in preventing disability worsening. Also, this benefit is associated with a small increased risk of infection, atrioventricular block, and possibly basal cell carcinoma<sup>49</sup>.

**ALEMTUZUMAB** Alemtuzumab is a monoclonal antibody that binds to CD52, a protein present on the surface of mature lymphocytes, but not on the stem cells from which these lymphocytes are derived. After treatment with alemtuzumab, these CD52-bearing lymphocytes are targeted for destruction. CD52 has been implicated in the activation and migration of T lymphocytes. Alemtuzumab mediates lysis of these cells, suppressing the neuroinflammatory responses in MS<sup>50</sup>. Combined data from 3 trials, involving 1694 patients, concludes there is evidence that annual intravenous cycles of alemtuzumab reduces the proportion of patients with relapses, disease progression, change of EDSS score and developing new T2 lesions on MRI.<sup>100</sup> The main side effects of alemtuzumab were infusion reactions, infections, and autoimmune disorders. Immune thrombocytopenia (ITP) developed in 1 percent of patients at two years, and in 3 percent at three years.<sup>101</sup>

**MITOXANTRONE** Mitoxantrone has immunosuppressive properties by reducing the number of T cells, inhibiting T helper cell function, and augmenting T cell suppressor activity.<sup>102</sup> The largest trial of mitoxantrone in MS was a single multicenter, double-blind trial of 194 patients with worsening RRMS or SPMS.<sup>103</sup> Treatment with mitoxantrone was associated with significant clinical benefits compared with placebo on multivariate analysis, reducing progression of disability and clinical exacerbations. Because of cardiac toxicity and possible association with a low risk of developing therapy-related acute leukemia, mitoxantrone should be reserved for patients with rapidly advancing disease who have failed other therapies<sup>51</sup>.

**OCRELIZUMAB** Ocrelizumab is a chimeric anti-CD20 monoclonal antibody. It selectively depletes CD20-expressing B lymphocytes while preserving the capacity for B lymphocyte reconstitution and pre-existing humoral immunity<sup>52,53</sup>. A phase 3 trial in 732 patients with primary progressive multiple sclerosis showed that ocrelizumab was associated with lower rates of clinical and MRI progression than placebo. Improvement was reported 12 weeks after the first treatment. Most report adverse events were infusion-related reactions, upper respiratory tract infections, and oral herpes infections<sup>54</sup>.

**CLADRIBINE** Cladribine is a prodrug, but its active metabolite, cladribine triphosphate, accumulates within the cell, resulting in disruption of cellular metabolism, DNA damage and subsequent apoptosis. Cladribine preferentially targets lymphocytes owing to their relatively high ratio of DCK to 5'-nucleotidase, producing rapid and sustained reductions in CD4+ and CD8+ cells and rapid, though more transient, effects on CD19+ B lymphocyte. Cladribine is relatively sparing of other immune cells<sup>55</sup>. A study in 1326 patients with RRMS, treatment with cladribine tablets significantly reduced relapse rates. Adverse events that were more frequent in the cladribine groups included lymphocytopenia (21.6% in the 3.5-mg group and 31.5% in the 5.25-mg group, vs. 1.8%) and herpes zoster (8 patients and 12 patients, respectively, vs. no patients)<sup>56</sup>.

**METHYLPREDNISOLONE** Methylprednisolone (MP), an immunosuppressive drug, is prescribed to MS patients as an acute treatment of a relapse, and has been shown to accelerate neurological recovery<sup>57</sup>. **Chapter 3** describes a first in human study with a new formulation of MP, 2B3-201. This compound consists of liposomes containing methylprednisolone. The liposomes have PEG (polyethylene glycol, also known as macrogol) molecules attached, ensuring a long residence time in the body,<sup>58,59</sup> and glutathione molecules attached to PEG molecules, improving blood-brain-barrier passage<sup>60,61</sup>. These characteristics in effect change regular methylprednisolone to a slow-release methylprednisolone, with benefits such as lower dosing frequency because of long residue time and lower peak concentrations and peak concentration related side effects.

Figure 1 displays the challenge in treatment development: the search for compounds with a high efficacy and limited burden. Remyelinating and neuroprotective therapies are a new class of medication in MS, for which little data is available on efficacy and burden.

## FUTURE OF TREATMENTS IN MS

Although a number of DMDS for the treatment of the inflammatory phase are available, the need for treating neurodegeneration and halting the progression of disability remyelinating and neuroprotective therapies is still unmet<sup>62</sup>. Below eight promising drug candidates are discussed that may have the potential to enhance remyelination or positively affect the CNS (table 3).

**ANTI-LINGO-1 ANTIBODIES** LINGO-1, a membrane protein, originally attained prominence as an essential subunit of a tripartite receptor complex containing LINGO-1,

Nogo-66 receptor (NGR1), and TNF receptor superfamily members P75<sup>NTR</sup> or Troy/Taj<sup>63</sup>. This complex mediates inhibitory effects of CNS myelin proteins on axon growth<sup>64</sup>. Exposure of mice to an inhibitory monoclonal antibody to LINGO-1 was found to promote spinal cord remyelination in an experimental model of MS, the experimental autoimmune encephalitis (EAE) model<sup>65</sup>. This and similar results of subsequent studies motivated development of opicinumab (BIIB033, Biogen), a LINGO-1 monoclonal antibody suitable for use in humans. Although a phase 2 study with this compound did demonstrate a difference in remyelination between opicinumab and placebo, this effect was only significant in a subgroup of the study population<sup>66</sup>.

**RHIGM22 ANTIBODIES** RHIGM22 is a monoclonal IgM antibody that binds myelin tracts and mature oligodendrocytes, induces calcium influx in astrocytes, oligodendrocyte progenitor cells (OPCs) and pre-mature oligodendrocytes in culture. The antibody promotes remyelination in animal studies<sup>67,68</sup>. One of these animal studies used the cuprizone model, in which the toxin cuprizone leads to demyelination of the central nervous system, demonstrated that treatment with RHIGM22 accelerated remyelination of the demyelinated corpus callosum, and enhancing effects were also accompanied by increased differentiation of OPCs into mature oligodendrocytes<sup>69</sup>. The first clinical studies in humans are ongoing and results are not yet available.

**OLESOXIME** Olesoxime is an experimental neuroprotective compound that was being developed for amyotrophic lateral sclerosis (ALS)<sup>70</sup> and spinal muscular atrophy (SMA)<sup>71</sup>. It has a number of potentially neuroprotective and neuroregenerative properties, including accelerated maturation of oligodendrocytes and promoting remyelination in cuprizone mouse models of demyelination<sup>72</sup>. A first study in MS patients has started, and preliminary results report olesoxime is safe and well tolerated in patients with MS.

**ASIC1 BLOCKERS** Blockade of the neuronal proton-gated acid-sensing ion channel 1 (ASIC1) can support cellular protection, which is increased within axons and oligodendrocytes in acute multiple sclerosis lesions<sup>73</sup>. Blocking ASIC1 with amiloride exerts neuroprotective and myeloprotective effects in experimental models of multiple sclerosis<sup>74</sup>. A pilot study suggest that amiloride may exert neuroprotective effects in patients with progressive multiple sclerosis<sup>75</sup>.

**BENZTROPINE** Benztropine functions by a mechanism that involves direct antagonism of M1 and/or M3 muscarinic receptors with subsequent oligodendrocyte maturation. Benztropine has shown to significantly decreases clinical severity in the EAE model<sup>76</sup>. Clinical trials with benztropine have not been announced yet.

**GUANABENZ** Guanabenz is a  $\alpha_2$  adrenergic receptor agonist. It protects oligodendrocytes by preventing dephosphorylation of eIF2, thereby increasing oligodendrocyte survival, and leading to prevention of myelin loss. Preclinical studies demonstrated improvement of deficits in the EAE model<sup>77</sup>. A clinical study has been initiated, but no results have been reported yet.



**QUETIAPINE FUMARATE** Quetiapine fumarate stimulates proliferation and maturation of oligodendrocytes, increases neurotrophic factors, and inhibits activated microglia, astrocytes, and T lymphocytes. It was shown to have remyelinating and neuroprotective properties in the EAE mouse model<sup>78</sup>. A clinical study has not been initiated yet.

**CLEAN SURFACE GOLD NANOPARTICLES** Animal studies with clean-surface gold nanoparticles showed remyelination in the cuprizone model. In **chapter 4** we discuss the first-in-human study with these gold nanoparticles (CNM-AU8), performed in 86 healthy male and female subjects to evaluate safety and pharmacokinetics.

## BIOMARKERS IN MULTIPLE SCLEROSIS

### Definition

The World Health Organization defined a biomarker as ‘any substance, structure, or process that can be measured in the body or its products and influence or predict the incidence of outcome or disease’<sup>79,80</sup>. Biomarkers in multiple sclerosis can be used to assess disease susceptibility, disease progression and response to treatment<sup>81</sup>. Biomarkers in response to treatment can be used to assess target engagement, pharmacodynamics, safety and proof-of-concept<sup>82</sup>.

### Current biomarkers

Current frequently used biomarkers in MS diagnosis and treatment management are oligoclonal bands (OCB) in the CSF, neurofilament light, white matter lesions on MRI and JC viral titer<sup>81</sup>. While oligoclonal bands may be considered a diagnostic biomarker, white matter lesions on MRI are diagnostic and used as biomarkers for treatment response, and JC viral titer is a biomarker related primarily to risk of side effects. An immunologic abnormality in MS patients is the presence of intrathecal synthesis of immunoglobulin G (IgG) in an oligoclonal pattern, measured in the CSF<sup>83,84</sup> and it was the first biomarker in the diagnostic criteria of MS in 1983<sup>85</sup>. Although OCBs were removed from the 2010 McDonald criteria for RRMS, they still are a criterion for the diagnosis of primary progressive MS<sup>86</sup>. Results of a recent biomarker study support the value of serum neurofilament light as a sensitive and clinically meaningful blood biomarker to monitor tissue damage and the effects of therapies in MS<sup>87</sup>.

MRI provides a substantial variety of neuroinflammation biomarkers. T1 lesions with contrast enhancement can be considered a biomarker of acute neuroinflammation and Blood-Brain-Barrier (BBB) disruption<sup>88,89</sup>. Hyperintense T2-weighted lesions reflect a combination of mechanisms like inflammation, demyelination, axonal damage and oedema and has a high diagnostic value in MS<sup>90</sup>. Hypotense T1-weighted lesions (black holes) are considered satisfactory biomarkers of axonal damage<sup>91</sup>. Both whole brain atrophy and grey matter atrophy are used as prognostic biomarkers in MS<sup>92,93</sup>. However, MRI

techniques lack in adequate correlation with neurodegeneration and disability progression, the so-called ‘clinic-radiological paradox’.<sup>94-96</sup>

### Potential biomarkers

As mentioned earlier, more pharmaceutical compounds will target remyelination and trials with potential neuroreparative or neuroregenerative agents will need appropriate biomarkers. One of the biggest difficulties in the development of remyelination therapies for MS is the demonstration of remyelination in living patients<sup>97,98</sup>. Conventional MRI sequences have limited specificity for myelination. Imaging modalities which are potentially more specific to myelin content in vivo are magnetisation transfer ratio (MTR), restricted proton fraction f (from quantitative magnetisation transfer measurements), myelin water fraction and diffusion tensor imaging (DTI) metrics, and positron emission tomography (PET) imaging. Although MTR and DTI measures probably offer the most realistic and feasible outcome measures for such trials, they don’t have sufficiently high sensitivity or specificity to myelin, or correlation with clinical features<sup>94,99</sup>. The inadequacy of imaging biomarkers to quantify the process of myelin formation, and the need for a pharmacodynamic measure that could be used for studies with compounds that enhance remyelination, led us to set up and validate a more accurate method to measure (re)myelination.

In **chapter 5** we describe the development of a method to determine myelin turnover by labelling myelin with deuterium. First, the method was designed with the help of pre-clinical analyses and modelling. Subsequently the feasibility of the method was assessed in a clinical study subjects. Healthy subjects drank heavy (70% deuterated) water for a period of 10 weeks, and deuterium incorporation of myelin breakdown products (beta-galactosylceramide) in the cerebrospinal fluid (CSF) was measured with mass spectrometry, after which the level of incorporation was quantified using modelling techniques. In a second study this labelling experiment was repeated in patients with MS with the goal to quantify myelin turnover and assess the feasibility of this method to be used in patients with MS. The results of this study are described in **chapter 6**.

Demyelination of nerves leads to conduction abnormalities and hence to neurological symptoms. Demyelination of the fasciculus longitudinalis medialis in the brainstem leads to slowing of the adducting eye in horizontal eye movements, which, when it leads to clinical symptoms is called an internuclear ophthalmoplegia (INO). We validated a method to accurately measure eye movements in patients with MS and an INO to be used to demonstrate pharmacological effects of compounds that influence nerve conduction (**chapter 7**). We accurately tracked eye movement in patients with MS and an internuclear ophthalmoplegia. As validation of a method is best done with a compound that has proven to be effective, we used fampridine (4-Aminopyridine) in this study as treatment. Fampridine caused a significant improvement in eye movements, as measured using a highly sensitive method to use eye movements. This method may also be used to quantify the effects of a compounds that enhance remyelination and thereby improve nerve conduction.

REFERENCES

1 Annual review of immunology. 2005;23:683-747.

2 Thompson AJ, Baranzini SE, Geurts J, Hemmer B, Ciccarelli O. Multiple sclerosis. *Lancet* (London, England). 2018;391(10130):1622-36.

3 Compston A, Coles A. Multiple sclerosis. *Lancet* (London, England). 2008;372(9648):1502-17.

4 Bruck W. The pathology of multiple sclerosis is the result of focal inflammatory demyelination with axonal damage. *Journal of neurology*. 2005;252 Suppl 5:v3-9.

5 Moore KL, Agur AMR, Dalley AF. Essential clinical anatomy 2014. Lublin FD, Reingold SC. Defining the clinical course of multiple sclerosis: Results of an international survey. *Neurology*. 1996;46(4):907-11.

7 Youl BD, Turano G, Miller DH, Towell AD, MacManus DG, Moore SG, et al. The pathophysiology of acute optic neuritis. An association of gadolinium leakage with clinical and electrophysiological deficits. *Brain*. 1991;114 (Pt 6):2437-50.

8 Black JA, Liu S, Hains BC, Saab CY, Waxman SG. Long-term protection of central axons with phenytoin in monophasic and chronic-relapsing EAE. *Brain*. 2006;129 (Pt 12):3196-208.

9 Smith KJ. Axonal protection in multiple sclerosis—a particular need during remyelination? *Brain*. 2006;129 (Pt 12):3147-9.

10 Barkhof F, Bruck W, De Groot CJ, Bergers E, Hulshof S, Geurts J, et al. Remyelinated lesions in multiple sclerosis: magnetic resonance image appearance. *Archives of neurology*. 2003;60(8):1073-81.

11 Reich DS, Lucchinetti CF, Calabresi PA. Multiple Sclerosis. *The New England Journal of Medicine*. 2018;378(2):169-80.

12 Alizadeh A, Dyck SM, Karimi-Abdolrezaee S. Myelin damage and repair in pathologic CNS: challenges and prospects. *Frontiers in Molecular Neuroscience*. 2015;8:35.

13 Bramow S, Frischer JM, Lassmann H, Koch-Henriksen N, Lucchinetti CF, Sorensen PS, et al. Demyelination versus remyelination in progressive multiple sclerosis. *Brain*. 2010;133(10):2983-98.

14 Lovas G, Szilagyí N, Majtenyi K, Palkovits M, Komoly S. Axonal changes in chronic demyelinated cervical spinal cord plaques. *Brain*. 2000;123 (Pt 2):308-17.

15 Mews I, Bergmann M, Bunkowski S, Gullotta F, Bruck W. Oligodendrocyte and axon pathology in clinically silent multiple sclerosis lesions. *Multiple sclerosis* (Houndmills, Basingstoke, England). 1998;4(2):55-62.

16 Mallucci G, Peruzzotti-Jametti L, Bernstock JD, Pluchino S. The role of immune cells, glia and neurons in white and gray matter pathology in multiple sclerosis. *Progress in neurobiology*. 2015;0:1-22.

17 Garg N, Smith TW. An update on immunopathogenesis, diagnosis, and treatment of multiple sclerosis. *Brain and behavior*. 2015;5(9):e00362.

18 Shah P. Symptomatic management in multiple sclerosis. *Ann Indian Acad Neurol*. 2015;18(Suppl 1):S35-42.

19 Coles A. Newer therapies for multiple sclerosis. *Annals of Indian Academy of Neurology*. 2015;18(Suppl 1):S50-S4.

20 Parkin J, Cohen B. An overview of the immune system. *The Lancet*. 2001;357(9270):1777-89.

21 listed\*\* na. Interferon beta-1β is effective in relapsing-remitting multiple sclerosis. I. Clinical results of a multicenter, randomized, double-blind, placebo-controlled trial. The IFNB Multiple Sclerosis Study Group. *Neurology*. 1993;43(4):655-61.

22 Paolicelli D, Direnzo V, Trojano M. Review of interferon beta-1β in the treatment of early and relapsing multiple sclerosis. *Biologics: Targets & Therapy*. 2009;3:369-76.

23 Calabresi PA, Kieseier BC, Arnold DL, Balcer LJ, Boyko A, Pelletier J, et al. Pegylated interferon beta-1a for relapsing-remitting multiple sclerosis (ADVANCE): a randomised, phase 3, double-blind study. *The Lancet Neurology*. 2014;13(7):657-65.

24 Rio J, Nos C, Bonaventura I, Arroyo R, Genis D, Sureda B, et al. Corticosteroids, ibuprofen, and acetaminophen for IFNβ-1a flu symptoms in MS: a randomized trial. *Neurology*. 2004;63(3):525-8.

25 Tremlett HL, Yoshida EM, Oger J. Liver injury associated with the beta-interferons for MS: a comparison between the three products. *Neurology*. 2004;62(4):628-31.

26 Arnon R, Aharoni R. Mechanism of action of glatiramer acetate in multiple sclerosis and its potential for the development of new applications. *Proceedings of the National Academy of Sciences of the United States of America*. 2004;101(Suppl 2):15493-8.

27 Johnson KP, Brooks BR, Cohen JA, Ford CC, Goldstein J, Lisak RP, et al. Copolymer 1 reduces relapse rate and improves disability in relapsing-remitting multiple sclerosis: results of a phase III multicenter, double-blind placebo-controlled trial. The Copolymer 1 Multiple Sclerosis Study Group. *Neurology*. 1995;45(7):1268-76.

28 Johnson KP, Brooks BR, Cohen JA, Ford CC, Goldstein J, Lisak RP, et al. Extended use of glatiramer acetate (Copaxone) is well tolerated and maintains its clinical effect on multiple sclerosis relapse rate and degree of disability. *Copolymer 1 Multiple Sclerosis Study Group*. *Neurology*. 1998;50(3):701-8.

29 Khan O, Rieckmann P, Boyko A, Selmaj K, Zivadinov R. Three times weekly glatiramer acetate in relapsing-remitting multiple sclerosis. *Annals of neurology*. 2013;73(6):705-13.

30 Zeyda M, Poglitsch M, Geyeregger R, Smolen JS, Zlabinger GJ, Horl WH, et al. Disruption of the interaction of T cells with antigen-presenting cells by the active leflunomide metabolite teriflunomide: involvement of impaired integrin activation and immunologic synapse formation. *Arthritis and rheumatism*. 2005;52(9):2730-9.

31 O'Connor P, Wolinsky JS, Confavreux C, Comi G, Kappos L, Olsson TP, et al. Randomized Trial of Oral Teriflunomide for Relapsing Multiple Sclerosis. *New England Journal of Medicine*. 2011;365(14):1293-303.

32 Confavreux C, O'Connor P, Comi G, Freedman MS, Miller AE, Olsson TP, et al. Oral teriflunomide for patients with relapsing multiple sclerosis (TOWER): a randomised, double-blind, placebo-controlled, phase 3 trial. *The Lancet Neurology*. 13(3):247-56.

33 Scannevin RH, Chollate S, Jung MY, Shacklett M, Patel H, Bista P, et al. Fumarates promote cytoprotection of central nervous system cells against oxidative stress via the nuclear factor (erythroid-derived 2)-like 2 pathway. *The Journal of pharmacology and experimental therapeutics*. 2012;341(1):274-84.

34 Linker RA, Lee DH, Ryan S, van Dam AM, Conrad R, Bista P, et al. Fumaric acid esters exert neuroprotective effects in neuroinflammation via activation of the Nrf2 antioxidant pathway. *Brain*. 2011;134(Pt 3):678-92.

35 Gold R, Kappos L, Arnold DL, Bar-Or A, Giovannoni G, Selmaj K, et al. Placebo-Controlled Phase 3 Study of Oral BG-12 for Relapsing Multiple Sclerosis. *New England Journal of Medicine*. 2012;367(12):1098-107.

36 Fox RJ, Miller DH, Phillips JT, Hutchinson M, Havrdova E, Kita M, et al. Placebo-controlled phase 3 study of oral BG-12 or glatiramer in multiple sclerosis. *The New England journal of medicine*. 2012;367(12):1087-97.

37 Rice GP, Hartung HP, Calabresi PA. Anti-alpha4 integrin therapy for multiple sclerosis: mechanisms and rationale. *Neurology*. 2005;64(8):1336-42.

38 Pucci E, Giuliani G, Solari A, Simi S, Minozzi S, Di Pietrantonj C, et al. Natalizumab for relapsing remitting multiple sclerosis. *The Cochrane database of systematic reviews*. 2011(10):Cd007621.

39 Polman CH, O'Connor PW, Havrdova E, Hutchinson M, Kappos L, Miller DH, et al. A randomized, placebo-controlled trial of natalizumab for relapsing multiple sclerosis. *The New England journal of medicine*. 2006;354(9):899-910.

40 Rudick RA, Stuart WH, Calabresi PA, Confavreux C, Galetta SL, Radue EW, et al. Natalizumab plus interferon beta-1a for relapsing multiple sclerosis. *The New England journal of medicine*. 2006;354(9):911-23.

41 Tramacere I, Del Giovane C, Salanti G, D'Amico R, Filippini G. Immunomodulators and immunosuppressants for relapsing-remitting multiple sclerosis: a network meta-analysis. *The Cochrane database of systematic reviews*. 2015(9):Cd011381.

42 Antoniol C, Stankoff B. Immunological Markers for PML Prediction in MS Patients Treated with Natalizumab. *Frontiers in immunology*. 2014;5:668.

43 Brew BJ, Davies NW, Cinque P, Clifford DB, Nath A. Progressive multifocal leukoencephalopathy and other forms of JC virus disease. *Nature reviews Neurology*. 2010;6(12):667-79.

44 Outteryck O, Zephir H, Salleron J, Ongagna JC, Etcheberria A, Collongues N, et al. JC-virus seroconversion in multiple sclerosis patients receiving natalizumab. *Multiple sclerosis* (Houndmills, Basingstoke, England). 2014;20(7):822-9.

45 Olsson T, Achiron A, Alfredsson L, Berger T, Brassat D, Chan A, et al. Anti-JC virus antibody prevalence in a multinational multiple sclerosis cohort. *Multiple sclerosis* (Houndmills, Basingstoke, England). 2013;19(11):1533-8.

46 Plavina T, Subramanyam B, Bloomgren G, Richman S, Pace A, Lee S, et al. Anti-JC virus antibody levels in serum or plasma further define risk of natalizumab-associated progressive multifocal leukoencephalopathy. *Annals of neurology*. 2014;76(6):802-12.

47 Berger JR, Houff SA, Gurwell J, Vega N, Miller CS, Danaher RJ. JC virus antibody status underestimates infection rates. *Annals of neurology*. 2013;74(1):84-90.

48 Cohen JA, Chun J. Mechanisms of fingolimod's efficacy and adverse effects in multiple sclerosis. *Annals of neurology*. 2011;69(5):759-77.

49 La Mantia L, Tramacere I, Firwana B, Pacchetti I, Palumbo R, Filippini G. Fingolimod for relapsing-remitting multiple sclerosis. *The Cochrane database of systematic reviews*. 2016;4:Cd009371.

50 Ruck T, Bittner S, Wiendl H, Meuth SG. Alemtuzumab in Multiple Sclerosis: Mechanism of Action and Beyond. *International journal of molecular sciences*. 2015;16(7):16414-39.

51 Goodin DS, Arnason BG, Coyle PK, Frohman EM, Paty DW. The use of mitoxantrone (Novantrone) for the treatment of multiple sclerosis: report of the Therapeutics and Technology Assessment Subcommittee of the American Academy of Neurology. *Neurology*. 2003;61(10):1332-8.

52 McGinley MP, Moss BP, Cohen JA. Safety of monoclonal antibodies for the treatment of multiple sclerosis. *Expert Opinion on Drug Safety*. 2017;16(1):89-100.

53 DiLillo DJ, Hamaguchi Y, Ueda Y, Yang K, Uchida J, Haas KM, et al. Maintenance of Long-Lived Plasma Cells and Serological Memory Despite Mature and Memory B Cell Depletion during CD20 Immunotherapy in Mice. *The Journal of Immunology*. 2008;180(1):361-71.

54 Montalban X, Hauser SL, Kappos L, Arnold DL, Bar-Or A, Comi G, et al. Ocrelizumab versus Placebo in Primary Progressive Multiple Sclerosis. *The New England journal of medicine*. 2017;376(3):209-20.

55 Beutler E. Cladribine (2-chlorodeoxyadenosine). *Lancet* (London, England). 1992;340(8825):952-6.

56 Giovannoni G, Comi G, Cook S, Rammohan K, Rieckmann P, Soelberg Sorensen P, et al. A placebo-controlled trial of oral cladribine for relapsing multiple sclerosis. *The New England journal of medicine*. 2010;362(5):416-26.

57 Nos C, Sastre-Garriga J, Borràs C, Río J, Tintoré M, Montalban X. Clinical impact of intravenous methylprednisolone in attacks of multiple sclerosis. *Multiple Sclerosis Journal*. 2004;10(4):413-6.

58 Linker RA, Weller C, Luhder F, Mohr A, Schmidt J, Knauth M, et al. Liposomal glucocorticosteroids in treatment of chronic autoimmune demyelination: long-term protective effects and enhanced efficacy of methylprednisolone formulations. *Experimental neurology*. 2008;211(2):397-406.

59 Schmidt J, Metselaar JM, Wauben MH, Toyka KV, Storm G, Gold R. Drug targeting by long-circulating liposomal glucocorticosteroids increases therapeutic efficacy in a model of multiple sclerosis. *Brain*. 2003;126(Pt 8):1895-904.

60 Gaillard PJ, Visser CC, Appeldoorn CCM, Rip J. Enhanced brain drug delivery: safely crossing the blood-brain barrier. *Drug Discovery Today: Technologies*. 2012;9(2):e155-e60.

61 Kannan R, Chakrabarti R, Tang D, Kim KJ, Kaplowitz N. GSH transport in human cerebrovascular endothelial cells and human astrocytes: evidence for luminal localization of Na<sup>+</sup>-dependent GSH transport in hCec. *Brain research*. 2000;852(2):374-82.

62 Coditu C, Constantinescu CS, Tanasescu R. The future of multiple sclerosis treatments. *Expert Review of Neurotherapeutics*. 2016 10/21/2016:1341-56.

63 Mi S, Lee X, Shao Z, Thill G, Ji B, Relton J, et al. LINGO-1 is a component of the Nogo-66 receptor/p75 signaling complex. *Nat Neurosci*. 2004;7(3):221-8.

64 Shao Z, Browning JL, Lee X, Scott ML, Shulga-Morskaya S, Allaire N, et al. TAJ/TROY, an Orphan TNF Receptor Family Member, Binds Nogo-66 Receptor 1 and Regulates Axonal Regeneration. *Neuron*. 2005;45(3):353-9.

65 Mi S, Hu B, Hahm K, Luo Y, Kam Hui ES, Yuan Q, et al. LINGO-1 antagonist promotes spinal cord remyelination and axonal integrity in MOG-induced experimental autoimmune encephalomyelitis. *Nat Med*. 2007;13(10):1228-33.

66 Cadavid D, Balcer L, Galetta S, Aktas O, Ziemssen T, Vanopdenbosch L, et al. Safety and efficacy of opicinumab in acute optic neuritis (RENEW): a randomised, placebo-controlled, phase 2 trial. *The Lancet Neurology*. 2017;16(3):189-99.

67 Watzlawik J, Holicky E, Edberg DD, Marks DL, Warrington AE, Wright BR, et al. Human remyelination promoting antibody inhibits apoptotic signaling and differentiation through Lyn kinase in primary rat oligodendrocytes. *Glia*. 2010;58(15):1782-93.

68 Watzlawik JO, Warrington AE, Rodriguez M. PDGF is required for remyelination-promoting IGM stimulation of oligodendrocyte progenitor cell proliferation. *PLoS one*. 2013;8(2):e55149.

69 Mullin AP, Cui C, Wang Y, Wang J, Troy E, Caggiano AO, et al. RHIGM22 enhances remyelination in the brain of the cuprizone mouse model of demyelination. *Neurobiology of disease*. 2017;105:142-55.

70 Martin LJ. Olesoxime, a cholesterol-like neuroprotectant for the potential treatment of amyotrophic lateral sclerosis. *IDrugs: the investigational drugs journal*. 2010;13(8):568-80.

71 Bertini E, Dessau E, Mercuri E, Muntoni F, Kirschner J, Reid C, et al. Safety and efficacy of olesoxime in patients with type 2 or non-ambulatory type 3 spinal muscular atrophy: a randomised, double-blind, placebo-controlled phase 2 trial. *The Lancet Neurology*. 2017;16(7):513-22.

72 Magalon K, Zimmer C, Cayre M, Khaldi J, Bourbon C, Robles I, et al. Olesoxime accelerates myelination and promotes repair in models of demyelination. *Annals of neurology*. 2012;71(2):213-26.

73 Vergo S, Craner MJ, Etzensperger R, Attfield K, Friese MA, Newcombe J, et al. Acid-sensing ion channel 1 is involved in both axonal injury and demyelination in multiple sclerosis and its animal model. *Brain*. 2011;134(2):571-84.

74 Friese MA, Craner MJ, Etzensperger R, Vergo S, Wemmie JA, Welsh MJ, et al. Acid-sensing ion channel-1 contributes to axonal degeneration in autoimmune inflammation of the central nervous system. *Nat Med*. 2007;13(12):1483-9.

75 Arun T, Tomassini V, Bardella E, de Ruiter MB, Matthews L, Leite MI, et al. Targeting ASIC1 in primary progressive multiple sclerosis: evidence of neuroprotection with amiloride. *Brain*. 2013;136(Pt 1):106-15.

76 Deshmukh VA, Tardif V, Lysiotis CA, Green CC, Kerman B, Kim HJ, et al. A regenerative approach to the treatment of multiple sclerosis. *Nature*. 2013;502(7471):327-32.

77 Way SW, Podojil JR, Clayton BL, Zaremba A, Collins TL, Kunjamma RB, et al. Pharmaceutical integrated stress response enhancement protects oligodendrocytes and provides a potential multiple sclerosis therapeutic. *Nature communications*. 2015;6:6532.

78 Zhornitsky S, Wee Yong V, Koch MW, Mackie A, Potvin S, Patten SB, et al. Quetiapine fumarate for the treatment of multiple sclerosis: focus on myelin repair. *CNS neuroscience & therapeutics*. 2013;19(10):737-44.

79 Organisation wh. WHO International Programme on Chemical Safety. Biomarkers in Risk Assessment: Validity and Validation. 2001.

80 Strimbu K, Tavel JA. What are biomarkers? Current opinion in HIV and AIDS. 2010;5(6):463-6.

81 Housley WJ, Pitt D, Hafler DA. Biomarkers in multiple sclerosis. *Clinical immunology* (Orlando, Fla). 2015;161(1):51-8.

82 Zhao X, Modur V, Carayannopoulos LN, Laterza OF. Biomarkers in Pharmacological Research. *Clinical chemistry*. 2015;61(11):1343-53.

83 Corrae J, de los Milagros Bassani Molinas M. Oligoclonal bands and antibody responses in Multiple Sclerosis. *Journal of neurology*. 2002;249(4):375-89.

84 Davenport RD, Keren DE. Oligoclonal bands in cerebrospinal fluids: significance of corresponding bands in serum for diagnosis of multiple sclerosis. *Clinical chemistry*. 1988;34(4):764-5.

85 Poser CM, Paty DW, Scheinberg L, McDonald WI, Davis FA, Ebers GC, et al. New diagnostic criteria for multiple sclerosis: Guidelines for research protocols. *Annals of neurology*. 1983;13(3):227-31.

86 Polman CH, Reingold SC, Banwell B, Clanet M, Cohen JA, Filippi M, et al. Diagnostic criteria for multiple sclerosis: 2010 Revisions to the McDonald criteria. *Annals of neurology*. 2011;69(2):292-302.

87 Disanto G, Barro C, Benkert P, Naegelin Y, Schadelin S, Giardiello A, et al. Serum Neurofilament light: A biomarker of neuronal damage in multiple sclerosis. *Annals of neurology*. 2017;81(6):857-70.

88 Shinohara RT, Goldsmith J, Mateen FJ, Crainiceanu C, Reich DS. Predicting breakdown of the blood-brain barrier in multiple sclerosis without contrast agents. *AJNR American journal of neuroradiology*. 2012;33(8):1586-90.

89 Katsavos S, Anagnostouli M. Biomarkers in Multiple Sclerosis: An Up-to-Date Overview. *Multiple sclerosis international*. 2013;2013:340508.

90 Brex PA, Ciccarelli O, O'Riordan JI, Sailer M, Thompson AJ, Miller DH. A longitudinal study of abnormalities on MRI and disability from multiple sclerosis. *The New England journal of medicine*. 2002;346(3):158-64.

91 Brex PA, Parker GJ, Leary SM, Molyneux PD, Barker GJ, Davie CA, et al. Lesion heterogeneity in multiple sclerosis: a study of the relations between appearances on T1 weighted images, T1 relaxation times, and metabolite concentrations. *Journal of neurology, neurosurgery, and psychiatry*. 2000;68(5):627-32.

92 Dalton CM, Chard DT, Davies GR, Miszkiel KA, Altmann DR, Fernando K, et al. Early development of multiple sclerosis is associated with progressive grey matter atrophy in patients presenting with clinically isolated syndromes. *Brain*. 2004;127(Pt 5):1101-7.

93 Fisher E, Rudick RA, Simon JH, Cutter G, Baier M, Lee JC, et al. Eight-year follow-up study of brain atrophy in patients with ms. *Neurology*. 2002;59(9):1412-20.

94 Dekker I, Wattjes MP. Brain and Spinal Cord MR Imaging Features in Multiple Sclerosis and Variants. *Neuroimaging clinics of North America*. 2017;27(2):205-27.

95 Hackmack K, Weygandt M, Wuerfel J, Pfueller CF, Bellmann-Strobl J, Paul F, et al. Can we overcome the 'clinico-radiological paradox' in multiple sclerosis? *Journal of neurology*. 2012;259(10):2151-60.

96 Barkhof F. The clinico-radiological paradox in multiple sclerosis revisited. *Current Opinion in Neurology*. 2002;15(3):239-45.

97 Bothwell M. Mechanisms and Medicines for Remyelination. *Annual review of medicine*. 2017;68:431-43.

98 Harlow DE, Honce JM, Miravalle AA. Remyelination Therapy in Multiple Sclerosis. *Frontiers in Neurology*. 2015;6:257.

99 Mallik S, Samson RS, Wheeler-Kingshott CA, Miller DH. Imaging outcomes for trials of remyelination in multiple sclerosis. *Journal of neurology, neurosurgery, and psychiatry*. 2014 2014:1396-404.

100 Zhang J, Shi S, Zhang Y, Luo J, Xiao Y, Meng L, Yang X. alemtuzumab versus interferon beta 1a for relapsing-remitting multiple sclerosis. *Cochrane Database of Systematic Reviews 2017, Issue 11*. Art. No.: CD010968. DOI: 10.1002/14651858.CD010968.pub2.

101 A.J. Coles, E. Fox, A. Vladic, S.K. Gazda, V. Brinar, K.W. Selmaj, A. Skoromets, I. Stolyarov, A. Bass, H. Sullivan, D.H. Margolin, S.L. Lake, S. Moran, J. Palmer, M.S. Smith, D.A.S. Compston 'Alemtuzumab more effective than interferon  $\beta$ -1a at 5-year follow-up of CAMMS223 Clinical Trial', *Neurology Apr 2012, 78 (14) 1069-1078*; DOI: 10.1212/WNL.0b013e31824e8ee7

102 Martinelli Boneschi F, Vacchi L, Rovaris M, Capra R, Comi G. Mitoxantrone for multiple sclerosis. *Cochrane Database of Systematic Reviews 2013, Issue 5*. Art. No.: CD002127. DOI: 10.1002/14651858.CD002127.PUB3.

103 Hartung, Hans-Peter et al. Mitoxantrone in progressive multiple sclerosis: a placebo-controlled, double-blind, randomised, multicentre trial *The Lancet*, Volume 360, Issue 9350, 2018 - 2025

TABLE 1 – Mechanisms of demyelination in multiple sclerosis, derived from Bruck, 2005<sup>4</sup>.

Primary immune mechanisms	Secondary mechanisms
T lymphocytes	Excitotoxicity
Cytotoxins	Free radicals
Nitric oxide	Death ligands and receptors
Antibodies	Toxins
Complement	Viruses

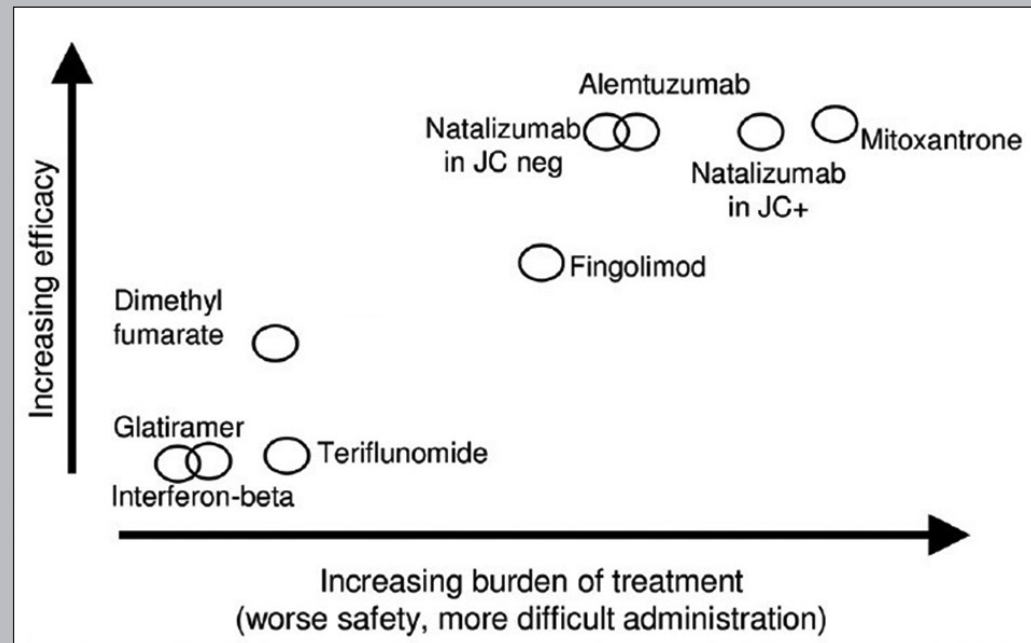
TABLE 2 – Disease Modifying Drugs, registered in the Netherlands.

Compound	Target	Development phase
Interferons	Immunomodulatory cytokine	Registered compound
Glatiramer acetate	Immunomodulatory: competition with various myelin antigens presentation to T lymphocyte	Registered compound
Teriflunomide	Inhibits pyrimidine biosynthesis what leads to impaired proliferation of T lymphocyte	Registered compound
Dimethyl fumarate	Neuroprotective effect through Nrf2-mediated oxidative stress response	Registered compound
Natalizumab	Antibody against alpha-4 integrins, decreases migration of immune cells	Registered compound
Fingolimod	Prevents lymphocytes from moving to the CNS	Registered compound
Alemtuzumab	Mediates lysis of immune cells, suppressing the neuroinflammatory responses in MS	Registered compound
Ocrelizumab	Selectively depletes CD20-expressing B lymphocytes	Registered compound
Cladribine	Causes apoptosis of T lymphocyte	Registered compound
Mitoxantrone	Immunosuppressive properties: reducing the number of B lymphocyte, inhibiting T helper cell function, and augmenting T lymphocyte suppressor activity	Registered compound

TABLE 3 – Compounds in developmental phase, selected on those that influence CNS.

Compound	Target	Development phase
Anti-LINGO-1 antibodies	Promotes remyelination	Phase II
RHIGM22 antibodies	Promotes remyelination	Phase I-II
Olesoxime	Neuroprotective and neuroregenerative properties	Phase I
ASIC1 blockers	Neuroprotective and myeloprotective effects	Pilot study
Benzotropine	Oligodendrocyte maturation	Animal studies
Guanabenz	Increasing oligodendrocyte survival	Phase I
Quetiapine fumarate	Remyelinating and neuroprotective properties	Animal studies
Clean surface gold nanoparticles	Enhance remyelination	Phase I

**FIGURE 1** – Frequently used medication in multiple sclerosis, modified from Coles 2015<sup>19</sup>. Ocrelizumab and cladribine are not in this figure.



## II

### EFFECTS ON SPASTICITY AND NEUROPATHIC PAIN OF AN ORAL FORMULATION OF $\Delta^9$ -TETRAHYDROCANNABINOL IN PATIENTS WITH PROGRESSIVE MULTIPLE SCLEROSIS

Published in: *Clinical Therapeutics* 2018 Sep;40(9):1467-1482

G van Amerongen<sup>1</sup>, K Kanhai<sup>1</sup>, AC Baakman<sup>1</sup>, J Heuberger<sup>1</sup>, E Klaassen<sup>1</sup>, TL Beumer<sup>2</sup>, RLM Strijers<sup>3</sup>, J Killestein<sup>3</sup>, JMA van Gerven<sup>1</sup>, AF Cohen<sup>1</sup>, GJ Groeneveld<sup>1,3</sup>

<sup>1</sup> Centre for Human Drug Research (CHDR), Leiden, the Netherlands

<sup>2</sup> Echo Pharmaceuticals, Weesp, the Netherlands

<sup>3</sup> Department of Neurology and Clinical Neurophysiology, vU University Medical Center, Amsterdam, the Netherlands

## ABSTRACT

**PURPOSE** The aim of the present study was to evaluate the efficacy of an oral formulation of  $\Delta 9$ -tetrahydrocannabinol (ECP002A) in patients with progressive multiple sclerosis (MS).

**METHODS** This accelerated proof-of-concept study consisted of 2 phases: a crossover challenge (dose-finding) phase and a 4-week, parallel, randomized, placebo-controlled treatment phase. Twenty-four patients with progressive MS and moderate spasticity were enrolled. During the treatment phase, biomarkers for efficacy and secondary pharmacodynamic effects were measured at baseline and after 2 and 4 weeks of treatment. Serum samples were collected to determine pharmacokinetic properties and perform population modeling. Safety and tolerability profiles were assessed based on adverse events and safety measurements.

**FINDINGS** Pain was significantly reduced when measured directly after administration of ECP002A in the clinic but not when measured in a daily diary. A similar pattern was observed in subjective muscle spasticity. Other clinical outcomes were not significantly different between active treatment and placebo. Cognitive testing indicated that there was no decline in cognition after 2 or 4 weeks of treatment attributable to ECP002A compared with placebo.

**IMPLICATIONS** This study specifically underlines the added value of thorough investigation of pharmacokinetic and pharmacodynamic associations in the target population. Despite the complex interplay of psychoactive effects and analgesia, the current oral formulation of  $\Delta 9$ -tetrahydrocannabinol may play a role in the treatment of spasticity and pain associated with MS because it was well tolerated and had a stable pharmacokinetic profile.

## INTRODUCTION

Multiple sclerosis (MS) is an inflammatory disease of the nervous system characterized by highly variable clinical aspects and an unpredictable course<sup>1</sup>. Of the many symptoms encountered in MS, muscle spasticity and spasms occur in up to 75% of patients<sup>2</sup>. These symptoms often lead to considerable distress from reduced mobility and interference with activities of daily living. Other disabling features include sensory symptoms (eg, pain), present in up to 86% of the patients<sup>3</sup>. Spasticity refers to feelings of stiffness and a wide range of involuntary muscle spasms (sustained muscle contractions or sudden movements). Spasticity may be as mild as the feeling of tightness of muscles or may be so severe as to produce painful, uncontrollable spasms of extremities. Spasticity may also produce feelings of pain or tightness in and around joints and can cause lower back pain. Although spasticity can occur in any limb, it is much more common in the legs. The endogenous cannabinoid system appears to be tonically active in the control of spasticity<sup>4,5</sup>, and cannabinoids have been proposed in MS because of their ability to reduce the subjective feeling of spasticity<sup>6</sup>. Cannabinoids modulate motor cortical excitability probably through the presynaptic cannabinoid receptor CB1 that controls the release of neurotransmitters from axonal terminals<sup>7,8</sup>.  $\Delta 9$ -Tetrahydrocannabinol ( $\Delta 9$ -THC) is one of the cannabinoids in the Cannabis sativa plant and a direct partial agonist of the cannabinoid receptor CB1. Several studies have examined the effect of (synthetic forms of)  $\Delta 9$ -THC in the treatment of multiple sclerosis. No significant effects of doses between 10 and 25 mg (total daily dose, twice-daily dosing) of oral  $\Delta 9$ -THC were observed on spasticity as measured on the Ashworth scale in a large population. However, a small but clinically relevant benefit of treatment with cannabis extract or  $\Delta 9$ -THC capsules of dosages up to 25 mg/d was found in secondary outcome measures of perception of spasticity and mobility<sup>9</sup>. Several other studies have also found an effect of  $\Delta 9$ -THC on subjective measures of spasticity<sup>10,11</sup> and pain in patients with MS<sup>9,12</sup> at different dosing regimens. Another study comparing the effects of an oral formulation of  $\Delta 9$ -THC to a cannabis plant extract and to placebo did not reveal efficacy in the treatment of spasticity of either product<sup>13</sup>.

Oral bioavailability of  $\Delta 9$ -THC is variable because of significant first-pass effect, and the current formulation of  $\Delta 9$ -THC, ECP002A, was found in a Phase I study to have superior pharmacokinetic (PK) properties to previous formulations, leading to more stable  $\Delta 9$ -THC plasma levels without high peaks and thus expected early onset of treatment effects<sup>14</sup>. It has a tablet formulation of pure  $\Delta 9$ -THC that was produced using an emulsifying drug delivery technology (Alitra [Echo Pharmaceuticals B.V., Weesp, the Netherlands]). This technology was designed to improve the uptake of poorly soluble lipophilic compounds, using less surfactant (<10% w/w). The present study was designed to investigate the PK properties, tolerability, and effects on spasticity and pain of this formulation in a cohort of 24 patients with primary and secondary progressive MS, using a crossover challenge (dose-finding) phase and a 28-day parallel treatment period.

## METHODS

This study was designed as a hybrid between a typical multiple-dose study to investigate PK, pharmacodynamic (PD), and safety profiles and a first-in-patient study to establish proof of concept and hence considered to be an accelerated proof-of-concept study that consisted of 2 phases. The challenge phase was designed as a randomized, double-blind, placebo-controlled, 2-way crossover design to determine the optimal effective dose of ECP002A to treat spasticity of each individual and limit the risk of adverse events, using PK/PD modeling. Each of the 2 visits in the challenge phase consisted of up-titration of 3 consecutive drug administrations with a 100-minute interval in ascending order. If well tolerated, the 3 dose levels were predetermined to be 3, 5, and 8 mg, leading to a total daily dose of 16 mg, which was based on the PK and PD findings in the previous study<sup>14</sup>. Between the administrations of  $\Delta 9$ -THC or placebo, different measurements for safety profile, tolerability, and biomarkers were performed. Between the 2 visits was a washout period of 7 to 14 days.

The 4-week treatment phase was performed in a randomized, double-blind, placebo-controlled parallel fashion to determine the safety profile, tolerability, and efficacy of ECP002A in patients with MS with spasticity and pain. On the basis of the findings of the challenge phase, patients start with a predetermined daily dose divided over 3 intakes. After 2 weeks of treatment, the dose for each patient was evaluated and increased when considered appropriate. The study was approved by the Medical Ethics Committee of the vU University Medical Center (Amsterdam, the Netherlands).

The study was conducted according to the Dutch Act on Medical Research Involving Human Subjects and in compliance with Good Clinical Practice and the Declaration of Helsinki. The study is registered in the European Union Clinical Trials Register under protocol number 2010-022033-28 and in the Dutch clinical trial registry ([www.toetsingonline.nl](http://www.toetsingonline.nl)) under dossier number NL34443.029.10. The study was performed by the Centre for Human Drug Research (Leiden, the Netherlands) and vU University Medical Center (Amsterdam, the Netherlands) and was funded by Echo Pharmaceuticals.

Twenty-four patients 18 years or older with a diagnosis of progressive (primary or secondary) MS according to the revised McDonald criteria<sup>15</sup> who had a disease duration of >1 year and were clinically stable for at least 30 days before the start of the challenge phase were to be enrolled. In addition, patients had to have moderate spasticity as defined by an Ashworth score of  $\geq 2$  (range, 0-4) and a Kurtzke Expanded Disability Status Scale score between 4.5 and 7.5 at baseline (range, 0-10). Spasmolytic therapy was allowed, given that dosage and treatment regimen was stable for at least 30 days before study participation and remained stable throughout study participation. Current use of  $\Delta 9$ -THC was exclusionary, as confirmed per urine drug screen. All patients provided written informed consent before participation.

ECP002A and matching placebo tablets were manufactured and provided under the responsibility of Echo Pharmaceuticals BV. Tablets were available in the strengths 1.5 and 5 mg of  $\Delta 9$ -THC and contained no other active ingredients. On the basis of the observed

PK profile in the first-in-human study, the dosing regimen for the treatment phase was fixed on intake thrice daily of the starting dose as determined during the challenge phase.

Both the challenge and treatment phase included biomarkers for *efficacy* and *secondary PD effects*. Both types consisted of objective and subjective measurements. The end points for the challenge phase were a set of biomarkers for *efficacy* (objective spasticity: the ratio of the maximum amplitude of the Hoffmann reflex to the maximum M response, recorded over the soleus muscle after electrophysiologic stimulation of the popliteal nerve (H/M ratio)<sup>16,17</sup> and subjective spasticity and pain expressed using a Numerical Rating Scale (NRS)) and biomarkers for *secondary PD effects* (changes in internal and external perception [feeling high] as measured with the visual analog scale (VAS) Bowdle<sup>18</sup>, changes in alertness, mood, and calmness as measured with the VAS Bond and Lader<sup>19</sup> and postural instability), and PK end points. The primary end point for the treatment phase was the H/M ratio<sup>16,17</sup>. Secondary end points were biomarkers for *efficacy* that were either measured in the clinic (Ashworth score<sup>20</sup>, subjective spasticity (NRS), number of spasms<sup>21</sup> and pain using an NRS<sup>22</sup> and the McGill Pain Questionnaire<sup>23,24,25</sup>) or measured at home using a daily diary (subjective spasticity (NRS), number of spasms and pain (NRS)). Furthermore, a set of functional outcome measures was selected to assess treatment effects: Expanded Disability Status Scale<sup>26</sup>, the Patient's Global Impression of Change<sup>22</sup>, quality of sleep as determined by the Pittsburgh Sleep Quality Index<sup>27</sup>, walking distance recorded by the Timed 25-Foot Walk Test<sup>28</sup>, the Fatigue Severity Scale<sup>29</sup>. Finally, the same biomarkers for *secondary PD effects* were included, namely, VAS Bowdle, VAS Bond and Lader, and postural instability, in addition to a test to assess visual perception, attention, and working memory, the Symbol Digit Substitution Test<sup>30</sup>, and heart rate<sup>31</sup>.

A sample size of 24 patients (including active and placebo treatment) was determined to have 90% power to detect a difference in the mean H/M ratio (change from baseline) between placebo and ECP002A of 20%, assuming an SD of differences of 21%, using a paired *t*-test with a 0.050 2-sided significance level. For both the challenge and treatment phases, a randomization schedule was prepared under the responsibility of an independent statistician within Centre for Human Drug Research but not involved in the execution of the study. All staff involved in the clinical execution of the study were blinded until all data were collected and the database was locked. For the treatment phase, block randomization was applied. The schedule was sent to the hospital pharmacy, and sealed envelopes for code breaking were available for the investigator. Treatment allocation was performed on the basis of the date of eligibility of the individual because the identification numbers are assigned at that moment.

The results of the PD endpoints were compared between the ECP002A- and placebo-treated group with an analysis of (co)variance with treatment, time, and treatment by time as fixed factors and individual as the random factor and, if available, the mean baseline measurement as covariate. Within the model, contrasts are calculated over all measurements, only the measurements of week 2, and only the measurements of week 4. The Kenward-Roger approximation was used to estimate denominator degrees of freedom, and model parameters were estimated using the restricted maximum likelihood method.

The general treatment effect and specific contrasts were reported with the estimated differences and 95% CIs, the least square mean (LSM) estimates, and *P* values. Graphs of the LSM estimates over time by treatment were presented with 95% CIs as error bars.

Because body sway and Timed 25-Foot Walk Test data were not normally distributed, the data were log-transformed before analysis and back-transformed after analysis. VAS Bowdle subscale scores were log transformed (log10) after a value of 2 was added to each score to avoid log transformation from zero. Combined internal, external, and feeling high scores were calculated on log transformed data.

All calculations of the PD parameters were performed using SAS for Windows, version 9.1.3 (SAS Institute, Cary, North Carolina). No adjustments for multiple comparisons were used.

### Post Hoc analysis

On review of the data, the authors noted that some patients indicated having experienced no subjective spasticity or pain at the start of the treatment phase because of the erratic nature of these symptoms of MS. Therefore, a subgroup analysis was performed that only included patients who indicated experiencing subjective spasticity (*n* = 17) or pain (*n* = 17) at the start of treatment. In addition, to differentiate short-term from long-term treatment effects, an additional analysis was performed in which the measurements immediately after the first dosing at the start of the treatment phase were excluded from the model, and only measurements of week 2 and 4 were used to estimate contrasts.

### PK modeling

The population PK analysis focused on identifying 1- and 2-compartmental structural models with first-order absorption and elimination to describe the data. The random-effects structure that was applied included a proportional residual error distribution and log-normal distributions for the interindividual variability of the PK parameters. The latter was established using an exponential transformation of a normal random-effects distribution. Various types of variance-covariance matrices were tested for the interindividual variability. The estimated population values (both fixed and random effects) were used to determine individual empirical Bayes estimates (post hoc estimates) of the PK parameters and related values such as after single dose:  $AUC_{0-\infty}$ ,  $C_{max}$ , and  $t_{1/2}$ . Calculations were performed using R, version 2.12.0 (R Foundation for Statistical Computing, Vienna, Austria). The analyses closely followed the guidelines of the US Food and Drug Administration and European Medicines Agency for performing and reporting population PK analyses.

## RESULTS

During the clinical execution, a total of 213 potential patients were identified (figure 1). Seventy-three patients were found eligible for screening after telephone prescreening, of

whom 66 were screened. Between August 2011 and January 2013, a total of 24 patients were enrolled. Baseline characteristics are given in table 1; there were no relevant differences between the treatment groups. All randomized patients completed the challenge phase and were subsequently enrolled in the treatment phase. One patient (randomized to receive placebo) dropped out during treatment phase because of intolerable adverse events.

### Challenge phase

None of the measurements included to assess the acute effects on spasticity or pain improved significantly after 3 consecutive dose administrations of ECP002A during the challenge phase (table 2). The H/M ratio and NRS scores for pain and spasticity were not significantly different between the ECP002A and placebo treatment groups. Several biomarkers for PD effects were measured during the challenge phase. On a group level, postural instability, heart rate, and internal and external perception were significantly affected by ECP002A administration compared with placebo. The VAS scores for alertness, calmness, and mood were not significantly affected differently by ECP002A than by placebo.

### PK/PD modeling

To overcome individual differences in tolerability, this study protocol was designed with PK/PD modeling implemented as an aid to determine individual dose per patient. Results from the crossover challenge phase were modeled to assess the individual dose at which desired effects would occur in the absence of adverse events. However, because of a lack of a robust PD response during the challenge phase (spasticity in H/M ratio or NRS scores) or other secondary PD effects (eg, VAS for feeling high), a PK/PD model could not be established on an individual level as intended. Because of large variability in acute PD response, a prediction of plasma concentrations needed to exert a desired PD effect could not be made. The pragmatic approach that we chose instead was up-titration to the level of tolerability to adverse events.

During the challenge phase, the highest consecutive dose of 8 mg was not reached in 2 patients because of adverse events. Twelve patients did not experience any adverse events during the challenge phase and were dosed at the maximum allowed starting dose per protocol of 24 mg/d (intake of 8 mg thrice daily). Seven of these patients were randomized to receive active treatment. The remaining 5 patients randomized to receive active treatment started at a dose of 15 mg/d (intake of 5 mg thrice daily) because they experienced intolerable adverse events after administration of 8 mg during the challenge phase. Daily doses prescribed in the treatment phase are presented in figure 2. After 2 weeks of treatment, the daily dose was increased with 4.5 mg in all patients, except 1. For 2 patients, the dose was subsequently decreased to the starting dose (15 and 24 mg/d, respectively) because of adverse events, indicating that the maximum tolerated dose was reached for these patients.

## Treatment phase

Treatment effects were measured using different types of outcome measures, which we categorized as objective or subjective measures of efficacy or secondary PD response results. The results of the measures of efficacy are summarized in table 3. No significant treatment effect was observed on the objective end points for spasticity: H/M ratio and Ashworth score. Measures of subjective spasticity did reveal a long-term treatment effect in a post hoc analysis that included patients who reported spasticity at the start of the treatment phase ( $n = 18$ ): a nonsignificant reduction of 0.94 point (95% CI, -2.05 to 0.17;  $P = 0.0910$ ). In addition, in a post hoc analyses of long-term treatment effects in patients who reported pain at the start of treatment ( $n = 17$ ), pain rating was significantly reduced overall during 4 weeks of treatment with ECP002A (LSM, 2.74 for active treatment versus 4.25 for placebo; LSM estimated difference, 1.51; 95% CI, -2.75 to -0.28;  $P = 0.0198$ ) (figure 3). When spasticity and pain were measured with a daily diary at home, no significant treatment effect was observed for either pain (-0.47; 95% CI, -2.66 to 1.71;  $P = 0.6581$ ) or spasticity (-0.09; 95% CI, -1.99 to 1.81;  $P = 0.9195$ ). Fatigue, measured using the Fatigue Severity Scale, was significantly reduced after 2 weeks of ECP002A treatment compared with placebo (LSM estimated difference, -0.74; 95% CI, -1.43 to -0.04;  $P = 0.0382$ ). This difference was not significant overall (-0.42; 95% CI, -1.03 to 0.20;  $P = 0.1769$ ). Other functional outcome measures for efficacy, including the Expanded Disability Status Scale, Timed 25-Foot Walk Test, Patient's Global Impression of Change, and Pittsburgh Sleep Quality Index, did not significantly improve during 4 weeks of treatment (table 3).

Other secondary PD effects were assessed using 2 objective biomarkers and 2 subjective questionnaires. The results are described in table 4. None of the tests evidenced a clinically relevant or statistically significant decline of postural stability, cognitive functioning, mood, or psychotomimetic effects. During each treatment visit, the patients were asked which treatment they assumed to be receiving to assess possible bias among patients. At the end of the treatment, 5 patients (41.7%) in the placebo arm guessed correctly that they had received placebo treatment and 5 (41.7%) patients were not sure, whereas 8 patients (66.7%) receiving active treatment guessed correctly that they had been receiving active treatment. Presumed treatment allocation was included in the statistical analyses but was not a significant factor in treatment response.

A responder analysis was performed in which responders for spasticity and pain (NRS) were identified and compared in terms of baseline characteristics. This analysis did not yield significant differences in baseline characteristics between responders and nonresponders.

## PK profiles

The PK profiles were derived from the data collected during the challenge and treatment phases. An overview of the population parameter estimates of the final 1-compartment PK model for  $\Delta 9$ -THC is shown in table 5. The model includes interindividual variability on the elimination rate constant ( $k_{20}$ ) ( $\omega 2$  estimate, 0.038; SE, 0.018; shrinkage, 32.3%)

and interoccasion variability on the absorption rate constant ( $k_a$ ) ( $\omega 2$  estimate, 0.47; SE, 0.087; shrinkage, 6.8%–43.1%). The parameter estimate for  $k_a$  is  $0.0033 \text{ min}^{-1}$  (95% CI, 0.0025–0.0042). The parameter estimate for  $k_{20}$  is  $0.036 \text{ min}^{-1}$  (95% CI, 0.022–0.058). The  $V_d$  is estimated at 285 L (95% CI, 170–479). The proportional residual error was an  $\sigma^2$  estimate of 0.18 (SE, 0.018; shrinkage, 9.4%).

## Safety profiles

In total, 200 adverse events were recorded, most of which were classified as mild. Nine treatment-emergent adverse events (4.5%) were considered moderate, and 1 diagnosis (0.5%) of euphoric mood was judged as severe because it led to inability to work or perform daily activities. A summary table of all adverse events that were observed more than once is provided in table 6. The most commonly reported adverse events were dizziness and euphoric mood, followed by headache, somnolence, and fatigue. Whenever a patient reported to be feeling high, this was recorded as euphoric mood in accordance with Medical Dictionary for Regulatory Activities coding, regardless of whether the patient reported euphoria. Feeling abnormal was used to describe changes in internal or external perception, without a patient specifically mentioning the word high. Adverse events related to disease state and commonly present in this population, including muscular weakness, muscle spasticity, tremor, or paresthesia, were recorded only if there was an increase compared with before the start of the study, as experienced by the patient. During the treatment phase, 5 adverse events led to a dose adjustment or omission of dose increase after 2 weeks of treatment. No serious adverse events occurred during this study. Individual patients reported psychiatric symptoms, including confusion, disorientation, irritability, or apathy, but this was not endemic for treatment with ECP002A. One patient reported adverse events that ultimately led to termination of the participation of this patient after 6 days of placebo treatment. Four (33.3%) of 12 patients receiving active treatment reported an increase in muscular weakness, which was considered moderate in 1 patient. The safety profile observed during active treatment in this study corresponds with the expected adverse event profile for this class of drugs.

## DISCUSSION

This was a phase II, accelerated, proof-of-concept study to investigate the adverse effect profile, tolerability, PD properties, and PK properties of an oral formulation of  $\Delta 9$ -THC in patients with progressive MS and spasticity. The present study was performed immediately after the first-in-human study in healthy volunteers. This study was designed as a hybrid between a typical multiple-dose study to investigate PK, PD, and safety profiles and a first-in-patient study to establish proof of concept. In this small study ( $n = 24$ ) we met these objectives. The challenge phase in the study design proved to be an elegant way to investigate PK, PD, and safety profiles and decide on an appropriate starting dose per individual patient to avoid cumbersome and inefficient up-titration during the treatment phase. Moreover, the placebo-controlled crossover setting reduced the risk of bias. Even though



dose selection for the treatment phase on an individual level was less refined than initially intended because of variability in acute PD response, which impeded determination of a starting dose using PK and PD modeling, the challenge phase still led to an effective treatment phase of 4 weeks in which a PD treatment effect could be found in the target population. The effect sizes in terms of treatment effect of the oral formulation of  $\Delta 9$ -THC on the clinical end points of subjective spasticity, pain, and various other clinical end points are consistent with the findings of earlier studies on this topic<sup>11,32</sup>.

Overall, treatment with ECP002A was well tolerated. The most frequently observed events of dizziness, somnolence, and changes in mood, including euphoric mood, were related to the primary pharmacologic mechanism of action. As such, these events were in line with what was expected. One-third ( $n = 4$ ) of the patients treated with ECP002A reported muscular weakness during the treatment phase. This muscular weakness may be a part of the causal pathway of reduced muscle tension, leading to the intended treatment of spasticity.

Subjective spasticity measured with an NRS repeatedly during the treatment visits on weeks 0, 2, and 4 improved after 2 and 4 weeks of treatment, which was significant at 2 weeks of treatment. The same pattern was observed in a more pronounced way for the NRS for pain measured as an NRS repeatedly during each treatment visit revealed an overall improvement in favor of treatment compared with placebo. For both spasticity and pain, post hoc analyses were performed, which only included patients with any subjective spasticity and pain at the start of treatment because patients with an NRS spasticity or pain score of 0 at baseline would not have been susceptible to improvement, thus leading to a statistical floor effect. For spasticity, the NRS analysis in 18 patients emphasized the pattern that was already seen in the intention-to-treat analysis: a reduction in subjective spasticity, which was significant after 2 weeks of treatment but not after 4 weeks of treatment and no overall significant treatment effect. The NRS for pain ( $n = 17$ ) revealed a significant overall treatment effect and an overall reduction in pain of 1.27 points. To differentiate between acute and (sub)chronic treatment effects, an additional analysis was performed that included the results of the baseline and weeks 2 and 4 and omitted those measurements taken immediately after the first dosing administration of the treatment phase. These analyses accentuated the pattern that was observed in the intention-to-treat analysis. No significant treatment effect was observed for the objective measurements of spasticity: H/M ratio and Ashworth scale. In addition, subjective spasticity and pain measured with an NRS using a daily diary during the treatment phase revealed a limited decrease in level of subjective spasticity and pain in patients treated with active treatment compared with placebo, which was not statistically significant.

The data-intensive study design allowed for a thorough investigation of the association between short-term and long-term PD and PK properties in the target population. The observed difference between short-term and daily treatment effects brought to light the importance of timing of measuring subjective treatment effects.

The discrepancy between the objective and subjective measures of spasticity seen in this study has previously also been observed in Phase II and III trials of cannabinoids and even occasionally for currently first-line spasmolytics in patients with MS<sup>33</sup>. According to

the reviews by Rog<sup>10</sup> and Lakhan and Rowland<sup>11</sup>, only 1 study<sup>34</sup> reported an improvement in Ashworth score, whereas multiple studies reported only subjective improvement of spasticity. In the aforementioned reviews and clinical studies, the validity of the Ashworth scale as an outcome measure for clinically relevant improvement has been questioned, partially because of its limited sensitivity for detecting small changes, as is the case for any objective measure of spasticity<sup>35</sup>. With the goal to further elucidate the pharmacologic mechanism of action of  $\Delta 9$ -THC on spasticity in patients with MS in this data-intensive clinical study, this end point was included in the protocol nonetheless. Even though the study was performed in a double-blind fashion, cannabinoids are known to induce subjective psychoactive effects, which are potentially undermining blinding of study treatment allocation. This could introduce bias, especially when measuring subjective outcome measures. However, it is impossible to disentangle desired spasmolytic treatment effects from psychoactive unblinding effects because they both result from modulation of the cannabinoid system and even possibly share the same pathway.

In 2 of the 3 other studies where the effects of  $\Delta 9$ -THC on the H/M ratio were investigated, no significant treatment effects were seen after 4 to 6 weeks of treatment with oromucosal cannabis-based therapy<sup>36,37,38</sup>. In the present study, the baseline H/M ratio values observed in the soleus muscle were relatively low compared with what is generally considered hyperreflexia or muscle spasticity<sup>39</sup>. This can possibly be explained by the extent of muscle tone observed in these patients: if muscle tone is increased for a prolonged period, reflexes are often diminished because of reduced excitability of the muscle. This phenomenon was distributed unevenly among the treatment groups because it was observed at the start of treatment and during the challenge phase preceding the treatment phase and is thus considered a group difference resulting from chance.

During the challenge phase objective (postural stability) and subjective (alterations in internal or external perception or mood) PD effects were affected by ECP002A compared with placebo. However, these PD effects were not observed during the 4-week treatment phase: patients receiving active treatment did not have an increase in postural instability after 2 or 4 weeks of treatment compared with placebo. In addition, the minor psychoactive effects observed after short-term administration of ECP002A during the challenge phase were not observed during the treatment phase. A comparable pattern was observed in the Symbol Digit Substitution Test, a measure of attention, short-term memory, and psychomotor speed, which revealed a slight deterioration after 2 weeks of treatment with ECP002A compared with placebo. This difference, however, was reversed after 4 weeks of treatment, suggesting an improvement in reaction time. This slim statistical difference was skewed because of a ceiling effect and is considered not clinically relevant. It indicates, however, that no clinically relevant deterioration in attention and cognitive functioning had taken place during 4 weeks of treatment with ECP002A. These findings appear to imply habituation to the (undesirable) psychoactive effects, which was also observed in previous studies investigating the potential for cannabinoids in therapeutic applications<sup>40</sup>.

To our knowledge, the first PK model for  $\Delta 9$ -THC in this patient population was created based on the data that were collected during the challenge and treatment phases. The current PK model exhibits the flip-flop kinetics phenomenon, where the  $k_a < k_{20}$ , and

the terminal phase is therefore determined by  $k_a$ . Although resulting in the best model fit, it is known from previously published PK models<sup>41</sup> that this is not true for  $\Delta 9$ -THC. The reason for this discrepancy is that the mathematical description of the data with a 1-compartment oral absorption model can be identical when the value for  $k_a$  and  $k_{20}$  are interchanged and the value for  $V_{app}$  is then scaled. Such a more physiologically plausible fit with  $k_a > k_{20}$  could not be accomplished with the current data; therefore, this should be taken into consideration when interpreting the values for  $k_a$ ,  $k_{20}$ , and  $V_d$ . In line with the variability in PD outcomes observed in this trial, moderate variability in PK properties was observed during both the challenge and treatment phases compared with the phase I trial investigating the PK and PD properties of ECP002A<sup>14</sup>. Thus, this increased variability is most likely attributable to an increase in variability observed in a heterogeneous patient population compared with healthy volunteers. The PK modeling reveals a relatively high typical apparent clearance (10.27 L/min) and typical apparent (central)  $V_d$  compared with previous findings, which is most likely related to a lower bioavailability (previously estimated between 4% and 12%)<sup>42</sup>. In addition, a slower absorption rate was observed compared with what was observed in a previous study investigating ECP002A in healthy individuals<sup>14</sup>. This was most likely caused by a reduced gastrointestinal motility, which has previously been reported in patients with MS<sup>43</sup>.

In this 4-week study, the subjective measures of the severity of experienced spasticity and pain revealed a treatment effect compared with placebo. These findings are in line with what has been previously reported on the effects of cannabinoids in patients with MS, when measured in the clinic. However, assessment of subjective effects using a daily diary yielded discrepant results, underlining the importance of selecting the appropriate method for determining treatment effects, when patients are treated at home. The mild adverse event profile indicates overall good tolerability for this formulation of  $\Delta 9$ -THC. The PK modeling provided insight in the relatively large variability in absorption between and within patients, thereby underlining the rationale for this combined crossover and parallel study design.

According to recent reviews<sup>44,45</sup>, there currently is moderate evidence supporting the use of cannabinoids ( $\Delta 9$ -THC alone or in combination with cannabidiol) for the treatment of spasticity and pain in patients with MS. Even though research thus far has focused on different formulations of cannabinoids (eg, nabiximols), the findings of the present study indicate that the current formulation has the potential to play a role in the treatment of symptoms, including spasticity and pain associated with MS.

In conclusion, this study found that the current formulation of ECP002A exerts a similar effect on spasticity and pain as other  $\Delta 9$ -THC formulations that was detectable after 2 weeks of treatment and was well tolerated in the target population. Based on our and other observations, spasticity and pain appear to be influenced by spasticity and pain appear to be influenced by  $\Delta 9$ -THC through higher-level central nervous system modulation of perception of spasticity rather than electrophysiologic muscle spasticity itself. Accordingly, ECP002A may have a role in symptomatic treatment of spasticity and pain in MS.

## REFERENCES

- Compston A., Ebers G., Lassmann H., McDonald I., Werkele H. *McAlpine's multiple sclerosis*, third Edition, London: Churchill Livingstone, 1998.
- Paisley S, Beard S, Hunn A, Wight J. Clinical effectiveness of oral treatments for spasticity in multiple sclerosis: a systematic review. *Mult.Scler.* 2002; 8: 319-329.
- Solaro C, Bricchetto G, Amato MP, Cocco E, Colombo B, D'Aleo G, Gasperini C, Ghezzi A, Martinelli V, Milanese C, Patti F, Trojano M, Verdun E, Mancardi GL. The prevalence of pain in multiple sclerosis: a multicenter cross-sectional study. *Neurology* 2004; 63: 919-921.
- Jean-Gilles L, Feng S, Tench CR, Chapman V, Kendall DA, Barrett DA, Constantinescu CS. Plasma endocannabinoid levels in multiple sclerosis. *J Neurol Sci* 2009; 287: 212-215.
- Scotter EL, Abood ME, Glass M. The endocannabinoid system as a target for the treatment of neurodegenerative disease. *Br J Pharmacol* 2010; 160: 480-498.
- Collin C, Davies P, Mutiboko IK, Ratcliffe S. Randomized controlled trial of cannabis-based medicine in spasticity caused by multiple sclerosis. *Eur J Neurol.* 2007; 14: 290-296.
- Iversen L. Cannabis and the brain. *Brain* 2003; 126: 1252-1270.
- Schlicker E, Kathmann M. Modulation of transmitter release via presynaptic cannabinoid receptors. *Trends Pharmacol Sci.* 2001; 22: 565-572.
- Zajicek J, Fox P, Sanders H, Wright D, Vickery J, Nunn A, Thompson A. Cannabinoids for treatment of spasticity and other symptoms related to multiple sclerosis (CAMS study): multicentre randomised placebo-controlled trial. *Lancet* 2003; 362: 1517-1526.
- Rog DJ. Cannabis-based medicines in multiple sclerosis—a review of clinical studies. *Immunobiology.* 2010; 215: 658-672.
- Lakhan SE, Rowland M. Whole plant cannabis extracts in the treatment of spasticity in multiple sclerosis: a systematic review. *BMC Neurol* 2009; 9: 59.
- Svensden KB, Jensen TS, Bach FW. Does the cannabinoid dronabinol reduce central pain in multiple sclerosis? Randomised double blind placebo controlled crossover trial. *BMJ* 2004; 329: 253.
- Killestein J, Hoogervorst EL, Reif M, Kalkers NF, Van Loenen AC, Staats PG, Gorter RW, Uitendhaag BM, Polman CH. Safety, tolerability, and efficacy of orally administered cannabinoids in MS. *Neurology* 2002; 58: 1404-1407.
- Klumpers LE, Beumer TL, van Hasselt JG, Lippmaa A, Karger LB, Kleinloog HD, Freijer JL, de Kam ML, van Gerven JM. Novel Delta(9)-tetrahydrocannabinol formulation Namisol(R) has beneficial pharmacokinetics and promising pharmacodynamic effects. *Br J Clin Pharmacol* 2012; 74: 42-53.
- Polman CH, Reingold SC, Edan G, Filippi M, Hartung HP, Kappos L, Lublin FD, Metz LM, McFarland HF, O'Connor PW, Sandberg-Wollheim M, Thompson AJ, Weinschenker BG, Wolinsky JS. Diagnostic criteria for multiple sclerosis: 2005 revisions to the 'McDonald Criteria'. *Ann.Neurol.* 2005; 58: 840-846.
- Eisen A. Electromyography in disorders of muscle tone. *Can J Neurol Sci* 1987; 14: 501-505.
- Matthews WB. Ratio of maximum H reflex to maximum M response as a measure of spasticity. *J Neurol Neurosurg Psychiatry* 1966; 29: 201-204.
- Bowdle TA, Radant AD, Cowley DS, Kharasch ED, Strassman RJ, Roy-Byrne PP. Psychedelic effects of ketamine in healthy volunteers: relationship to steady-state plasma concentrations. *Anesthesiology* 1998; 88: 82-88.
- Bond A, Lader M. The use of analogue scales in rating subjective feelings. *Br J Med Psychol* 1974; 47: 211-218.
- Bohannon RW, Smith MB. Interrater reliability of a modified Ashworth scale of muscle spasticity. *Phys.Ther* 1987; 67: 206-207.
- Penn RD. Intrathecal baclofen for severe spasticity. *Ann.N.Y.Acad.Sci.* 1988; 531: 157-166.
- Farrar JT, Young JP, Jr., LaMoreaux L, Werth JL, Poole RM. Clinical importance of changes in chronic pain intensity measured on an 11-point numerical pain rating scale. *Pain* 2001; 94: 149-158.
- Melzack R. The short-form McGill Pain Questionnaire. *Pain* 1987; 30: 191-197.
- Wright KD, Asmundson GJ, McCreary DR. Factorial validity of the short-form McGill pain questionnaire (SF-MPQ). *Eur J Pain* 2001; 5: 279-284.
- Bolton JE, Wilkinson RC. Responsiveness of pain scales: a comparison of three pain intensity measures in chiropractic patients. *J Manipulative.Physiol Ther* 1998; 21: 1-7.
- Kurtzke JF. Rating neurologic impairment in multiple sclerosis: an expanded disability status scale (EDSS). *Neurology* 1983; 33: 1444-1452.
- Buysse DJ, Reynolds CF, III, Monk TH, Berman SR, Kupfer DJ. The Pittsburgh Sleep Quality Index: a new instrument for psychiatric practice and research. *Psychiatry Res* 1989; 28: 193-213.
- Cohen JA, Fischer JS, Bolibrush DM, Jak AJ, Kniker JE, Mertz LA, Skaramagas TT, Cutter GR. Intrarater and interrater reliability of the ms functional composite outcome measure. *Neurology* 2000; 54: 802-806.
- Krupp LB, LaRocca NG, Muir-Nash J, Steinberg AD. The fatigue severity scale. Application to patients with multiple sclerosis and systemic lupus erythematosus. *Arch.Neurol.* 1989; 46: 1121-1123.
- Wilson WH, Ellinwood EH, Mathew RJ, Johnson K. Effects of marijuana on performance of a computerized cognitive-neuromotor test battery. *Psychiatry Res* 1994; 51: 115-125.
- Strougo A, Zuurman L, Roy C, Pinquier JL, van Gerven JM, Cohen AF, Schoemaker RC. Modelling of the concentration-effect relationship of THC on central nervous system parameters and heart rate – insight into its mechanisms of action and a tool for clinical research and development of cannabinoids. *J Psychopharmacol.* 2008; 22: 717-726.
- Chohan H, Greenfield AL, Yadav V, Graves J. Use of Cannabinoids for Spasticity and Pain Management in MS. *Curr Treat.Options Neurol* 2016; 18: 1.
- Beard S, Hunn A, Wight J. Treatments for spasticity and pain in multiple sclerosis: a systematic review. *Health Technol.Assess.* 2003; 7: 111, IX-111, 111.
- Vaney C, Heinzel-Gutenbrunner M, Jobin P, Tschopp F, Gattlen B, Hagen U, Schnelle M, Reif M. Efficacy, safety and tolerability of an orally administered cannabis extract in the treatment of spasticity in patients with multiple sclerosis: a randomized, double-blind, placebo-controlled, crossover study. *Mult.Scler.* 2004; 10: 417-424.
- Thaera GM, Wellik KE, Carter JL, Demaerschalk BM, Wingerchuk DM. Do cannabinoids reduce multiple sclerosis-related spasticity? *Neurologist.* 2009; 15: 369-371.
- Centonze D, Mori F, Koch G, Buttari F, Codeca C, Rossi S, Cencioni MT, Bari M, Fiore S, Bernardi G, Battistini L, Maccarrone M. Lack of effect of cannabis-based treatment on clinical and laboratory measures in multiple sclerosis. *Neurol Sci* 2009; 30: 531-534.
- Leocani L, Nuara A, Houdayer E, Schiavetti I, Del CU, Amadio S, Straffi L, Rossi P, Martinelli V, Vila C, Sormani MP, Comi G. Sativex((R)) and clinical-neurophysiological measures of spasticity in progressive multiple sclerosis. *J Neurol* 2015; 262: 2520-2527.
- Russo M, Calabro RS, Naro A, Sessa E, Rifici C, D'Aleo G, Leo A, De LR, Quararone A, Bramanti P. Sativex in the management of multiple sclerosis-related spasticity: role of the corticospinal modulation. *Neural Plast.* 2015; 2015: 656582.
- Kumru H, Murillo N, Samsó JV, Valls-Sole J, Edwards D, Pelayo R, Valero-Cabre A, Tormos JM, Pascual-Leone A. Reduction of Spasticity With Repetitive Transcranial Magnetic Stimulation in Patients With Spinal Cord Injury. *Neurorehabil.Neural Repair* 2010; 24: 435-441.
- Croxford JL. Therapeutic potential of cannabinoids in CNS disease. *CNS Drugs* 2003; 17: 179-202.
- Heuberger JA, Guan Z, Oyetayo OO, Klumpers L, Morrison PD, Beumer TL, van Gerven JM, Cohen AF, Freijer J. Population pharmacokinetic model of THC integrates oral, intravenous, and pulmonary dosing and characterizes short- and long-term pharmacokinetics. *Clin Pharmacokinet* 2015; 54: 209-219.
- McGilveray IJ. Pharmacokinetics of cannabinoids. *Pain Res Manag.* 2005; 10 Suppl A: 15A-22A.
- el-Maghraby TA, Shalaby NM, Al-Tawdy MH, Salem SS. Gastric motility dysfunction in patients with multiple sclerosis assessed by gastric emptying scintigraphy. *Can J Gastroenterol.* 2005; 19: 141-145.
- Chohan H, Greenfield AL, Yadav V, Graves J. Use of Cannabinoids for Spasticity and Pain Management in MS. *Curr Treat.Options Neurol* 2016; 18: 1.
- Whiting PE, Wolff RE, Deshpande S, Di NM, Duffy S, Hernandez AV, Keurentjes JC, Lang S, Misso K, Ryder S, Schmidtkofer S, Westwood M, Kleijnen J. Cannabinoids for Medical Use: A Systematic Review and Meta-analysis. *JAMA* 2015; 313: 2456-2473.

TABLE 1 – Baseline characteristics.

		Total (N=24)	Δ9-THC (N=12)	Placebo (N=12)
Age,y	Mean (SD)	54.3 (8.9)	57.3 (9.0)	51.4 (8.0)
	Range	38-73	41-73	38-64
Sex, No. (%)	Male	8 (33.3%)	4 (33.3%)	4 (33.3%)
	Female	16 (66.7%)	8 (66.7%)	8 (66.7%)
Disease Duration,y	Mean (SD)	11.5 (5.8)	10.3 (6.5)	12.6 (4.9)
	Range	3-27	3-27	6-21
Spasticity, No. (%)	Modified Ashworth score of 2	16 (66.7%)	8 (66.7%)	8 (66.7%)
	Modified Ashworth score of 3	8 (33.3%)	4 (33.3%)	4 (33.3%)
EDSS total score	Mean (SD)	6.2 (0.9)	6.2 (1.2)	6.3 (0.5)
	Range	4.5-7.5	4.5-7.5	5.5-7.5

EDSS = Kurtzke Expanded Disability Status Scale

TABLE 2 – Summary of analysis of measures of pharmacological effects during the challenge phase.

Parameter	LSM		Estimate of Difference 95% CI	LSM Change From Baseline	
	Placebo	Active		Placebo	Active
OBJECTIVE AND SUBJECTIVE MEASURES FOR EFFICACY					
H/M Ratio	0.333	0.326	-0.007 (-0.070, 0.057) p=0.8238	-0.002	-0.008
NRS: spasticity	3.35	3.64	0.28 (-0.01, 0.58) p=0.0595	-0.73	-0.45
NRS: neuropathic pain	2.75	2.71	-0.03 (-0.41, 0.34) p=0.8470	-0.23	-0.27
OBJECTIVE MEASUREMENTS FOR SECONDARY PHARMACODYNAMIC EFFECTS					
Body sway, mm	775.3	919.4	18.6% (5.9%, 32.8%) p=0.0067	-2.0%	16.3%
Heart rate, beats/min	71.1	74.6	3.5 (1.4, 5.7) p=0.0025	-1.0	2.5
SUBJECTIVE MEASUREMENTS FOR SECONDARY PHARMACODYNAMIC EFFECTS					
VAS External log, mm	0.323	0.384	0.061 (0.028, 0.094) p=0.0009	-0.022	0.040
VAS Internal log, mm	0.321	0.352	0.030 (0.003, 0.057) p=0.0295	-0.030	0.000
VAS feeling high log, mm	0.322	0.542	0.220 (0.067, 0.373) p=0.0070	0.019	0.239
VAS Alertness, mm	54.5	52.7	-1.7 (-4.1, 0.6) p=0.1342	1.3	-0.4
VAS Calmness, mm	53.8	54.7	0.9 (-1.5, 3.3) p=0.4289	1.8	2.7
VAS Mood, mm	55.2	56.0	0.8 (-0.4, 2.0) p=0.1699	0.5	1.4

H/M ratio = ratio of the maximum amplitude of the Hoffmann reflex to the maximum M response; LSM = Least Square Means; NRS = Numerical Rating Scale; VAS = Visual Analogue Scale.

TABLE 3 – Summary of analyses of measures for efficacy during treatment phase.

Parameter	LSM		Estimate of Difference (95% CI)			LSM Change From Baseline	
	Placebo	Active	Overall	Week 2	Week 4	Placebo	Active
OBJECTIVE EFFICACY							
H/M ratio (Score 0-1)	0.385	0.386	0.001 (-0.178, 0.179) P=0.9929	-0.009 (-0.198, 0.180) P=0.9216	0.031 (-0.069, 0.131) P=0.5269	0.052	0.053
Ashworth (Score 1-4)	1.70	1.60	-0.11 (-0.41, 0.19) P=0.4615	-0.10 (-0.52, 0.31) P=0.6142	-0.11 (-0.53, 0.30) P=0.5888	-0.21	-0.32
SUBJECTIVE EFFICACY							
NRS: spasticity (Score 1-10)	3.61	3.23	-0.38 (-1.30, 0.53) P=0.3907	-1.00 (-1.98, -0.03) P=0.0445	-0.31 (-1.29, 0.66) P=0.5176	-0.22	-0.61
NRS: spasticity (Score 1-10): subgroup (N=18)	4.50	3.81	-0.69 (-1.79, 0.42) P=0.2038	-1.23 (-2.39, -0.07) P=0.0387	-0.84 (-2.00, 0.32) P=0.1450	-0.46	-1.15
NRS: spasticity (Score 1-10): subgroup (N=18) long-term treatment	4.52	3.57	-0.94 (-2.05, 0.17) P=0.0910				
NRS: pain (Score 1-10)	2.95	2.15	-0.81 (-1.66, 0.04) P=0.0618	-1.09 (-1.98, -0.20) P=0.0183	-0.85 (-1.74, 0.04) P=0.0612	-0.21	-1.02
NRS: pain (Score 1-10): subgroup (n=17)	4.26	2.99	-1.27 (-2.50, -0.04) P=0.0439	-1.69 (-2.96, -0.41) P=0.0124	-1.38 (-2.65, -0.10) P=0.0360	-0.27	-1.54
NRS: pain (Score 1-10): subgroup (n=17) Long-term treatment	4.25	2.74	-1.51 (-2.75, -0.28) P=0.0198				
Diary: spasticity (Score 1-10)	3.65	3.56	-0.09 (-1.99, 1.81) P=0.9195				
Diary: pain (Score 1-10)	2.57	2.10	-0.47 (-2.66, 1.71) P=0.6581				
EDSS (Score 1-10): subanalysis	6.42	6.39	-0.03 (-0.22, 0.17) P=0.7650	-0.12 (-0.34, 0.11) P=0.2935	0.06 (-0.16, 0.28) P=0.5759	-0.05	-0.08
T25 feet walk (ft/sec): subanalysis	3.70	3.87	4.8% (-7.8, 19.1%) P=0.4425	4.0% (-9.1, 19.0%) P=0.5481	5.6% (-7.8, 21.0%) P=0.4080	7.5%	12.6%
PGIC (Score 1-7)	4.08	3.59	-0.49 (-1.19, 0.21) P=0.1632	-0.58 (-1.33, 0.16) P=0.1213	-0.39 (-1.14, 0.35) P=0.2900	-0.22	-0.71
PSQI (Score 0-21)	4.15	5.15	1.00 (-0.83, 2.84) P=0.2688	0.36 (-1.62, 2.33) P=0.7147	1.64 (-0.33, 3.62) P=0.0996	-1.41	-0.41
FSS (Score 1-7)	4.33	3.92	-0.42 (-1.03, 0.20) P=0.1769	-0.74 (-1.43, -0.04) P=0.0382	-0.44 (-1.13, 0.25) P=0.2065	-0.13	-0.55

EDSS = Kurtzke Expanded Disability Status Scale; FSS = Fatigue Severity Scale; H/M ratio = ratio of the maximum amplitude of the Hoffmann reflex to the maximum M response; LSM = Least Square Means; NRS = Numerical Rating Scale; PGIC = Patients Global Impression of Change; PSQI = Pittsburgh Sleep Quality Index; T25 feet walk = Timed 25 feet walk

**TABLE 4 – Summary of analyses of measures for secondary pharmacodynamic effects during treatment phase.**

Parameter	LSM		Treatment P-value	Estimate of difference (95% CI)			LSM Change From Baseline	
	Placebo	Active		Overall	Week 2	Week 4	Placebo	Active
<b>OBJECTIVE MEASUREMENTS</b>								
Body sway, mm	861.8	887.4	0.7024	3.0% (-12.5%, 21.2%) p=0.7024	9.8% (-7.7%, 30.7%) p=0.2722	0.5% (-15.8%, 20.0%) p=0.9527	-6.4%	-3.7%
SDST: total No of correct responses	55.5	55.8	0.0671	0.3 (-0.0, 0.6) p=0.0671	-1.2 (-2.7, 0.3) p=0.1298	2.5 (0.9, 4.0) p=0.0017	-0.1	0.2
SDST: Percentage of correct responses	97.73	97.84	0.0275	0.11 (0.01, 0.20) P=0.0275	0.16 (-0.92, 1.23) p=0.7745	1.58 (0.50, 2.66) p=0.0042	-0.08	0.03
SDST: Average reaction time, msec	2944.1	2929.9	0.1521	-14.2 (-34.2, 5.77) p=0.1521	137.1 (30.01, 244.2) p=0.0123	-147 (-255, -39.0) p=0.0078	-4.29	-18.50
<b>SUBJECTIVE MEASUREMENTS</b>								
VAS Bowdle: External log, mm	0.312	0.340	0.2153	0.028 (-0.18, 0.075) p=0.2153	0.038 (-0.13, 0.089) p=0.1421	0.034 (-0.18, 0.085) p=0.1890	-0.000	0.028
VAS Bowdle: Internal log, mm	0.325	0.320	0.6331	-0.05 (-0.26, 0.016) p=0.6331	-0.02 (-0.26, 0.021) p=0.8285	-0.10 (-0.33, 0.013) p=0.4011	-0.010	-0.015
VAS Bowdle: feeling high log, mm	0.365	0.475	0.2020	0.110 (-0.63, 0.283) p=0.2020	0.113 (-0.74, 0.300) p=0.2277	0.159 (-0.28, 0.346) p=0.0935	0.064	0.174
VAS Bond and Lader: Alertness, mm	51.2	52.1	0.3295	0.8 (-0.9, 2.6) p=0.3295	0.7 (-1.2, 2.7) p=0.4550	0.9 (-1.0, 2.9) p=0.3348	-0.7	0.2
VAS Bond and Lader: Calmness, mm	50.4	52.6	0.1422	2.2 (-0.8, 5.3) p=0.1422	3.3 (0.1, 6.6) p=0.0462	2.1 (-1.2, 5.3) p=0.2046	0.1	2.4
VAS Bond and Lader: Mood, mm	52.0	53.9	0.2469	1.9 (-1.4, 5.2) p=0.2469	2.0 (-1.5, 5.4) p=0.2470	2.6 (-0.8, 6.0) p=0.1283	-0.1	1.8

SDST = Symbol Digit Substitution Test; VAS = Visual Analogue Scale

**TABLE 5 – Population parameter estimates of 1-compartment PK model for Δ9-tetrahydrocannabinol.**

Parameter	Finding (95% CI)	% CV
$k_a$ , min <sup>-1</sup>	0.0033 (0.0025; 0.0042)	77.7
Lag time, min	5.26 (5.11; 5.41)	-
$V_d$ , L	285 (170; 479)	
$k_{20}$ , min <sup>-1</sup>	0.036 (0.022; 0.058)	19.6
$Cl/F$ , L*min <sup>-1</sup>	10.27 (8.72; 12.1)	19.6
$T_{1/2}$ , min	213.6 (165; 275)	77.8

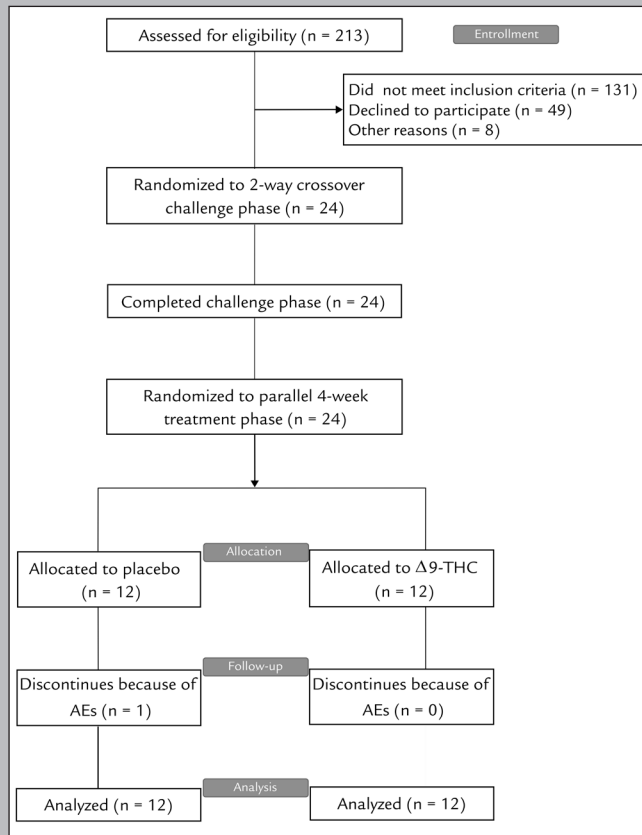
$k_a$  = Absorption rate constant,  $k_{20}$  = Elimination rate constant.

**TABLE 6 – Overview of adverse events and incidence of events reported more than once.**

Adverse Event	Dose finding phase No. (%)		Treatment phase No. (%)	
	Δ9-THC (n = 24)	Placebo (n = 24)	Δ9-THC (n = 12)	Placebo (n = 12)
Number of subjects with at least one adverse event	20 (83.3)	10 (41.7)	10 (83.3)	7 (58.3)
Number of different adverse events	15	9	34	15
<b>Overview of adverse events (incidence &gt;1)</b>				
<b>NERVOUS SYSTEM</b>				
Dizziness	6 (25.0%)	1 (4.2%)	7 (58.3%)	1 (8.3%)
Headache	3 (12.5%)	2 (8.3%)	6 (50.0%)	3 (25.0%)
Somnolence	6 (25.0%)	-	3 (25.0%)	2 (16.7%)
Muscular weakness	1 (4.2%)	1 (4.2%)	4 (33.3%)	1 (8.3%)
Muscle spasticity	-	-	3 (25.0%)	3 (25.0%)
Paresthesia	-	1 (4.2%)	2 (16.7%)	-
Tremor	1 (4.2%)	-	2 (16.7%)	-
Tinnitus	-	-	2 (16.7%)	-
<b>PSYCHIATRIC / MOOD</b>				
Euphoric mood	5 (20.8%)	1 (4.2%)	4 (33.3%)	2 (16.7%)
Disturbance in attention	1 (4.2%)	1 (4.2%)	-	-
Insomnia	-	-	1 (8.3%)	1 (8.3%)
<b>GENERAL DISORDERS AND ADMINISTRATION SITE CONDITIONS</b>				
Fatigue	3 (12.5%)	2 (8.3%)	2 (16.7%)	3 (25.0%)
Feeling abnormal	4 (16.7%)	-	1 (8.3%)	2 (16.7%)
Feeling hot	1 (4.2%)	-	2 (16.7%)	2 (16.7%)
<b>GASTROINTESTINAL</b>				
Dry mouth	1 (4.2%)	-	2 (16.7%)	-
Nausea	1 (4.2%)	-	-	1 (8.3%)
Increased appetite	1 (4.2%)	-	1 (8.3%)	-

Δ9-THC = Δ9-tetrahydrocannabinol.

**FIGURE 1 – Disposition of patients.**



AEs = Adverse effects; Δ9-THC = Δ9-tetrahydrocannabinol.

**FIGURE 2 – Total daily dose of Δ9-THC prescribed per subject in the treatment phase (intake thrice daily) (N=12).**

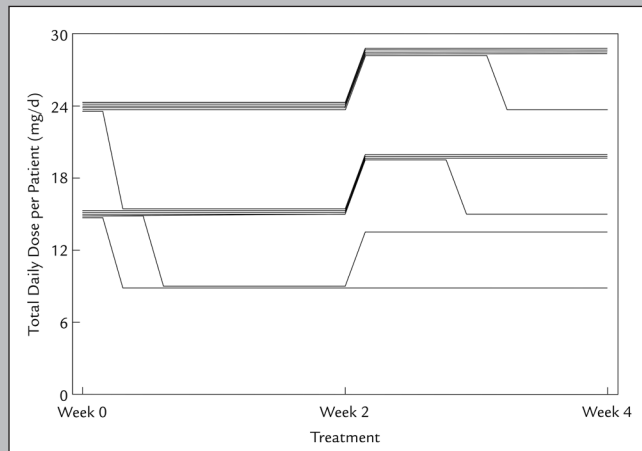
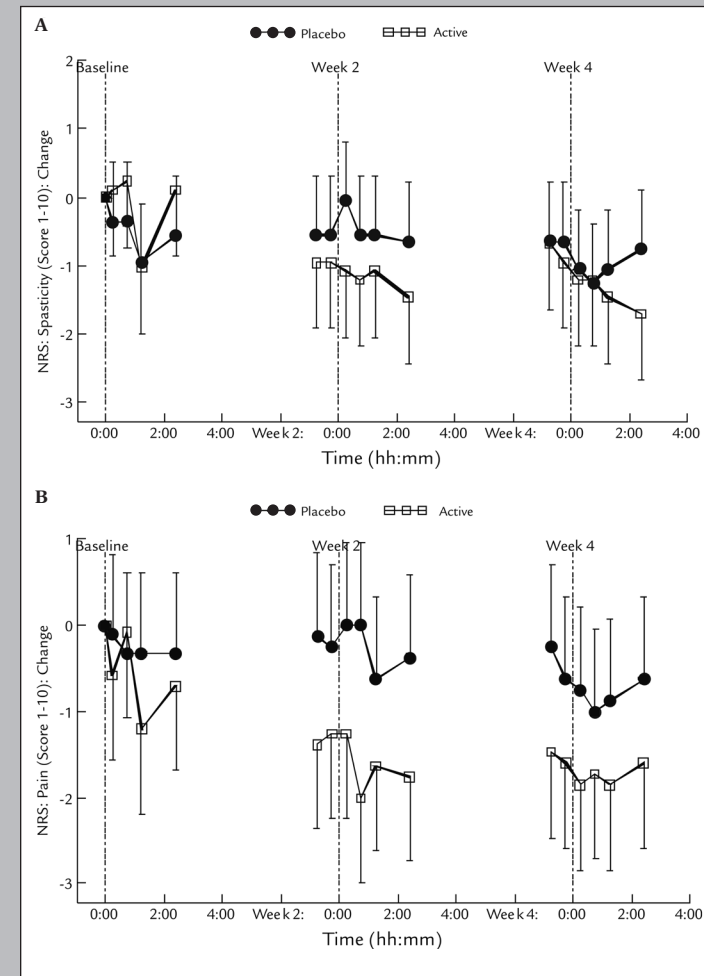


**FIGURE 3 – Post hoc analyses: least square mean change from baseline time profile for Numerical Rating Scale (NRS) scores for spasticity (N=18) (A) and pain (n=17) (B).**



# III

## **GSH-PEGYLATED LIPOSOMAL METHYLPREDNISOLONE IN COMPARISON TO FREE METHYLPREDNISOLONE: SLOW RELEASE CHARACTERISTICS AND PROLONGED LYMPHOCYTE DEPRESSION IN A FIRST-IN-HUMAN STUDY**

**Published in: British Journal of Clinical Pharmacology (BJCP) 2018  
May;84(5):1020-1028.**

**K.M.S. Kanhai<sup>1</sup>, R.G.J.A. Zuiker<sup>1</sup>, I. Stavrakaki<sup>2</sup>, W. Gladdines<sup>2</sup>, P.J. Gaillard<sup>2,3</sup>,  
E.S. Klaassen<sup>1</sup>, G.J. Groeneveld<sup>1</sup>**

<sup>1</sup> Centre for Human Drug Research (CHDR), Leiden, the Netherlands

<sup>2</sup> Former to-BBB technologies bv, Leiden, the Netherlands

<sup>3</sup> 2-BBB Medicines bv, Leiden, the Netherlands

## ABSTRACT

**AIM** Intravenous high-dose free methylprednisolone hemisuccinate (MP) is the primary treatment for an acute relapse in relapsing-remitting (RR) multiple sclerosis (MS). However, it is inconvenient and its side effects are undesirable. Both dose and dosing frequency can be reduced by incorporating free MP in glutathione (GSH) PEGylated liposomes, creating a slow-release formulation with reduced toxicity and prolonged peripheral efficacy. This first-in-human study was designed to assess the safety, pharmacokinetics (PK) and pharmacodynamics (PD) of GSH-PEGylated liposomes containing MP (2B3-201).

**METHODS** The first part was a double-blind, 3-way cross over study in 18 healthy male subjects, receiving ascending doses of 2B3-201, active comparator (free MP) or placebo. Part 2 of the study was an open-label infusion of 2B3-201 (different doses), exploring pre-treatment with antihistamines and different infusion schedules in another 18 healthy male subjects, and a cross-over study in 6 healthy female subjects. MP plasma concentrations, lymphocyte counts, ACTH, osteocalcin and fasting glucose were determined. Safety and tolerability profiles were assessed based on adverse events, safety measurements and CNS tests.

**RESULTS** The most frequent recorded AE related to 2B3-201 was an infusion related reaction (89%). 2B3-201 was shown to have a plasma half-life between 24 and 37 hours and caused a prolonged decrease in the lymphocyte count, ACTH and osteocalcin, and a rise in fasting glucose.

**CONCLUSION** 2B3-201 is considered safe, with no clinically relevant changes in (CNS) safety parameters and no serious adverse events. In addition, 2B3-201 shows a long plasma half-life and prolonged immunosuppressive effects.

## INTRODUCTION

Multiple sclerosis (MS) is one of the most prevalent neuro-inflammatory diseases and the leading cause of chronic disability in young adults. In MS, central nervous system (CNS) infiltration of leukocytes leads to overt inflammation and demyelination and results in neuronal dysfunction<sup>1</sup>. High-dose methylprednisolone hemisuccinate (free MP), given 500-1000 mg daily for 3 to 5 consecutive days, is the primary treatment for an acute relapse in relapsing-remitting (RR) multiple sclerosis<sup>2</sup>. However, it is often given intravenously and causes undesirable short term and long-term side effects include insomnia, depression and agitation<sup>3,4</sup>.

Both dose and dosing frequency of glucocorticoids may significantly be reduced by incorporating steroids in (PEGylated) liposomes, which is expected to result in reduced systemic toxicity while maintaining peripheral efficacy<sup>5</sup>. The additional conjugation of glutathione (GSH) to target active GSH transporters on the blood-brain barrier (BBB), has been shown to facilitate the delivery of the liposome-encapsulated drug into the brain<sup>6,7</sup>.

2B3-201 is methylprednisolone hemisuccinate encapsulated in GSH-PEGylated liposomes and is developed with the aim to enhance the sustained delivery of MP into the brain, thereby potentially augmenting CNS activity. Preclinical studies in animal models showed that 2B3-201 at therapeutic levels in animal models had fewer behavioural side effects (unpublished) and a superior efficacy compared to methylprednisolone hemisuccinate<sup>8-10</sup>. Also, plasma circulation of 2B3-201 derived MP was significantly increased by encapsulation in GSH-PEGylated liposomes<sup>11</sup>. Based on these preclinical data we expected in human subjects a longer half-life and fewer side effects of 2B3-201 when compared to MP.

In this first-in-human study we aimed to assess the safety, pharmacokinetic and pharmacodynamic profile of 2B3-201 in healthy male and female subjects. Plasma concentrations of lymphocytes, osteocalcin, ACTH and fasting glucose were used as pharmacodynamic endpoints, as intravenous administration of prednisolone causes rapid inhibition of the hypothalamic-pituitary-adrenal (HPA) axis<sup>12</sup>, glucose homeostasis disturbances, and depletion of osteocalcin<sup>13,14</sup> and lymphocytes<sup>15</sup>. CNS effects were measured with the NeuroCart<sup>16</sup>.

## MATERIALS

### Design

Initially a randomized, double-blind, placebo- and active comparator- controlled 3-way crossover study with three cohorts of 6 healthy males each, was performed. Subsequently the study was extended while applying a parallel open label design with four cohorts, each containing 6 healthy subjects.

In cohorts 1, 2 and 3, a single dose of 150 mg, 300 mg and 450 mg 2B3-201 respectively was tested and compared to free MP and placebo (table 1). The time interval between the occasions in the cross-over parts was 1 week. Cohorts 4, 5 and 6 had a single dose of 300 mg (cohort 5) and 450 mg (cohorts 4 and 6) 2B3-201 tested while applying altered infusion

schedules and pre-treatment with clemastine. Cohort 7 included females and compared 450 mg 2B3-201 to 1000 mg of free MP in a double-blind crossover design.

An interim analysis was conducted after completion of cohorts 1, 2 and 3 at which safety, pharmacokinetics and pharmacodynamics results were evaluated and a decision to continue to the next cohort was made.

The study was approved by the Medical Ethics Committee of the BEBO Foundation (Assen, The Netherlands). The study was conducted according to the Dutch Act on Medical Research Involving Human Subjects (WMO) and in compliance with Good Clinical Practice (ICH-GCP) and the Declaration of Helsinki.

## Subjects

Forty-six healthy subjects were recruited via the CHDR database and advertisements. All subjects gave written informed consent and were subsequently medically screened before entry into the study. Healthy subjects were not allowed to smoke more than ten cigarettes per day and had to refrain from smoking during the study days. In the 48 h prior to the study days they were asked not to drink alcohol and to avoid xanthine-containing drinks. The use of medication was not allowed during the study period (except occasional use of paracetamol, up to 1 g per day). Healthy subjects with a positive Mantoux test and/or recent (less than 1 month prior to screening) or current significant infection, were not enrolled.

## Treatments

7 study cohorts with a total of 46 subjects received an infusion with 150 mg, 300 mg or 450 mg 2B3-201, 300 mg or 1000 mg free MP, or placebo. An overview of all cohorts can be found in table 1. Subjects in cohorts 1-3 had 3 study periods, during which they either received 2B3-201, free MP or placebo (5% dextrose). Cohorts 4 and 6 received open label infusions of 450 mg 2B3-201, and cohort 4 also assessed the pre-treatment effect of 2 mg clemastine on adverse events. Subjects in cohort 5 received 300 mg 2B3-201, and were also pre-treated with clemastine. In cohort 6 a longer infusion duration was assessed. In cohort 7 healthy female subjects received 450 mg 2B3-201 while being pre-treated with clemastine, and 1000 mg free MP in a double blind two-way cross-over fashion.

## Safety

Adverse events, electrocardiogram (ECG), lymphocyte count, fasting glucose, blood pressure, and heart rate measurements were collected throughout the study. Twelve-lead ECG recordings were made using Electrocardiograph Marquette 800/5500 or Dash 3000. Blood pressure and heart rate were assessed using a Nihon-Kohden BSM-1101K monitor or a Colin Pressmate BP 8800 or a Dash 4000. All ECG, blood pressure and heart rate measurements were performed after subjects had been resting in a supine position for at least 5 min.

## Pharmacokinetics

Whole blood samples were taken for assay of the active component methylprednisolone and the encapsulated pro-drug methylprednisolone hemisuccinate. Blood samples were taken 0.25 h pre-dose and 0.25, 0.5, 1, 2, 4, 6, 8, 12, 24, 26, 48 and 72 hours post-dose for all cohorts, and up to 288 hours for cohorts 4-7. The blood was drawn in 2 mL NaF/K-oxalate tubes, directly placed on ice and then centrifuged (2000 g, 10 min, at 2-8°C), transferred to 2 mL Sarsted tubes and stored at -80°C within 30 min after sampling. The concentrations of methylprednisolone and methylprednisolone hemisuccinate (MPHS) in human sodium fluoride/potassium oxalate plasma were determined using a validated liquid chromatography with tandem mass spectrometry (LC-MS/MS) assays by Analytical Biochemical Lab (Assen, the Netherlands). The Lower Limit of Detection (LLOQ) was 1 ng/mL for methylprednisolone. Concentrations for methylprednisolone were calculated by interpolation from a calibration curve while applying a range of 1-1000 ng/mL.

The following pharmacokinetic variables were calculated: Area under the plasma concentration-time curve (AUC) from time 0 to the time of the last quantifiable concentration ( $AUC_{0-t}$ ) and from time 0 extrapolated to infinity ( $AUC_{0-inf}$ ), maximal observed plasma drug concentration ( $C_{max}$ ), time to maximum observed plasma drug concentration ( $t_{max}$ ), half-life ( $t_{1/2}$ ), volume of distribution (Vd) and clearance. For the non-compartmental analysis only MP concentrations up to 74 hours were used.

## Pharmacodynamics

**LYMPHOCYTE COUNT** Time points for measurement of lymphocytes were 2 hours pre-dose (cohorts 1-3 only), 15 minutes pre-dose (cohorts 4-7) and 1, 2, 4, 8, 12, 24, 48 and 72 hours post dose for all cohorts, and up to 288 hours post dose for cohorts 4-7. The 2 mL EDTA-sample was directly, without pre-processing, sent to a hospital haematology and chemistry lab for analysis. The normal range for lymphocyte count was  $1.00-3.50 \times 10^9/L$ .

**OSTEOCALCIN** Serum osteocalcin was measured several times per occasion: pre-dose on day 0, 8, 24, 48 and 72 hours post dose for all cohorts, and up to 288 hours post dose for cohorts 4-7. Intact osteocalcin was measured in serum with ELISA<sup>13</sup>, the normal range used was 0.4-4.0 nmol/L.

**ACTH** ACTH was measured 12 times per occasion. Samples were taken 0.25 h pre-dose and 0.25, 0.5, 1, 2, 4, 6, 8, 12, 24, 26, 48 and 72 hours post-dose for all cohorts, and up to 288 hours post dose for cohorts 4-7. The ACTH samples (2 mL in an EDTA-tube) were put on ice directly, and centrifuged within 10 minutes. Normal range was <75 ng/L.

**FASTING GLUCOSE** As a pharmacodynamics and safety marker, measurement of fasting glucose levels was performed. Samples were taken pre-dose, 2, 6, 12, 24 and 72 hours post dose for all cohorts, and up to 288 hours for cohorts 4-7. 2 mL was collected in a NaF tube, the used normal range was 3.1-6.4 mmol/L.



**COMPLEMENT AND IGE** To confirm if the observed infusion related reactions in cohort 1 were complement mediated and not allergic reactions, we measured for cohorts 2-7 complement factors SC5b-9, C3a, C4d and Bb (4 mL blood EDTA tube) and IgE (2 mL blood, EDTA tube). These samples were taken pre-dose (depending on cohort at -20, -9 or -7 minutes) and 5, 30 and 120 minutes after start of the infusion.

**CNS TESTS** CNS tests performed with the NeuroCart included: pharmaco-EEG<sup>17-19</sup>, maze learning<sup>20</sup>, visual verbal learning test, Stroop test<sup>21</sup>, adaptive tracking<sup>22</sup>, VAS Bond & Lader<sup>23</sup> and VAS Bowdle<sup>24</sup> and saccadic and smooth pursuit eye movements<sup>25</sup>.

## Statistics

To compare the pharmacodynamics and pharmacokinetics between treatments the mean and SD were calculated per time point by treatment. Cohorts with the same treatment are combined into one treatment group. For MP values below LLOQ are set to 0 ng/mL before dosing and set to half of LLOQ (0.5 ng/mL) after dosing. For ACTH all values below LLOQ were set to half of LLOQ (2.5 ng/L).

## RESULTS

### Demographics

A total of 46 subjects participated in the study of which 41 completed the study. 5 subjects retracted consent during the study, 4 of them were replaced. The subjects that participated in this study were all healthy young adults, subjects' characteristics are listed in table 2.

### Safety

No clinically relevant changes were observed in ECG, physical examination and vital signs (temperature, heart rate, systolic and diastolic blood pressure). Safety laboratory assessments for blood hematology, chemistry and urinalysis also showed no clinically meaningful abnormalities with the exception of a decrease in lymphocytes, which will be discussed in more detail in the pharmacodynamics section.

The most frequently reported adverse events related to 2B3-201 were infusion related reactions, defined as any sign or symptom experienced by the subject within 4 hours after the start of the infusion<sup>26,27</sup>. Symptoms related to infusion that occurred within 4 hours after start of the infusion, such as chest discomfort, urticaria, angioedema and back pain, were clustered<sup>28</sup>. Infusion reaction related symptoms were reported by 41 of the 46 healthy subjects (89%). Other frequently reported adverse events were somnolence (15%), gastroesophageal reflux disease (8%), back pain (not assessed as an infusion related reaction) (8%), fatigue (8%) and dizziness (8%).

Pre-treatment with 2 mg clemastine (cohorts 4, 5 and 7) at 20 minutes before infusion did not result in fewer infusion related reactions: all subjects in these cohorts showed

symptoms of an infusion related reaction (see table 3). Not all infusion related reactions resulted in (temporary) halt of the infusion and/or lowering of the infusion speed.

All adverse events were mild in severity, short lasting and self-limiting. One adverse event related to 1000 mg free MP was classified as moderate: a male subject (cohort 1) developed an acute tonsillitis with fever 3 days after the infusion. He was subsequently treated with feniticillin and fully recovered.

Complement and IgE measurements showed that 2B3-201 caused a parallel rise of C3a and Bb and no increase in C4d and IgE levels were observed (figure 1).

## Pharmacokinetics

A concentration-time graph for methylprednisolone plasma concentration at different dose levels of 2B3-201 derived MP and free MP is shown in figure 2. Pharmacokinetic parameters per cohort are listed in table 4. Plasma concentrations of 2B3-201 derived MP were measured up to 7 days (300 and 450 mg), for 300 mg and 1000 mg free MP concentrations were measurable until two days after infusion.

2B3-201 derived MP had a maximum plasma concentration of 545 mg/mL (450 mg 2B3-201), which contrasts the maximum plasma concentration of 7290 ng/mL for free MP (1000 mg). The  $t_{max}$  was 5.9 hours for 2B3-201 derived MP while free MP had a  $t_{max}$  of 2.16-4.2 hours. Plasma half-life for 2B3-201 derived MP was between 24 and 37 h. Free MP had a half-life of 2.2-4 hr. A t-test showed a significant difference in AUC and  $C_{max}$  (p-values of respectively 0.003 and 0.006) between males and females and in weight (p-value = 0.03), but not in BMI. Observed differences were tested for correlation with weight and BMI with a Spearman correlation. Correlation was found for weight, with values of -0.335 (weight and  $C_{max}$ , p-value=0.03) and -0.39 (weight and AUC, p-value=0.01), however not for BMI, with values of 0.11 (BMI and  $C_{max}$ ) and 0.052 (BMI and AUC). Concentrations and pharmacokinetic parameters for MPHS are not reported (data on file).

## Pharmacodynamics

**LYMPHOCYTES** The effects of 2B3-201 derived MP, free MP and placebo on lymphocytes are shown in figure 3a. Administration of 2B3-201 and free MP resulted in a maximal decrease in lymphocyte count 6 to 12 hours after dosing. The decrease in lymphocyte count, persisted for 2 days after dosing after 150 mg 2B3-201 administration, for 3 days after dosing with 300 and 450 mg 2B3-201. Infusion of 300 mg and 1000 mg free MP resulted in a maximal decrease for 24 hours. 7 days after dosing lymphocytes values for all active groups had returned to baseline.

**ACTH** ACTH concentrations were below the lower limit of quantification for almost all subjects 3 hours after administration of active study medication. The decrease of ACTH was sustained for 3 days (150 mg) and 4 days (300 and 450 mg) in the 2B3-201 dosing groups, whereas for free MP ACTH plasma levels were no longer decreased after the first day after dosing, demonstrated a slight compensatory increase on days 2 and 3, and had returned to baseline values from day 4 onwards.

**OSTEOCALCIN** All the active treatment groups showed a decrease in osteocalcin concentrations in the first 24 hours after dosing. In the 1000 mg MP dosing group, osteocalcin concentrations started to rise again after 24 hours. For the 2B3-201 dosing groups, the decrease in osteocalcin concentrations persisted for at least 4 days.

**FASTING GLUCOSE** An increase in fasting glucose was visible for all active treatment groups. Peak concentrations were measured 12 hours after dosing for free MP cohorts, and 15 hours after dosing for 2B3-201 cohorts. Fasting glucose concentrations were below 6 mmol/L (the upper limit of subjects in fasting condition) after 2 days for cohorts with free MP and 150 mg 2B3-201. For subjects who received 300 mg and 450 mg 2B3-201, fasting blood glucose had returned to levels below 6 mmol/L after 4 days.

**CNS TESTS** No relevant changes in the effects on CNS between 2B3-201 and free MP could be observed.

## DISCUSSION

This first-in-human study with 2B3-201, a formulation of methylprednisolone-encapsulated GSH-PEG liposomes, showed prolonged methylprednisolone concentrations in serum, and as a consequence a sustained decrease in the levels of lymphocytes, osteocalcin and ACTH and increased fasting glucose over a longer period of time.

Based on pharmacokinetic properties, 2B3-201 acts like a slow release product. The estimated terminal half-life of 2B3-201 derived MP is ten times longer than free MP. Also, the  $C_{max}$  is lower for 2B3-201 (360-545 ng/mL) than for free MP (5120-7290 ng/mL). Based on graphical inspection, it is likely that the pharmacokinetics of 2B3-201 derived MP is characterized by first order kinetics. The observed pharmacokinetic profile of free MP corresponded with literature<sup>29,30</sup> and information in the Summary of Product Characteristics.

Pharmacokinetics of 450 mg 2B3-201 in women were different from 450 mg 2B3-201 in men: The  $C_{max}$  and AUC were higher, and the half-life was longer (table 4). This can be explained by relative lower weight of women resulting in a higher concentration of MP in serum, and a longer residence time of 2B3-201 compared to men, as the clearance is comparable (men: 0.09-0.11 L/hr, women: 0.09 L/hr).

A limitation of the cross-over part of the study was the time interval between the cohorts. In cohort 3, dosing of 450 mg of 2B3-201 resulted for two subjects in low concentrations of MP study in pre-dose samples at the start of subsequent occasions. However, we believe that this did not influence the major outcome as pharmacodynamic parameters lymphocytes, ACTH and fasting glucose were back to baseline in less than 7 days after the infusion. Also, the other 4 subjects in cohort 3 did not have measurable pre-dose pharmacokinetic results.

As a consequence of prolonged plasma concentrations of 2B3-201 derived MP, a pronounced decrease in lymphocytes was observed for all dose levels for 3 days, an effect that lasted markedly longer than in the free MP groups (1 day). Similar prolonged pharmacodynamic effects were observed for the decreases in concentrations of osteocalcin and

ACTH, as well as a rise in fasting blood glucose. All these effects were present over a longer period of time after dosing 2B3-201 in comparison to free MP. Even though we observed prolonged effects of 2B3-201, we could not observe significant differences in effects on CNS functioning between 2B3-201 and free MP.

Treatment with 2B3-201 led to the occurrence of mild infusion related reactions in 89% of all subjects. Increased levels of complement concentrations were found in all subjects after receiving 2B3-201 300 mg and 450 mg, although not all subjects reported symptoms related to an infusion reaction (table 3). From this study we can conclude that complement is activated due to administration of 2B3-201, resulting in a rise in C3a (figure 1). With a simultaneous rise of complement factor Bb (specific for the alternative pathway, figure 1), and a lack of rise in C4d (figure 1) concentration (specific for classical pathway), we can conclude that 2B3-201 activated the alternative complement activation pathway. IgE concentrations (figure 1) were not increased, indicating no anaphylactic reaction was initiated. These results correspond well with what is known as ‘complement activation related pseudo allergy’ (CARPA). The relationship between liposomal drug delivery and CARPA is well known, and the observed symptoms in this study match those previously described by others<sup>31-33</sup>.

There were a couple of adjustments described that may decrease the development of a CARPA reaction. First adjustment is to start the infusion with a low infusion rate<sup>31</sup>. We lowered the infusion rate during cohort 1. Also, lowering the infusion speed when symptoms occur, and re-challenging subjects has also reported to be effective<sup>28</sup>. The same could be observed in our study: the infusions of only 3 subjects were eventually permanently halted as a result of an infusion related reaction. All other subjects received the complete infusion.

Another study reported that a low concentration of liposomes in the infusion fluid also led to fewer infusion related reactions<sup>34</sup>, which was implemented in cohort 1. In cohorts 2-7 the concentrations of the liposomes were however still relatively high, as compared to the adjusted concentration in cohort 1 without the observed infusion related reactions. The effect of pre-treatment with clemastine has been discussed in literature<sup>28,34</sup>, and although this had not been effective in all studies, it was decided to administer 2 mg clemastine 20 minutes before start of the infusion in cohorts 4, 5 and 7. In our study design, subjects received 2B3-201 once, so a reported decrease of infusion related reaction with multiple dosing<sup>34</sup> of the same compound was not addressed.

Our current actions did not lead to a decrease in the number of reported infusion related reactions, although we did observe a reduced need to change the infusion speed because of infusion related reactions. Reducing the concentration of the liposomes at the start of the infusion may offer a solution in the future.

Methylprednisolone is first choice in medication for acute relapses in MS<sup>35,36</sup>. In certain European countries usually 3 consecutive days of infusions are given<sup>37</sup>. Based on study results in 2015 which revealed that use of oral administration of MP was non-inferior to intravenous MP<sup>38</sup>, the National Institute for health and Care Excellence (NICE, UK) adapted their guideline<sup>39</sup> accordingly. Nevertheless, use of intravenous MP remains part of clinical practice especially for patients who suffer from severe relapses and those who do not

respond to oral treatment. With these practices in mind, use of 2B3-201 as a one-day intravenous treatment may be a good alternative.

Moreover, to reduce the burden of 3-5 days of hospital visits, and healthcare costs related to the days of admissions in other countries, a single infusion of 2B3-201 could be beneficial for patients and reduce side effects caused by high doses of MP. In the current study, 2B3-201 derived MP was measurable and active for 7 days after infusion, resulting in a sustained decrease of lymphocyte count, ACTH and osteocalcin, and an increase in fasting glucose. Now, studies with single administrations in patients with RRMS and a relapse measuring clinical improvement and comparing single administrations of 2B3-201 to 3 day treatments with regular MP are warranted to demonstrate this further.

Despite the fact that the infusion related reactions were all mild and self-limiting, these reactions caused by 2B3-201 in the current setting were frequent and intense. MP treatment in MS reduces symptoms of the MS relapse on the short-term, but for most patients it does not influence the disease progression in the long-term<sup>36</sup>. It is important that the side effect profile is acceptable for the patient. The observed infusion related reactions, if not resolved, may therefore limit the future widespread use of 2B3-201 as a standard therapy for the treatment of relapses in patients with RRMS.

## REFERENCES

- Compston A, Coles A. Multiple sclerosis. *The Lancet*. 2008;372(9648):1502-17.
- van Winsen L, Polman C, Dijkstra C, Tilders F, Uitdehaag B. Suppressive effect of glucocorticoids on TNF-alpha production is associated with their clinical effect in multiple sclerosis. *Mult Scler*. 2010 4/2010:500-2.
- Tischner D, Reichardt H. Glucocorticoids in the control of neuroinflammation. *Mol Cell Endocrinol*. 2007 9/15/2007:62-70.
- Jongen PJ, Stavrakaki I, Voet B, Hoogervorst E, van Munster E, Linssen WH, et al. Patient-reported adverse effects of high-dose intravenous methylprednisolone treatment: a prospective web-based multi-center study in multiple sclerosis patients with a relapse. *J Neurol*. 2016;263(8):1641-51.
- Linker R, Weller C, Luhder F, Mohr A, Schmidt J, Knauth, et al. Liposomal glucocorticosteroids in treatment of chronic autoimmune demyelination: long-term protective effects and enhanced efficacy of methylprednisolone formulations. *Exp Neurol*. 2008 6/2008:397-406.
- Kannan R, Chakrabarti R, Tang D, Kim K, Kaplowitz N. GSH transport in human cerebrovascular endothelial cells and human astrocytes: evidence for luminal localization of Na<sup>+</sup>-dependent GSH transport in hCEC. *Brain Res*. 2000 1/10/2000:374-82.
- Gaillard P, Visser C, Appeldoorn C, Rip J. Enhanced brain drug delivery: safely crossing the blood-brain barrier. *Drug Discov Today Technol*. 2011 2011:71-4.
- Lee DH, Rotger C, Appeldoorn CC, Reijerkerk A, Gladdines W, Gaillard PJ, et al. Glutathione PEGylated liposomal methylprednisolone (2B3-201) attenuates CNS inflammation and degeneration in murine myelin oligodendrocyte glycoprotein induced experimental autoimmune encephalomyelitis. *J Neuroimmunol*. 2014;274(1-2):96-101.
- Evans MC, Gaillard PJ, de Boer M, Appeldoorn C, Dorland R, Sibson NR, et al. CNS-targeted glucocorticoid reduces pathology in mouse model of amyotrophic lateral sclerosis. *Acta Neuropathol Commun*. 2014;2:66.
- Reijerkerk A, Appeldoorn CC, Rip J, de Boer M, Gaillard PJ. Systemic treatment with glutathione PEGylated liposomal methylprednisolone (2B3-201) improves therapeutic efficacy in a model of ocular inflammation. *Invest Ophthalmol Vis Sci*. 2014;55(4):2788-94.
- Gaillard P, Appeldoorn C, Rip J, Dorland R, van der Pol S, Kooij G, et al. Enhanced brain delivery of liposomal methylprednisolone improved therapeutic efficacy in a model of neuroinflammation. *J Control Release*. 2012 12/28/2012:364-9.
- Russel G, Henley D, Leendertz J, Douthwaite J, Wood S, Stevens A, et al. Rapid glucocorticoid receptor-mediated inhibition of hypothalamic-pituitary-adrenal ultradian activity in healthy males. *J Neurosci*. 2010 4/28/2010:6106-15.
- Heuck C, Wolthers O. A placebo-controlled study of three osteocalcin assays for assessment of prednisolone-induced suppression of bone turnover. *J Endocrinol*. 1998 10/1998:127-31.
- Kuroki Y, Kaji H, Kawano S, Kanda F, Takai Y, Kajikawa M, et al. Short-term effects of glucocorticoid therapy on biochemical markers of bone metabolism in Japanese patients: a prospective study. *J Bone Miner Metab*. 2008 2008:271-8.
- Tornatore K, Venuto R, Logue G, Davis P. CD4+ and CD8+ lymphocyte and cortisol response patterns in elderly and young males after methylprednisolone exposure. *J Med*. 1998 1998:159-83.
- Groeneveld GJ, Hay JL, Van Gerven JM. Measuring blood-brain barrier penetration using the NeuroCart, a CNS test battery. *Drug Discov Today Technol*. 2016;20:27-34.
- Cohen AF, Ashby L, Crowley D, Land G, Peck AW, Miller AA. Lamotrigine (BW430C), a potential anticonvulsant. Effects on the central nervous system in comparison with phenytoin and diazepam. *Br J Clin Pharmacol*. 1985;20(6):619-29.
- Van Steveninck AL, Mandema JW, Tuk B, Van Dijk JG, Schoemaker HC, Danhof M, et al. A comparison of the concentration-effect relationships of midazolam for EEG-derived parameters and saccadic peak velocity. *Br J Clin Pharmacol*. 1993;36(2):109-15.
- Wauquier A. Aging and changes in phasic events during sleep. *Physiol Behav*. 1993;54(4):803-6.
- Milner B. Visually-guided maze learning in man: Effects of bilateral hippocampal, bilateral frontal, and unilateral cerebral lesions. *Neuropsychologia*. 1965;3(4):318-38.
- Laeng B, Lag T, Brennen T. Reduced Stroop interference for opponent colors may be due to input factors: evidence from individual differences and a neural network simulation. *J Exp Psychol Hum Percept Perform*. 2005;31(3):438-52.
- Borland RG, Nicholson AN. Visual motor co-ordination and dynamic visual acuity. *Br J Clin Pharmacol*. 1984;18 Suppl 1:69S-72S.
- Bond AJ, James DC, Lader MH. Sedative effects on physiological and psychological measures in anxious patients. *Psychol Med*. 1974;4(4):374-80.
- Bowdle TA, Radant AD, Cowley DS, Kharasch ED, Strassman RJ, Roy-Byrne PP. Sympathetic effects of ketamine in healthy volunteers: relationship to steady-state plasma concentrations. *Anesthesiology*. 1998;88(1):82-8.
- de Haas SL, de Visser SJ, van der Post JP, de Smet M, Schoemaker RC, Rijnbeek B, et al. Pharmacodynamic and pharmacokinetic effects of TPA023, a GABA(A) alpha(2,3) subtype-selective agonist, compared to lorazepam and placebo in healthy volunteers. *J Psychopharmacol*. 2007;21(4):374-83.
- Sampson H, Munoz-Furlong A, Campbell R, Adkinson NJ, Bock S, Branum A, et al. Second symposium on the definition and management of anaphylaxis: summary report—second National Institute of Allergy and Infectious Disease/Food Allergy and Anaphylaxis Network symposium. *Ann Emerg Med*. 2006 4/2006:373-80.
- Scarlet C. Anaphylaxis. *J Infus Nurs*. 2006 2/2006:39-44.
- Kang S, Saif M. Infusion-Related and Hypersensitivity Reactions of Monoclonal Antibodies Used to Treat Colorectal Cancer-Identification, Prevention, and Management. *J Support Oncol*. 2007 10/2007:451-7.
- Al-Habet S, Rogers H. Methylprednisolone pharmacokinetics after intravenous and oral administration. *Br J Clin Pharm*. 1989 1989:285-90.
- Mollmann H, Rohdewald P, Barth J, Verho M, Derendorf H. Pharmacokinetics and dose linearity testing of methylprednisolone phosphate. *Biopharm Drug Dispos*. 1989 9/1989:453-64.
- Chanan-Khan A, Szebeni J, Savay S, Liebes L, Rafique N, Alving C, et al. Complement activation following first exposure to pegylated liposomal doxorubicin (Doxil): possible role in hypersensitivity reactions. *Ann Oncol*. 2003 9/2003:1430-7.
- Roden M, Nelson L, Knudsen T, Jarosinski P, Starling J, Shiflett S, et al. Triad of acute infusion-related reactions associated with liposomal amphotericin B: analysis of clinical and epidemiological characteristics. *Clin Infect Dis*. 2003 5/15/2003:1213-20.
- Szebeni J. Complement activation-related pseudoallergy: a new class of drug-induced acute immune toxicity. *Toxicology*. 2005 12/15/2005:106-21.
- Szebeni J, Muggia F, Gabizon A, Barenholz Y. Activation of complement by therapeutic liposomes and other lipid excipient-based therapeutic products: Prediction and prevention. *Advanced Drug Delivery Reviews*. 2011;63(12):1020-30.
- Sellebjerg F, Barnes D, Midgard R, Montalban X, Rieckmann P, Selma JK, et al. EFNS guideline on treatment of multiple sclerosis relapses: report of an EFNS task force on treatment of multiple sclerosis relapses. *Eur J Neurol*. 2005 12/2005:939-46.
- Nos C, Sastre-Garriga J, Borrás C, Río J, Tintore M, Mantalban X. Clinical impact of intravenous methylprednisolone in attacks of multiple sclerosis. *Multiple Sclerosis*. 2004 3/30/2004:416.
- NVN. Nederlandse Vereniging voor Neurologie (Dutch Neurology Association): Database with guidelines (<https://richtlijndatabase.nl/NVN>)
- Le Page E, Veillard D, Laplaud D, Hamonic S, Wardi R, Lebrun C, et al. Oral versus intravenous high-dose methylprednisolone for treatment of relapses in patients with multiple sclerosis (COPOSEP): a randomised, controlled, double-blind, non-inferiority trial. *The Lancet*. 2015;386(9997):974-81.
- NICE. NICE guideline on treatment of acute exacerbation in MS <https://www.nice.org.uk/guidance/CG186/chapter/1-Recommendations#relapse-and-exacerbation>

TABLE 1 – Summary of study characteristics.

Cohort	1	2	3	4	5	6*	7
<b>2B3-201 dose</b>	150 mg	300 mg	450 mg	450 mg	300 mg	450 mg	450 mg
<b>Population</b>	Healthy males	Healthy males	Healthy males	Healthy males	Healthy males	Healthy males	Healthy females
<b>Design</b>	Randomized	Randomized	Randomized				Randomized
	Crossover	Crossover	Crossover				Crossover
	Placebo-controlled	Placebo-controlled	Placebo-controlled				
	Active comparator: methylprednisolone	Active comparator: methylprednisolone**	Active comparator: methylprednisolone				Active comparator: methylprednisolone
	Double blind	Double blind	Double blind	Open-label	Open-label	Open-label	Double blind
<b>Number of subjects</b>	6	6	6	6	6	6	6

\* Cohort 6 had an infusion that was twice as long, data from this cohort has not been used in our PK and PD analyses.

\*\* Dose of methylprednisolone was an intravenous infusion of 300 (cohort 2 only) or 1000 mg.

TABLE 2 – Subject characteristics.

Cohort	1	2	3	4	5	6	7
<b>2B3-201 dose</b>	150 mg	300 mg	450 mg	450 mg	300 mg	450 mg	450 mg
<b>Population</b>	Healthy males	Healthy males	Healthy males	Healthy males	Healthy males	Healthy males	Healthy females
<b>Age (years) mean (range)</b>	25 (20-30)	24.9 (19-36)	25.3 (20-45)	21.3 (19-25)	25.5 (20-35)	19.8 (18-23)	23 (20-30)
<b>Weight (kg) mean (range)</b>	77.6 (66-95)	71.3 (66-77)	75.5 (68-88)	81.1 (68.9-116.6)	71.0 (59.8-85.6)	72.1 (65.9-77.8)	66.8 (54.4-81.2)
<b>Height (cm) mean (range)</b>	183.9 (177-191)	179.9 (159-189)	183.4 (165-194)	184.9 (178.4-199.6)	177.3 (165.0-188.2)	184.2 (179.2-191.5)	171.5 (162.7-179.0)
<b>BMI (kg/m<sup>2</sup>) mean (range)</b>	23.0 (20-28)	22.1 (20-26)	22.6 (18-26)	23.5 (21.5-29.3)	22.7 (18.4-25.2)	21.2 (20.2-23.1)	22.8 (19.1-26.9)
<b>Number of subjects</b>	6	6	6 (1 dropout)	6	6	5 (1 dropout)	6 (2 dropouts)

TABLE 3 – Infusion related reactions (IRRS) per cohort.

Cohort	1	2	3	4	5	6	7
2B3-201 dose	150 mg	300 mg	450 mg	450 mg	300 mg	450 mg	450 mg
No. of IRRS	4	5	5	6	6	6	6
Infusion (temporary) stopped due to IRR symptoms	2	3	5	2	4	6	3

TABLE 4 – Pharmacokinetic parameters of methylprednisolone, calculated from 0-72 hours.

Dose (mg)	Cohort	Compound	C <sub>max</sub> (ng mL <sup>-1</sup> ) (SD)	t <sub>max</sub> (h)	AUC <sub>0-∞</sub> (ng h mL <sup>-1</sup> ) (SD)	K <sub>a</sub> (h <sup>-1</sup> ) (SD)	T <sub>1/2</sub> (h) (SD)
150	1 (n=6)	2B3-201	138 (37.1)	4.56 (1.3)	4370 (1000)	0.029 (0.0045)	24.4 (3.9)
300	2 (n=6)	2B3-201	375 (96.6)	4.48 (1.4)	13400 (3220)	0.028 (0.0032)	25 (2.5)
300	5 (n=6)	2B3-201	282 (35)	4.19 (0.9)	14800 (4060)	0.025 (0.0086)	31 (9.5)
450	3 (n=6)	2B3-201	501 (144)	4.85 (0.75)	17900 (2690)	0.024 (0.0029)	29.2 (3.5)
450	4 (n=6)	2B3-201	360 (57.5)	5.12 (1.4)	17400 (4020)	0.024 (0.0034)	28.9 (4.3)
450	7 (n=6)	2B3-201	545 (99.7)	5.90 (2.9)	31800 (15500)	0.0250 (0.010)	37.0 (29)
300	2 (n=6)	Free MP	2140 (371)	2.67 (0.20)	11900 (2490)	0.258 (0.039)	2.74 (0.44)
1000	1 (n=6)	Free MP	5930 (580)	2.16 (0.37)	27800 (7370)	0.286 (0.041)	2.47 (0.38)
1000	3 (n=6)	Free MP	5120 (1120)	3.95 (0.029)	28800 (10800)	0.286 (0.032)	2.45 (0.30)
1000	7 (n=6)	Free MP	7290 (1740)	4.20 (0.26)	42900 (13400)	0.208 (0.082)	3.81(1.6)

FIGURE 1 – Mean values of Bb, C4d, C3a en IgE concentrations for 2B3-201, methylprednisolone and placebo.

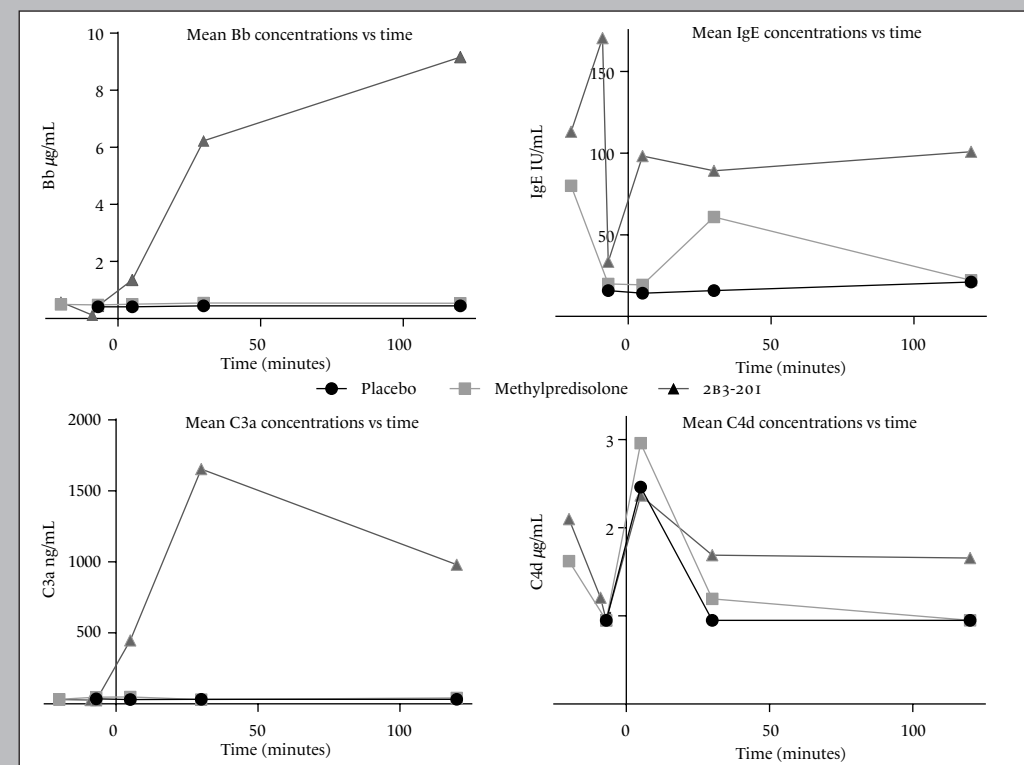


**FIGURE 2** – Serum methylprednisolone (MP) concentrations for 150, 300 and 450 mg 2B3-20I, and 300 and 1000 mg MP. The concentrations of 150 mg 2B3-20I have only been measured for 50 h.

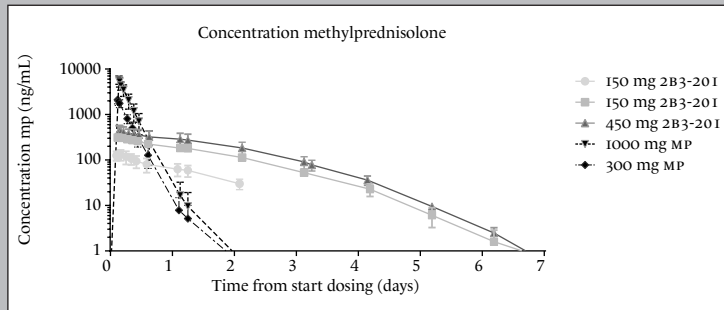
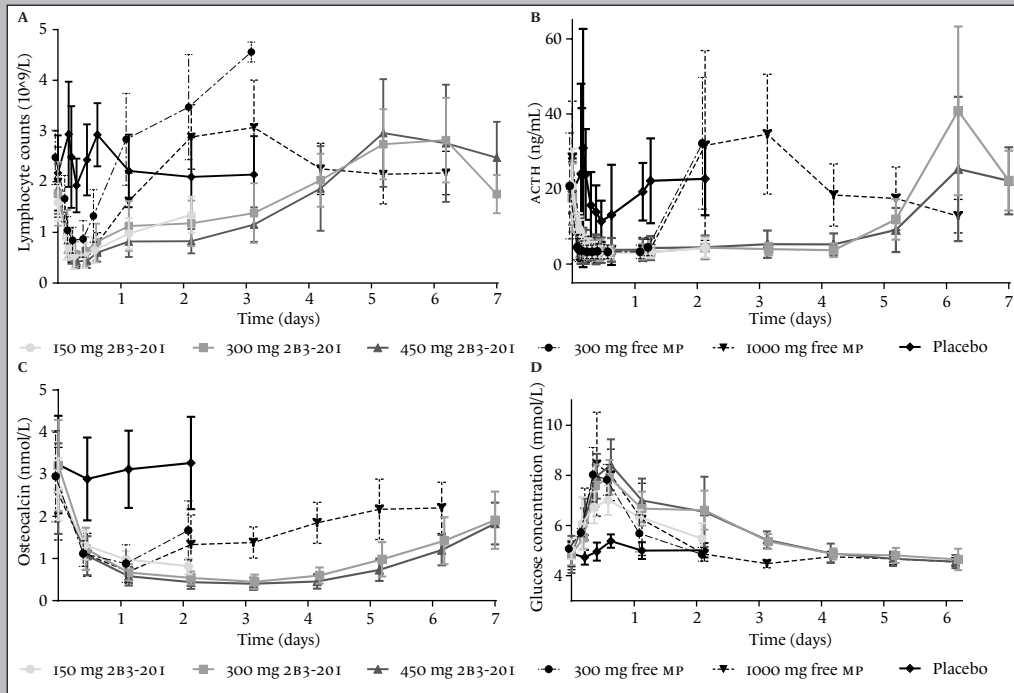


**FIGURE 3** – Pharmacodynamic measurements: graphs of lymphocyte count (A), ACTH concentrations (B), Osteocalcin concentrations (C) and fasting glucose concentrations (D) for different 2B3-20I doses, 300 and 1000 mg free methylprednisolone, and placebo.



# IV

## A FIRST-IN-HUMAN STUDY IN HEALTHY SUBJECTS OF CNM-AU8, GOLD NANOPARTICLES WITH REMYELINATING PROPERTIES.

KMS Kanhai<sup>1</sup>, RGJA Zuiker<sup>1</sup>, W Houghton<sup>2</sup>, WG Kramer<sup>3</sup>, K McBride<sup>4</sup>, M Moerland<sup>1</sup>, R Etherington<sup>2</sup>, GJ Groeneveld<sup>1</sup>

- 1 Centre for Human Drug Research (CHDR), Leiden, the Netherlands
- 2 Clene Nanomedicine, Salt Lake City, United States
- 3 Kramer Consultancy IIc, North Potomac, United States
- 4 Instat, San Diego, United States

## ABSTRACT

**AIMS** CNM-AU8 is a solution of clean-surface gold nanocrystals and being developed for its potentially immunomodulating and remyelinating effects, while leading to fewer side effects than registered gold-containing compounds. A first-in-human single ascending dose study (SAD), followed by a 21-days multiple ascending dose (MAD) study, was performed to assess the safety and pharmacokinetics (PK) of CNM-AU8. In vitro inflammatory challenge experiments were performed to investigate possible PD effects.

**METHODS** The SAD phase included 4 cohorts of 8 subjects (ratio active:placebo 6:2), MAD phase consisted of 4 cohorts of 12 subjects (ratio active:placebo 9:3). Dosages used were 15 mg, 30 mg, 60 mg and 90 mg CNM-AU8 or matching placebo. Safety and tolerability profiles were assessed based on adverse events (AES), vital signs, ECGs, routine laboratory measurements and extra kidney markers. Pharmacokinetic parameters were calculated using non-compartmental analyses and modelling. An in vitro inflammatory challenge was performed in whole human blood samples and PBMCs to investigate potential modulation of TLR9 signaling by CNM-AU8.

**RESULTS** The most frequent reported AE related to CNM-AU8 was abdominal pain (20%) CNM-AU8 had a plasma half-life between 11.5 to 26.2 days, and a first dose  $t_{max}$  between 3.3 and 3.5 hours. No anti-inflammatory effects of CNM-AU8 were observed in the in vitro challenge, and therefore no ex vivo PD measurements were implemented in the clinical study.

**CONCLUSIONS** This study demonstrates that CNM-AU8 has a good safety profile, which appears to be more favorable than existing gold formulations. The low concentrations and unusual pharmacokinetic profile correspond to the reported data on gold nanoparticles. The next step in the development is to determine whether CNM-AU8 possesses anti-inflammatory effects and remyelinating effects.

## INTRODUCTION

Gold has been used in the treatment of various diseases since the beginning of civilization and is mentioned in documents dating as early as 2500 BC<sup>1</sup>. Although it has been utilized for centuries, the exact mechanism of action of gold as a therapeutic agent remains uncertain<sup>1-3</sup>.

The negatively charged surface of gold particles can adhere strongly to proteins in serum, and more than 80% binds to albumin<sup>4</sup>. Which protein attaches to the gold particle subsequently determines its fate<sup>5</sup>. The protein-bound gold nano-particle (NP) distributes to different tissues in the body<sup>6</sup>, and has been found to be present at higher concentrations in inflamed tissue<sup>7</sup>. How gold particles influence immunological responses may be through internalization by macrophages, which has been previously reported<sup>5</sup>. It is hypothesized that gold ions alter the function of macrophages by inhibiting their lysosomal enzymes and lowering the production of pro-inflammatory cytokines<sup>8-13</sup>.

Currently, the gold complexes that are used in clinical practice (e.g. aurothiomalate and auranofin), are prescribed as immunomodulating therapies, predominantly in the treatment of rheumatoid arthritis<sup>14,15</sup>. However, side effects including pruritus, dermatitis, stomatitis, diarrhea, proteinuria, and less frequently hematological abnormalities, are reported in up to 50% of patients and are an important reason to discontinue therapy<sup>14,16</sup>.

It is hypothesized that adverse events related to gold complexes may be specifically related to the covalent formulations of the gold complexes rather than to the activity of gold per se<sup>14,17</sup>. For this reason, CNM-AU8 was developed, a highly concentrated suspension of non-covalently bound, clean-surface faceted gold nanocrystals.

In mice treated with cuprizone, a well-known pre-clinical model for demyelination<sup>18</sup>, CNM-AU8 consistently led to myelin protection and enhanced remyelination (unpublished, sponsor documents on file). For this reason CNM-AU8 is being developed for the treatment of demyelinating disorders such as multiple sclerosis (MS) and neuromyelitis optica (NMO).

In this first in human study we aimed to assess the safety and pharmacokinetics (PK) of CNM-AU8. First, a single ascending dose study (SAD) was performed, followed by 21-days multiple ascending dose (MAD) study. In vitro inflammatory challenge experiments were performed to investigate possible pharmacodynamic effects.

## METHODS

### Design

This was a first-in-human, randomized, double-blind, placebo-controlled, study in healthy male and female subjects. The study had two phases: a single ascending dose (SAD) phase and a multiple ascending dose (MAD) phase. The SAD study consisted of 4 cohorts with 8 subjects per cohort, randomly assigned to receive CNM-AU8 or placebo in a 3:1 ratio. Subsequently the MAD phase of the study was performed, which consisted of 4 cohorts of 12 subjects randomly assigned to receive CNM-AU8 or placebo (in a 3:1 ratio) once daily for 21 days.

An interim analysis was conducted after completion of each cohort. Safety data, collected until one week after last dosing, was used in interim safety reports and was evaluated before it was decided to continue to the next cohort.

The study was approved by the Medical Ethics Committee of the BEBO Foundation (Assen, The Netherlands). The study was conducted according to the Dutch Act on Medical Research Involving Human Subjects (WMO) and in compliance with Good Clinical Practice (ICH-GCP) and the Declaration of Helsinki.

## Subjects

Eighty healthy subjects between the age of 18 and 45 years (inclusive) were recruited via the research institute database and advertisements. All subjects gave written informed consent and were subsequently medically screened before entry into the study. Healthy subjects were not allowed to smoke and had to refrain from smoking during the study days. Subjects were asked not to drink alcohol from 3 days before start of the study until follow-up. The use of medication was not allowed during the study period, with the exception of hormonal contraceptives. Subjects were asked to use double-barrier contraception from two weeks before start of the study until 3 months after the study.

## Treatments

CNM-AU8 is an aqueous suspension of clean surfaced nanocrystals consisting of gold atoms self-organized into crystals of various faceted, geometrical shapes (hexagonal bi-pyramid, pentagonal bi-pyramid, tetrahedron, decahedron, planar spheroids). The faceted gold nanocrystal suspension is concentrated to 1 mg/mL (1,000 ppm) Au. The drug substance is pure elemental Au nanocrystals suspended in deionized water buffered with 0.545 mg/mL sodium bicarbonate (NaHCO<sub>3</sub>) resulting in an aqueous formulation. The colour of the suspension is dark red to purple with a pH within the range of 8.3 to 9.3. CNM-AU8 has been developed for oral administration. Dosages used in this study were 15 mg, 30 mg, 60 mg and 90 mg CNM-AU8 or matching placebo. Using the Food and Drug Administration guidelines<sup>19</sup> a starting dose of 15 mg was selected. Multiple safety and toxicology studies across diverse species (with maximum feasible dosing studies of CNM-AU8 up to 90 mg/kg/day) did not demonstrate any acute or sub chronic toxicities, and accordingly a maximum tolerated dose (MTD) was not identified. These studies did show incidental decrease of blood platelet count and accumulation of small amounts of gold in the kidneys, without affecting renal function. During a 28-day study in dogs with 10 mg/kg/day, a half-life ( $t_{1/2}$ ) of 333 hours, a  $C_{max}$  of 11.9 ng/mL, and a  $t_{max}$  at 24 hours were observed. The No Observed Adverse Effect Level (NOAEL) was 10 mg/kg/day. The planned CNM-AU8 dose levels in this study were 15, 30, 60, and 90 mg CNM-AU8. Based on the NOAEL, an equivalent human dose was determined to be approximately 5.4 mg/kg. In a 60-kg human subject, the selected starting dose of 15 mg CNM-AU8 represents a safety margin of 20-fold.

## Safety

Adverse events (AEs) were monitored and electrocardiogram (ECG), blood pressure, and heart rate measurements were performed throughout the study. Twelve-lead ECG recordings were performed using Electrocardiograph Marquette 800/5500 or Dash 3000. Blood pressure and heart rate were assessed using a Nihon-Kohden BSM-1101K monitor or a Colin Pressmate BP 8800 or a Dash 4000. All ECG, blood pressure and heart rate measurements were performed after subjects had been resting in a supine position for at least 5 minutes.

In addition to standard haematological, chemical and coagulation laboratory measurements, kidney injury markers Kidney Injury Marker-1 (KIM-1), alpha-glutathione S-transferase ( $\alpha$ -GST) and neutrophil gelatinase-associated lipocalin (NGAL)<sup>20</sup> were measured in the multiple dose cohorts. For KIM-1 analysis, 2 × 2.0 mL of urine was collected in Sarstedt tubes per time point and stored at -80°C. For  $\alpha$ -GST 2 × 800  $\mu$ L of urine was collected in Sarstedt tubes per time point, mixed with 200  $\mu$ L urine stabilizing buffer (BIO85STB, Argutus Medical®) and stored at -80°C.

For NGAL analysis, 2 × 2.0 mL of urine was collected in Sarstedt tubes per time point and stored at -80°C.

## Pharmacokinetics

Whole blood samples were taken for measurement of gold concentration in blood. In the SAD cohorts, blood for PK analysis was collected at 1, 2, 3, 4, 6, 8, 12, 24, 48, 72, 96, 120, 144, 168, 192, 216, 240, 264, 288, and 312 hours after dosing ( $\pm$  2 hours for blood samples collected from 24 hours onward). In the MAD cohorts, blood for PK analysis was collected during the day on days 1, 7, 14 and 21 (at 1, 2, 3, 4, 6, 8, 12 hours after dosing and 24 hours). During the other dosing days (days 3-6, 9-13, and 16-21) and on selected days after the last dosing (days 23-28, 32, 36, 40 and 49) one PK sample was taken per visit.

The blood was collected in tubes with potassium (K<sub>2</sub>) EDTA, transferred to 2 mL Sarstedt tubes and stored at -80°C. Blood concentrations of CNM-AU8 were determined using a validated Inductively Coupled Plasma – Mass Spectrometer (ICP-MS) analytical method by Clene Nanomedicine (Havre de Grace, United States). The Lower Limit of Detection (LLOQ) used was 1.5 ng/mL for the SAD part and subsequently upgraded to 0.75 ng/mL for the MAD part after introduction of new ICP-MS instrument with greater sensitivity.

## Pharmacodynamics

In a series of in-vitro experiments, inflammatory challenges were performed on PBMCs and hirudinized whole blood from 4 healthy volunteers (who did not participate in the Phase I clinical trial). We assessed the effect of CNM-AU8 on in vitro toll-like receptor -9 (TLR9)-mediated cytokine release after stimulation with well-characterized TLR9 agonists. PBMCs and whole blood samples were incubated with a concentration range of CNM-AU8 for 6 to 24 hours. Subsequently, TLR9 ligands CpG (Cytosine phosphodiester and Guanine

triphosphate) or ss-DNA/Iyovec were added to the culture, for an additional 3 to 24 hours. The response was quantified by measurement of cytokine release in culture supernatant (pan IFN $\alpha$ , IL-6, IL-1 $\beta$ , TNF $\alpha$ ). This in vitro study was performed to explore whether CNM-AU8 exerts anti-inflammatory effects. In that case, the TLR9 challenge would have been included as pharmacodynamic assay in the MAD part of the clinical study.

## Statistics

All PK parameters were calculated using non-compartmental analysis. Whole blood concentrations below LLOQ were taken as 0 for the calculation of the descriptive statistics for whole blood gold concentrations at each sampling time. All pharmacokinetic calculations were done and individual subject whole blood concentration-time graphs were prepared using SAS® for Windows® Version 9.4.

Individual pharmacokinetic parameters for CNM-AU8 were summarized with descriptive statistics. Pharmacokinetic parameters such as the maximum observed plasma concentration ( $C_{max}$ ), time to  $C_{max}$  ( $t_{max}$ ), the area under the plasma concentration versus time from time 0 to time of measurable plasma concentration after 24 hours ( $AUC_{0-24h}$ ) and terminal-phase half-life ( $t_{1/2}$ ) were calculated using non-compartmental analyses and pharmacokinetic modelling.

## RESULTS

The study was performed between April 2015 and October 2016. Cohort 1 (single dose of 15 mg) was repeated due to a new batch of CNM-AU8 during the study.

### Demographics

A total of 86 subjects participated in the phase 1 study of which 83 completed the study. Due to circumstances for cohort 5 (multiple dose, 15 mg) 10 subjects were enrolled (instead of the planned 12 subjects). Three subjects discontinued the study after dosing: one subject retracted consent during the follow-up phase of the MAD study, one subject of a MAD cohort missed only the last follow-up visit and drug administration for one subject dosing in a MAD cohort was stopped after a pregnancy was confirmed. The group of subjects that participated in this study was a healthy young adult population, the subjects' characteristics can be found in table 1.

### Safety

Overall for both the SAD and MAD phases of the study, routine clinical laboratory assessments, vital signs, ECGs, and physical examinations did not reveal clinically notable findings; none resulted in serious AES or AES leading to discontinuation of treatment. As no reference ranges for normal values for KIM-1,  $\alpha$ -GST, or NGAL have been established

to date, observed values from this study were compared to data previously obtained from healthy volunteers in other studies (data on file). Exploratory statistical analyses did not identify any relevant change from baseline of the three kidney injury markers (KIM-1,  $\alpha$ -GST, or NGAL) across the 4 dosing groups of CNM-AU8 (15 mg, 30 mg, 60 mg, and 90 mg) over the course of the MAD phase.

Most subjects receiving CNM-AU8 experienced at least one AE, but not all AES were related to the compound. The treatment-related AES reported by 3 subjects or more, are summarized in table 2. The most frequently reported, compound-related, AE for subjects who received CNM-AU8 was abdominal pain (20%). These symptoms were mild, mostly intermittent and all self-limiting. For subjects who received placebo, the most reported AE was headache (28%). Other frequently reported AES for CNM-AU8 were mainly gastrointestinal: diarrhea (7 subjects with CNM-AU8, 1 subject with placebo), nausea (5 subjects with CNM-AU8, 1 subject with placebo) and discolored feces (3 subjects with CNM-AU8, 0 subjects with placebo).

There were no serious AES, no AES leading to discontinuation of treatment, and no AES were considered severe.

### Pharmacokinetics

For the single dose cohorts, only one whole blood Au concentration was measured above the LLOQ (1.5 ng/mL), in one subject who received 15 mg CNM-AU8. Consequently, no PK analysis could be done for the SAD phase of the study, and the pharmacokinetic analysis was based completely on the multiple dose cohorts.

A concentration-time graph for gold plasma concentration at different dose levels of CNM-AU8 is shown in figure 1. Based on pre-specified fit criteria, the elimination  $t_{1/2}$  could be calculated for only 39% of the subjects and the geometric mean ranged from 277 to 628 hr (11.5 to 26.2 days). Steady-state plasma concentrations for all cohorts, based on the geometric mean whole blood concentrations, were reached by the end of the 2nd week of dosing (Day 14). The geometric mean whole blood concentrations from 1 week onward increased in a dose-related but not dose-proportional manner. This was also the case for days 14 and 21, where the increases in both  $C_{max}$  and  $AUC_{(0-24)}$  were less than dose proportional and the exponents for the power model for both parameters,  $\sim 0.43$ , were considerably lower than 1, indicating a less than dose proportional increase in exposure. Pharmacokinetic parameters per dose are shown in table 3.

### In vitro pharmacodynamic experiment

CNM-AU8 pretreatment of whole blood or PBMC cultures did not result in an inhibition of TLR9-driven cytokine release, as investigated in an in vitro experiment. In contrary, higher concentrations of CNM-AU8 enhanced NF $\kappa$ B- (IL-6, IL-1 $\beta$ , TNF $\alpha$ ), and IRF-mediated cytokine secretion (figure 2). Based on this outcome, it was decided to not implement a TLR9 challenge as ex vivo pharmacodynamic assay in the clinical study.



## DISCUSSION

This first-in-human study assessed single (SAD) and repeated doses (MAD) of oral CNM-AU8 over 21 consecutive days. The studied dose ranged from 15 to 90 mg CNM-AU8 and was considered safe and well tolerated. The main reported adverse event was mild self-limiting abdominal pain. Pharmacokinetics were characterised by a long half-life and were less than dose proportional.

Gastro-intestinal (GI) adverse events (AES) occurred in 32% of subjects after CNM-AU8 administration. This is comparable to the AE profile of auranofin, an oral gold-containing compound that leads to GI related AES in approximately 40% of cases<sup>1,21</sup>. It is important to mention that the treatment dosages of auranofin leading to adverse events are considerably lower than those of CNM-AU8; 3-9 mg compared to 15-90 mg respectively<sup>22</sup>. This seems to confirm the hypothesis that a gold formulation with less covalent bonds, as it the case for CNM-AU8, is associated with fewer adverse events<sup>14,17</sup>. GI side effects were rarely reported after intramuscular aurothiomalate administration leading to the assumption that route of administration may also be of importance<sup>1,23,24</sup>. It has been suggested that in response to auranofin elevated cyclic AMP in gut mucosal cells results in outpouring of intracellular contents, leading to GI complaints<sup>25</sup>, which can also be relevant for CNM-AU8 as this is an oral suspension.

Another side effect often associated with gold-containing compounds is rash, which has been related with its parenteral administration. It has been reported in 12% subjects taking auranofin and in 30-50% for aurothiomalate<sup>1</sup>. Although the exact mechanism is unknown, early studies report elevated IgE count in some patients<sup>26</sup> and a significant relationship between rash as side effect and smoking<sup>27</sup>. In our study, CNM-AU8 was orally administered and no rash was observed. Subjects in our study were requested to refrain from smoking from 2 months prior to the study until the final follow-up.

Literature reports 0-40% incidence of proteinuria due to use of auranofin or aurothiomalate<sup>28</sup> and that the use of therapeutic dosages can affect renal tubular cells<sup>29</sup>. This study did not detect any relevant increase or change from baseline across the 4 dosing groups of CNM-AU8 during the MAD phase for renal injury markers KIM-1,  $\alpha$ -GST and NGAL. As also no abnormalities in urine related to kidney failure and no symptoms associated with renal insufficiency were observed, we conclude that no nephrotoxic effect of CNM-AU8 has occurred in this study. We concluded that CNM-AU8 15-90 mg per dose for 21 days was safe and well tolerated.

The low concentrations of CNM-AU8 measured in blood are in line with reported biokinetics of gold nanoparticles: gastro-intestinal absorption is limited (animal studies report incomplete absorption of less than 5% within 24h)<sup>30,31</sup>. The passage of gold nanoparticles across the gastro-intestinal epithelium appears to proceed in a prolonged fashion. There is an ongoing debate on the absorption route, but the most recent data suggest entry into the circulation might be through the lymphatic pathway<sup>31</sup>. In animal studies, 10% of circulation nanoparticles is trapped by the liver after entry into the circulation and a part is redistributed again. The role of protein binding and interaction of circulating cellular elements on the biokinetics is not fully understood<sup>31</sup>.

Studies show a high accumulation of gold in secondary tissue, and gold detected 6 months after injection in expected organs (liver) and in less expected organs (brain, spinal cord, testis)<sup>6,30-33</sup>. This could explain the unusual PK curve of CNM-AU8 with gradually increasing concentrations, eventually reaching a plateau. Data suggest that biodistribution of gold nanoparticles is modulated over long periods of time, and it some have mentioned that short-term pharmacokinetic studies should be interpreted with great caution<sup>31</sup>.

This atypical behaviour of nanoparticles makes it difficult to compare CNM-AU8 pharmacokinetics to auranofin and aurothiomalate<sup>34</sup>. It is clear that these registered compounds lead to higher blood concentrations than CNM-AU8. Conversely, the long half-life that was reported for CNM-AU8 (11-26 days) is very comparable to that of auranofin (15-25 days), and of aurothiomalate (10-35 days)<sup>1,35</sup>. A long half-life can be explained by gold distributing widely into different tissues and it being inert. The body can't metabolise gold, and after distribution into the tissues it can be redistributed at a later time point<sup>36</sup>.

As CNM-AU8 was not intravenously administered, but orally, absolute bioavailability and volume of distribution could not be determined. Therefore these PK parameters of CNM-AU8 can't be compared to other compounds in the same class, such as e.g. the oral formulation of auranofin, which has a limited bio-availability of 20-30%<sup>34</sup>.

It is known that size and shape of the nanoparticle influence absorption in the intestine, accumulation, toxicity and interaction<sup>30,37,38</sup>. The size of the nanocrystal size of CNM-AU8 is 10-30 nm and can be expected to allow rapid absorption by intestinal epithelial cells compared to larger nanocrystal sizes, and has less tendency to accumulate in these cells when compared to larger non-particles<sup>37</sup>. The small size of the nanoparticle would suggest a good bio-distribution throughout the body, compared to larger-sized particles (50-100 nm).

Unfortunately, none of the animal studies that were performed with CNM-AU8 reported a minimal anticipated biologic effect level (MABEL). However, based on information from the cuprizone experiment we have tried to determine the human equivalent dose needed to observe a comparable pharmacological effect.

In the cuprizone experiment C57BL/6 mice were given CNM-AU8 (51 ppm) *ad libitum* for 5 weeks. Average fluid intake of mice is approximately 4 mL per day, which would result in a daily intake of 0.204 mg of CNM-AU8, which is approximately 8.16 mg/kg for a C57BL/6 mouse with an average weight of 25 grams<sup>39</sup>. The corresponding human equivalent dose<sup>40</sup> is 0.65 mg/kg. For a human subject weighing 65 kg this would be 42.2 mg. This should be well in the range of dosages tested in our study (15-90 mg per day).

An *in vitro* experiment in whole blood did not show any inhibitory effect of CNM-AU8 on TLR9-mediated inflammation. This design of the experiment was based on a report of Tsai et al from 2012, describing the effect of different sizes of gold nanoparticles on TLR9 signalling<sup>41</sup>. Rather than an inhibition of the inflammatory response by CNM-AU8, an enhancement of the TLR9-driven IFN $\alpha$  release was observed at higher gold concentrations. Based on this exploratory experiment, it was decided to not further explore the potential interference of CNM-AU8 in TLR9 signaling. Although this main objective of the study was to determine safety and pharmacokinetics, the absence of a pharmacodynamic marker is a limitation of this study.

The use of gold-containing medication has declined during the past decades<sup>1</sup>. This is likely the result of the high occurrence of side effects in combination with the limited efficacy. In the treatment of rheumatoid arthritis (RA), methotrexate became the mainstay of treatment due to a superior benefit to risk ratio. The current new gold formulation showed fewer side effects in this clinical study and demonstrated anti-inflammatory and remyelinating effects in nonclinical studies. CNM-AU8 was also tested in the experimental autoimmune encephalomyelitis (EAE) model for MS<sup>42</sup>. And although CNM-AU8 demonstrated remyelinating effects in the cuprizone model, treatment with CNM-AU8 in the EAE model had no beneficial effects. Despite these conflicting results, the clearly remyelinating effects in the cuprizone model were deemed an important reason to explore the effects in patients with demyelinating diseases such as NMO, for which there is still a great unmet medical need. Also, previous studies support the exploration of gold-formulation in neurological diseases<sup>3,8,24</sup>. CNM-AU8 may offer an important possible treatment option for NMO, MS, and perhaps other neurological disease.

As the compound seems to have a favorable safety profile, additional studies will show if limitations that are known for gold-containing compounds, are also applicable to CNM-AU8. This study demonstrates that CNM-AU8 has a good side effect profile, more favorable than old gold formulations. The next step in the development is to demonstrate CNM-AU8 possesses anti-inflammatory effects *in vivo* and remyelinating effects as observed in non-clinical studies.

## REFERENCES

- Kean WF, Kean IR. Clinical pharmacology of gold. *Inflammopharmacology*. 2008;16(3):112-25.
- Stuhlmeier KM. The anti-rheumatic gold salt aurothiomalate suppresses interleukin-beta-induced hyaluronan accumulation by blocking HAS1 transcription and by acting as a cox-2 transcriptional repressor. *The Journal of biological chemistry*. 2007;282(4):2250-8.
- Madeira JM, Bajwa E, Stuart MJ, Hashioka S, Klegeris A. Gold drug auranofin could reduce neuroinflammation by inhibiting microglia cytotoxic secretions and primed respiratory burst. *Journal of neuroimmunology*. 2014;276(1-2):71-9.
- Sadler PJ, Sue RE. The Chemistry of Gold Drugs. *Metal-Based Drugs*. 1994;1(2-3):107-44.
- Dykman LA, Khlebtsov NG. Immunological properties of gold nanoparticles. *Chemical Science*. 2017;8(3):1719-35.
- De Jong WH, Hagens WI, Krystek P, Burger MC, Sips AJAM, Geertsma RE. Particle size-dependent organ distribution of gold nanoparticles after intravenous administration. *Biomaterials*. 2008;29(12):1912-9.
- Vernon-Roberts B, Dore JL, Jessop JD, Henderson WJ. Selective concentration and localization of gold in macrophages of synovial and other tissues during and after chrysotherapy in rheumatoid patients. *Ann Rheum Dis*. 1976;35(6):477-86.
- Larsen A, Kolind K, Pedersen DS, Doering P, Pedersen MO, Danscher G, et al. Gold ions bio-released from metallic gold particles reduce inflammation and apoptosis and increase the regenerative responses in focal brain injury. *Histochem Cell Biol*. 2008;130(4):681-92.
- Persellin RH, Ziff M. The effect of gold salt on lysosomal enzymes of the peritoneal macrophage. *Arthritis Rheum*. 1966;9(1):57-65.
- Yanni G, Nabil M, Farahat MR, Poston RN, Panayi GS. Intramuscular gold decreases cytokine expression and macrophage numbers in the rheumatoid synovial membrane. *Ann Rheum Dis*. 1994;53(5):315-22.
- Sumbayev VV, Yasinska IM, Garcia CP, Gilliland D, Lall GS, Gibbs BF, et al. Gold nanoparticles downregulate interleukin-beta-induced pro-inflammatory responses. *Small (Weinheim an der Bergstrasse, Germany)*. 2013;9(3):472-7.
- Lee JY, Park W, Yi DK. Immunostimulatory effects of gold nanorod and silica-coated gold nanorod on RAW 264.7 mouse macrophages. *Toxicology letters*. 2012;209(1):51-7.
- Bancos S, Stevens DL, Tyner KM. Effect of silica and gold nanoparticles on macrophage proliferation, activation markers, cytokine production, and phagocytosis *in vitro*. *International journal of nanomedicine*. 2015;10:183-206.
- Dabrowiak JC. *Metals in Medicine*. John Wiley & Sons, Ltd; 2009. p. 283-310.
- Suarez-Almazor ME, Spooner C, Belseck E, Shea B. Auranofin versus placebo in rheumatoid arthritis. *Cochrane Database of Systematic Reviews*. 2000(2).
- Menninger H, Herborn G, Sander O, Blechschmidt J, Rau R. A 36 month comparative trial of methotrexate and gold sodium thiomalate in the treatment of early active and erosive rheumatoid arthritis. *British journal of rheumatology*. 1998;37(10):1060-8.
- Yei Ho S, Tiekink ERT. 79Au Gold-Based Metallotherapeutics: Use and Potential. *Metallotherapeutic Drugs and Metal-Based Diagnostic Agents*: John Wiley & Sons, Ltd; 2005. p. 507-27.
- Torkildsen Ø, Brunborg LA, Myhr KM, Bø L. The cuprizone model for demyelination. *Acta Neurologica Scandinavica*. 2008;117:72-6.
- FDA. Food and Drug Administration Guidance Document. Estimating the Maximum Safe Starting Dose in Initial Clinical Trials for Therapeutics in Adult Healthy Volunteers. CDER. July 2005;www.fda.gov/downloads/Drugs/GuidanceComplianceRegulatoryInformation/Guidances/ucm078932.pdf.
- Bonventre JV, Vaidya VS, Schmouder R, Feig P, Dieterle F. Next-generation biomarkers for detecting kidney toxicity. *Nature Biotechnology*. 2010;28:436.
- Capparelli EV, Bricker-Ford R, Rogers MJ, McKerrow JH, Reed SL. Phase I Clinical Trial Results of Auranofin, a Novel Antiparasitic Agent. *Antimicrob Agents Chemother*. 2016;61(1):e01947-16.
- Calin A, Saunders D, Bennett R, Jacox R, Kaplan D, O'Brien W, et al. Auranofin: 1 mg or 9 mg? The search for the appropriate dose. *The Journal of rheumatology Supplement*. 1982;8:146-8.
- van Riel PL, van de Putte LB, Gribnau FW, Macrae KD. Comparison of auranofin and aurothioglucose in the treatment of rheumatoid arthritis: a single blind study. *Clinical rheumatology*. 1984;3 Suppl 1:51-6.
- Roder C, Thomson MJ. Auranofin: Repurposing an Old Drug for a Golden New Age. *Drugs in R&D*. 2015;15(1):13-20.
- van Riel PL, Gribnau FW, van de Putte LB, Yap SH. Loose stools during auranofin treatment: clinical study and some pathogenetic possibilities. *The Journal of rheumatology*. 1983;10(2):222-6.
- Iveson JM, Scott DG, Perera WD, Cunliffe WJ, Wright V. Immunofluorescence of the skin in gold rashes-with particular reference to IgE. *Ann Rheum Dis*. 1977;36(6):520-3.
- Kay EA, Jayson MI. Risk factors that may influence development of side effects of gold sodium thiomalate. *Scandinavian journal of rheumatology*. 1987;16(4):241-5.
- Kean WF, Hart L, Buchanan WW. Auranofin. *British journal of rheumatology*. 1997;36(5):560-72.
- Merle LJ, Reidenberg MM, Camacho MT, Jones BR, Drayer DE. Renal injury in patients with rheumatoid arthritis treated with gold. *Clinical pharmacology and therapeutics*. 1980;28(2):216-22.
- Schleh C, Semmler-Behnke M, Lipka J, Wenk A, Hirn S, Schäffler M, et al. Size and surface charge of gold nanoparticles determine absorption across intestinal barriers and accumulation in secondary target organs after oral administration. *Nanotoxicology*. 2012;6(1):36-46.
- Schmid G, Kreyling WG, Simon U. Toxic effects and biodistribution of ultrasmall gold nanoparticles. *Archives of Toxicology*. 2017;91(9):3011-37.
- Cho WS, Cho M, Jeong J, Choi M, Han BS, Shin HS, et al. Size-dependent tissue kinetics of PEG-coated gold nanoparticles. *Toxicology and applied pharmacology*. 2010;245(1):116-23.
- Sonavane G, Tomoda K, Makino K. Biodistribution of colloidal gold nanoparticles after intravenous administration: effect of particle size. *Colloids and surfaces B, Biointerfaces*. 2008;66(2):274-80.
- Blocka KL, Paulus HE, Furst DE. Clinical pharmacokinetics of oral and injectable gold compounds. *Clinical pharmacokinetics*. 1986;11(2):133-43.
- Furst DE, Dromgoole SH. Comparative pharmacokinetics of triethylphosphine gold (auranofin) and gold sodium thiomalate (GST). *Clinical rheumatology*. 1984;3 Suppl 1:17-24.
- Naz F, Koul V, Srivastava A, Gupta YK, Dinda AK. Biokinetics of ultrafine gold nanoparticles (AuNPs) relating to redistribution and urinary excretion: a long-term *in vivo* study. *Journal of drug targeting*. 2016;24(8):720-9.
- Yao M, He L, McClements DJ, Xiao H. Uptake of Gold Nanoparticles by Intestinal Epithelial Cells: Impact of Particle Size on Their Absorption, Accumulation, and Toxicity. *Journal of Agricultural and Food Chemistry*. 2015;63(36):8044-9.
- Carnovale C, Bryant G, Shukla R, Bansal V. Size, shape and surface chemistry of nano-gold dictate its cellular interactions, uptake and toxicity. *Toxicology*. 2016;317:1-10.
- Zhang Q, Tordoff MG. No effect of dietary calcium on body weight of lean and obese mice and rats. *American journal of physiology Regulatory, integrative and comparative physiology*. 2004;286(4):R669-77.
- Nair AB, Jacob S. A simple practice guide for dose conversion between animals and human. *Journal of basic and clinical pharmacy*. 2016;7(2):27-31.
- Tsai CY, Lu SL, Hu CW, Yeh CS, Lee GB, Lei HY. Size-dependent attenuation of TLR9 signaling by gold nanoparticles in macrophages. *Journal of immunology (Baltimore, Md. : 1950)*. 2012;188(1):68-76.
- Constantinescu CS, Farooqi N, O'Brien K, Gran B. Experimental autoimmune encephalomyelitis (EAE) as a model for multiple sclerosis (MS). *British Journal of Pharmacology*. 2011;164(4):1079-106.

TABLE 1 – Subject disposition per treatment

	Single dose cohorts					Multiple dose cohorts				
	15 mg	30 mg	60 mg	90 mg	Placebo	15 mg	30 mg	60 mg	90 mg	Placebo
N	12	6	6	6	10	8	9	9	9	11
Male (%)	5 (41.7)	3 (50.0)	3 (50.0)	2 (33.3)	4 (40.0)	5 (62.5)	5 (55.6)	4 (44.4)	5 (55.6)	7 (63.6)
Female (%)	7 (58.3)	3 (50.0)	3 (50.0)	4 (66.7)	6 (60.0)	3 (37.5)	4 (44.4)	5 (55.6)	4 (44.4)	4 (36.4)
Mean age (years)	23.5	21.8	24.5	25.8	29.5	25.9	22.0	26.7	28.1	27.8
Mean height (cm)	176.4	173.7	179.3	169.3	173.3	174.2	181.2	174.0	174.2	177.8
Mean weight (kg)	69.8	66.8	77.2	64.7	75.6	70.0	76.2	70.8	72.5	77.3
BMI (kg/m <sup>2</sup> )	22.2	22.1	23.9	22.6	25.2	22.7	23.1	23.4	23.9	24.2

TABLE 2 – Summary of treatment-emergent adverse events reported by 3 subjects or more.

	Total (active/ Placebo)	Single dose cohorts				Multiple dose cohorts				Placebo (n=21)
		15 mg (n=12)	30 mg (n=6)	60 mg (n=6)	90 mg (n=6)	15 mg (n=8)	30 mg (n=9)	60 mg (n=9)	90 mg (n=9)	
Subjects with any related AE	34/13	2 (16.6)	2 (33.3)	5 (83.3)	5 (83.3)	5 (62.5)	4 (44.4)	3 (33.3)	8 (88.9)	13 (61.9)
Abdominal pain	13/2	0	0	0	0	1 (12.5)	5 (55.6)	2 (22.2)	4 (44.4)	2 (9.5)
Headache	11/6	1 (8.4)	0	1 (16.7)	0	1 (12.5)	1 (11.1)	1 (11.1)	6 (66.7)	6 (28.6)
Diarrhea	7/1	0	0	3 (50)	0	1 (12.5)	1 (11.1)	0	3 (33.3)	1 (4.8)
Nausea	5/1	0	0	0	0	1 (12.5)	0	1 (11.1)	3 (33.3)	1 (4.8)
Feces discolored	3/0	0	0	0	0	0	0	0	3 (33.3)	0

TABLE 3 – Overview of pharmacokinetic parameters per dose for multiple dose cohorts.

Parameter*		Multiple dose cohort 15 mg / day		Multiple dose cohort 30 mg / day		Multiple dose cohort 60 mg / day		Multiple dose cohort 90 mg / day	
		Mean	CV(%) or SD*	Mean	CV(%) or SD*	Mean	CV(%) or SD*	Mean	CV(%) or SD*
Day 1	C <sub>max</sub> (ng/mL)	‡	‡	2.818	113.94	1.853	105.57	5.678	53.11
	T <sub>max</sub> (hr) †	‡	‡	3.286	4.855	3.389	8.162	3.515	8.441
	AUC <sub>(0-24)</sub> (hr × ng/mL)	‡	‡	55.186	110.77	37.79	111.76	109.862	53.44
Day 7	C <sub>max</sub> (ng/mL)	1.219	30.16	1.792	61.37	1.494	47.33	1.724	93.35
	T <sub>max</sub> (hr) †	4.864	8.551	5.007	8.858	3	4.183	6.283	7.567
	AUC <sub>(0-24)</sub> (hr × ng/mL)	20.335	50.33	30.524	146.5	19.32	352.38	14.48	610.6
Day 14	C <sub>max</sub> (ng/mL)	1.399	32.96	1.641	65.94	1.975	74.27	2.27	75.81
	T <sub>max</sub> (hr) †	3.286	4.271	6.579	2.759	6.402	7.351	10.358	8.28
	AUC <sub>(0-24)</sub> (hr × ng/mL)	30.726	31.71	17.993	416.38	35.687	101.09	41.978	102.13
Day 21	C <sub>max</sub> (ng/mL)	1.53	38.26	1.982	39.89	2.348	60.57	3.326	118.99
	T <sub>max</sub> (hr) †	12.126	8.526	10.964	17.505	14.469	15.189	7.619	7.386
	AUC <sub>(0-24)</sub> (hr × ng/mL)	32.317	44.76	41.41	40.69	50.267	62.42	66.017	120.7
T <sub>1/2</sub> (hr)	276.694	35.47	512.941	61.55	355.75	29.89	628.487	17.84	

\* Geometric mean and geometric CV (%) except T<sub>max</sub> for which the median and SD is reported.

‡ Relative to the dose on the study day. † All concentrations were below loq and no PK parameters could be estimated.

FIGURE 1 – Geometric mean blood concentrations of gold after multiple oral administration of CNM-Au8 per dose level.

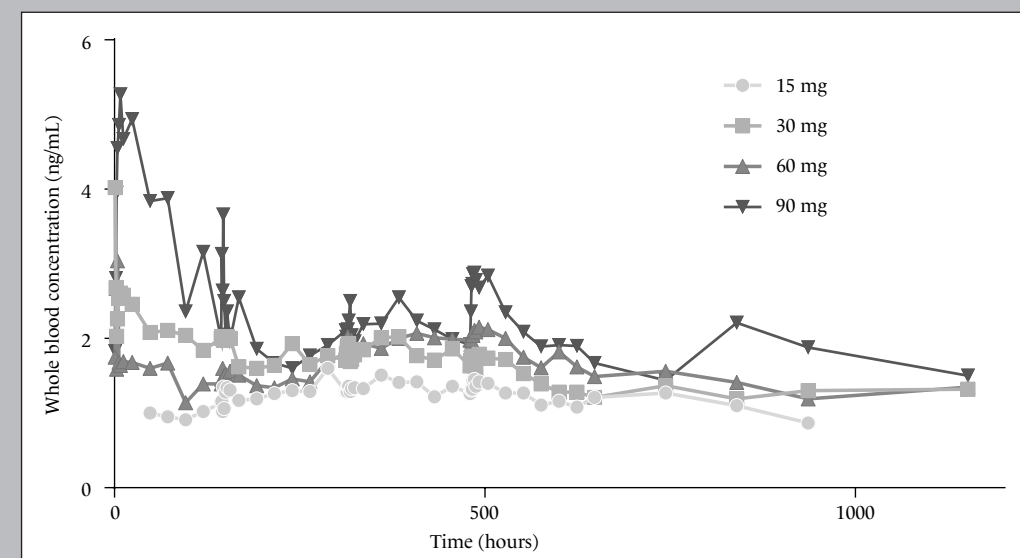
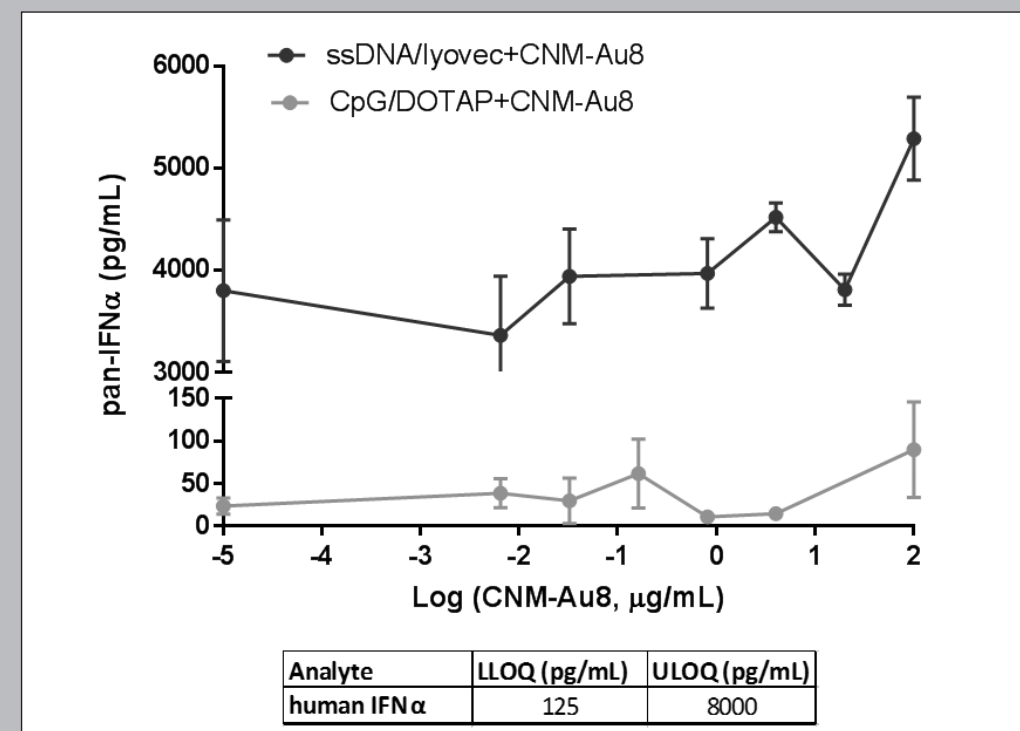


FIGURE 2 – CNM-Au8 concentration versus IFN $\alpha$  release in ssDNA/Iyovec-10  $\mu$ g/mL and CpG/DOTAP- (5  $\mu$ M) stimulated whole blood cultures from 1 healthy donor (6 hr incubation with CNM-Au8, followed by 24 hr incubation with TLR9 trigger).





# QUANTIFYING BETA-GALACTO- SYLCERAMIDE KINETICS IN CSF OF HEALTHY SUBJECTS USING DEUTERIUM LABELING

Published in: *Clinical and Translational Science (CTS)* (2016) 00, 1-7

K.M.S. Kanhai<sup>1</sup>, S.C. Goulooze<sup>1</sup>, J. Stevens<sup>1</sup>, J.L. Hay<sup>1</sup>, G. Dent<sup>2</sup>,  
A. Verma<sup>2</sup>, T. Hankemeier<sup>3</sup>, T. de Boer<sup>4</sup>, H. Meijering<sup>4</sup>, J.C. Chavez<sup>2</sup>,  
A.F. Cohen<sup>1</sup>, G.J. Groeneveld<sup>1</sup>

<sup>1</sup> Centre for Human Drug Research (CHDR), Leiden, the Netherlands

<sup>2</sup> Experimental Medicine, Biogen Cambridge, MA, USA

<sup>3</sup> Netherlands Metabolomics Centre, Leiden, the Netherlands

<sup>4</sup> Analytical Biochemical Laboratory bv, Assen, the Netherlands

## ABSTRACT

Therapeutics promoting myelin synthesis may enhance recovery in demyelinating diseases such as multiple sclerosis (MS). However, no suitable method exists to quantify myelination. The turnover of galactosylceramide (myelin component) is indicative of myelination in mice, but its turnover has not been determined in humans. Here, six healthy subjects consumed 120 mL 70% D<sub>2</sub>O daily for 70 days to label galactosylceramide. We then used mass spectrometry and compartmental modeling to quantify the turnover rate of galactosylceramide in cerebrospinal fluid. Maximum deuterium enrichment of body water ranged from 1.5 to 3.9%, while that of galactosylceramide was much lower: 0.05–0.14%. This suggests a slow turnover rate, which was confirmed by the model-estimated galactosylceramide turnover rate of 0.00168 day<sup>-1</sup>, which corresponds to a half-life of 413 days. Additional studies in patients with MS are needed to investigate whether galactosylceramide turnover could be used as an outcome measure in clinical trials with remyelination therapies.

## INTRODUCTION

Multiple sclerosis is a highly prevalent inflammatory disease that affects the central nervous system, causing progressive disability. Multiple sclerosis is characterized by a loss of myelin combined with incomplete remyelination, leading to a progressive demyelination of nerves in the central nervous system. Current treatments for multiple sclerosis are designed to inhibit the inflammatory component of the disease<sup>1</sup>. However, increasing the remyelination process is another promising strategy, which may improve patient outcome<sup>2</sup>. Enhancing remyelination may also be beneficial for other demyelinating diseases such as neuromyelitis optica, Krabbe disease and metachromatic leucodystrophy.

Because of interest in remyelinating therapies, there is a need for methodologies that quantify remyelination in a clinical setting. Unfortunately, no such methodology currently exists; the use of several imaging techniques has been explored, but no single technique is sufficiently sensitive, specific for myelin and correlated to clinical outcome<sup>3</sup>.

An alternative way to assess myelin kinetics would be to quantify the turnover rate of a relevant myelin component. Different components of myelin have a different turnover rates<sup>4,5</sup>. Although there are no lipids that are absolutely specific for myelin, galactosylceramide (a cerebroside, also known as galactosylcerebroside) is the most typical of myelin<sup>5</sup>. The half-replacement time of galactosylceramide is 94–250 days in adult mice, but has never been determined in humans<sup>4</sup>. In mice, the turnover of galactosylceramide has been reported to be a good measure of myelination, while several other myelin components correlated poorly with myelination<sup>6</sup>. By quantifying the turnover of galactosylceramide in humans, a measure for (altered) myelin kinetics might be obtained.

The ability to monitor demyelination and remyelination is essential to determine possible therapeutic efficacy of interventions that enhance remyelination. The imaging techniques that are currently being used to try to quantify this process are, however, not sufficiently sensitive or specific<sup>3</sup>.

The myelin sheath that surrounds most axons in the central nervous system is a spiral structure that arises from an extension of the plasma membrane of oligodendrocytes. The thickness of the myelin sheath is dynamic and may be modulated<sup>7</sup>. Myelin is composed of 40% water and 60% dry mass. The dry mass is composed of 70% lipids and 30% proteins; this high concentration of lipids facilitates the rapid conduction of action potentials along the nerve fiber. In the adult brain, the various components of myelin have specific turnover rates<sup>5</sup>. The most specific myelin degradation product is  $\beta$ -D-galactosylceramide (24:1) ( $\beta$ -GALC)<sup>5</sup>.

Stable isotope labeling is commonly used to study the *in vivo* kinetics of biomolecules<sup>8–11</sup>. This method relies on the labeling of a precursor and the subsequent quantification of the labeled target molecule over time. The stable isotope can be a direct precursor (e.g., a labeled amino acid for incorporation into proteins) or a more upstream precursor (e.g., deuterated water (D<sub>2</sub>O) or labeled glucose). Animal studies have shown that deuterium levels up to 15% are generally without harmful effects<sup>8,9,12</sup>. In humans, continuous administration of D<sub>2</sub>O administration over several months – resulting in deuterium levels of 1–2% in body water – did not result in adverse effects<sup>13,14</sup>.

After the stable isotope has been administered, mass spectrometry can be used to measure labeling of the target molecule. This technique separates molecules based on differences in mass (due to different isotope compositions), but not chemical structure. The resulting data can then be interpreted using several methods, for example mass isotopomer distribution analysis or compartmental modeling of both the precursor and target molecule<sup>15</sup>.

Here, we used a 70-day deuterium labeling protocol, combined with mass spectrometry and compartmental modeling, to estimate the turnover rate of  $\beta$ -D-galactosylceramide<sup>24,1</sup> ( $\beta$ -GALC) in healthy human subjects.

## MATERIALS AND METHODS

### Pre-study simulation

A pre-study simulation of the expected deuterium enrichment of body water and  $\beta$ -GALC was performed to support the study design. Assuming a daily body water clearance of 2 L and a total body water volume of 50 L, the half-life of deuterium in body water was set to a conservative estimate 17 days<sup>4,16</sup>. Because the turnover rate of  $\beta$ -GALC in humans is unknown, we used the reported half-life for young adult mice of 90 days<sup>4</sup>. After simulations of different study designs, a 70-day labeling period with daily consumption of 120 mL of 70% D<sub>2</sub>O was selected (figure 1). With this dosing regimen, the peak deuterium fraction in the total body water was estimated to reach 0.037 at day 70; after the dosing regimen ended, this fraction returned to baseline by day 200 (i.e., 130 days after the last D<sub>2</sub>O dose). The peak deuterium fraction in  $\beta$ -GALC was expected to reach 0.013 at approximately 30 days after the last D<sub>2</sub>O dose.

### Study design

During the study, the six healthy subjects were instructed to consume 120 mL of 70% D<sub>2</sub>O daily for 70 days. Weekly urine samples were collected and used to measure the percentage of D<sub>2</sub>O in the subject's total body water. The subjects also underwent four lumbar punctures (LPS) for CSF collection. Blood was collected for safety measurements (routine hematology and chemistry). The LPS and venous punctures were performed 35, 70, 94, and 167 days after the start of the study. Because initial results indicated slower kinetics of  $\beta$ -GALC than expected, the study protocol was amended to include an additional long-term LP. This LP was taken at approximately 1.5 (subjects 3-6) or 2.0 (subjects 1 and 2) years after the start of the study.

### Subjects

Healthy male or female subjects between 18 and 70 years old with a body mass index of 18 to 30 kg/m<sup>2</sup> were to be enrolled after having given written informed consent. The subjects underwent a full medical screening, including medical history, a physical examination, blood chemistry, hematology and virology (hepatitis B, C and HIV) urinalysis and electrocardiogram (ECG) to assess eligibility. Key exclusion criteria were: contraindications for

lumbar puncture, clinically significant abnormalities during screening, regular user of any illicit drugs or history of drug abuse or a positive drug screen at screening.

### Study approval

The study was approved by the Medical Ethics Committee of the BEBO Foundation (Assen, The Netherlands). The study was conducted according to the Dutch Act on Medical Research Involving Human Subjects (WMO) and in compliance with Good Clinical Practice (ICH-GCP) and the Declaration of Helsinki.

### Measurement of deuterium enrichment in the total body water

D<sub>2</sub>O content in total body water was calculated using a derivatization reaction with a ketone followed by gas chromatography/mass spectroscopy (GC-MS) analysis. The deuterium fraction in the urine sample was calculated using the ratio of deuterated to non-deuterated forms. Measuring D<sub>2</sub>O in urine established as reliable marker of body water D<sub>2</sub>O, and also used in other studies<sup>8,11,17</sup>. Urine was used because its collection is least invasive for subjects participating.

### Measurement of deuterium enrichment of $\beta$ -GALC

$\beta$ -GALC was extracted from the CSF using a chloroform-methanol mixture. After isolation and subsequent evaporation of the organic layer, an aliquot of the reconstituted sample was injected into a high-performance liquid chromatography system (Shimadzu Nexera LC30; 's Hertogenbosch, the Netherlands) equipped with a Kinetic C18 column (100×3.0 mm, 2.6  $\mu$ m; Phenomenex, Utrecht, the Netherlands) that was kept at ambient temperature. A gradient elution using 5% acetonitrile/95% water (v/v), 1% formic acid/5% acetonitrile/94% water (v/v/v), and acetonitrile as mobile phase was used to separate the  $\beta$ -GALC from matrix components and was delivered at a flow rate of 0.8 mL/min into the electrospray ionization chamber of the mass spectrometer. Quantification was achieved with MS-MS detection in positive ion mode using an AB SCIEX Triple Quad™ 5500 LC-MS/MS (Nieuwerkerk aan den IJssel, the Netherlands) equipped with a Turboion-spray™ interface at 650°C. The ion spray voltage was set at 5500 V. The source parameters: curtain gas Ion source gas 1 and 2, and collision gas were set at 30, 40, 60, and 6 psi, respectively. The compound parameters: the declustering potential (DP), collision energy (CE), entrance potential (EP), and collision cell exit potential (CEP) were 121, 129, 10, 15 V for  $\beta$ -GALC. Detection of the ions was carried out in the multiple-reaction monitoring mode (MRM), by monitoring the transition pairs of 810.6 → 630.6 amu (M0), m/z 811.6 → 631.6 (M1), m/z 812.6 → 632.6 (M2), m/z 813.6 → 633.6 (M3), m/z 814.6 → 634.6 (M4), m/z 815.6 → 635.6 (M5), m/z 816.6 → 636.6 (M6), ... and m/z 819.6 → 639.6 (M9), where Mi is the  $\beta$ -GALC mass isotopomer with i additional neutrons compared to the mass isotopomer without any heavy isotope (M0). Quadrupoles Q1 and Q3 were set on unit resolution. The analysis data obtained were processed by Analyst software™ (version 1.5)<sup>2</sup>.

The isotopomer data of  $\beta$ -GALC was used to calculate the change in average number of additional neutrons (the replacement of a hydrogen atom by a deuterium atom adds one neutron to  $\beta$ -GALC). This was then divided by the total number of hydrogen atoms in  $\beta$ -GALC<sup>78</sup> to yield the change from baseline of the average deuterium fraction of the hydrogen atoms in  $\beta$ -GALC<sup>18</sup>.

### Compartmental model

A compartmental model that describes the turnover of body water (precursor) and  $\beta$ -GALC (product) was fit to the data using the non-linear mixed effects modeling program NONMEM, version 7.3.0<sup>19</sup>. The first-order conditional estimation with interaction method was used to estimate typical parameter values and their inter-individual variability. Inter-individual variability was only included in the model when it significantly ( $p < 0.05$ ) improved the model fit (minus two times the log likelihood reported by NONMEM).

The body water turnover was characterized with two structural parameters: the daily water input/output and the size of the total body water pool. A theoretical estimate of subjects' total body water – based on their sex, height, weight and age – was used as a covariate for daily water input/output<sup>20</sup>. This model described the deuterium enrichment of body water over time.

The production of  $\beta$ -GALC from the (indirect) precursor body water was characterized with two structural parameters: fraction of  $\beta$ -GALC with a fast turnover, and the turnover rate of that fraction. The turnover rate of the remaining fraction of  $\beta$ -GALC (with a slow turnover) was assumed to have a negligible impact on the  $\beta$ -GALC deuterium enrichment in this study, and was therefore not estimated (i.e., assumed to be zero).

## RESULTS

### Clinical study

Six healthy adult subjects were enrolled in the study; their demographics are summarized in table 1. All subjects completed the study, and all of the reported adverse events were mild and transient. Most frequent reported adverse events were headache (14%) and nasopharyngitis (10%). No post-dural puncture headache occurred. All subjects appeared to reach steady state deuterium enrichment in body water during the 70-day labeling period. There was considerable inter-individual variability in the extent of body water enrichment, with maximum values ranging from 0.015 to 0.039. Body water enrichment decreased rapidly after the last D<sub>2</sub>O dose: to an average of 16.3% of maximum levels on day 93. The maximum deuterium enrichment of  $\beta$ -GALC was about 25-fold lower than that of body water and ranged from 0.0005 to 0.0014. The enrichment of  $\beta$ -GALC decreased slowly: at day 167, the  $\beta$ -GALC enrichment was still high (92% of maximum enrichment on average). Even 1.5–2.0 years after the start of the study, a measurable  $\beta$ -GALC enrichment above baseline was still present in all subjects (average 41% of maximum enrichment, see figure 2).

### Compartmental model output

Inter-individual variability was only estimated for daily water input/output; for the other structural parameters it did not result in a significantly improved model fit. The inter-individual differences in deuterium enrichment of  $\beta$ -GALC were attributed exclusively to differences in deuterium enrichment of body water (precursor). The compartmental model was used to fit the data, resulting in an adequate characterization of the deuterium enrichment of both body water and  $\beta$ -GALC (figure 3 and 4).

The final model's parameter estimates and variability are summarized in table 2. All parameters were estimated with good precision (i.e., low standard errors). The typical values for the daily water input/output (3.25 L) and the size of the total body water pool (35.5 L) correspond to a turnover rate constant of 0.092 or a body water half-life of 7.6 days. The estimated  $\beta$ -GALC turnover rate constant (of the fast fraction) is much lower: 0.00168, which corresponds to a half-life of 413 days. This slow  $\beta$ -GALC turnover is consistent with its relatively low, but long-lasting deuterium enrichment.

## DISCUSSION

Here, we report that orally administered deuterated water can be used to label and track the metabolism of  $\beta$ -GALC in human subjects, and these data can be used to estimate the turnover rate for this myelin breakdown product. The low, but long-lasting enrichment shows that  $\beta$ -GALC has a slow turnover. We used compartmental modeling to characterize this turnover, as it allowed us to account for differences in deuterium enrichment of body water between subjects and within subjects over time. With this empirical model, we estimated a half-life of 413 (352–499) days for  $\beta$ -GALC in CSF. Importantly, the turnover of  $\beta$ -GALC has been reported for mice<sup>21</sup>, but this has never been reported in human subjects. An estimated fraction of  $\beta$ -GALC with a fast turnover was included in the model to accurately describe the  $\beta$ -GALC enrichment data. While this factor does not have a direct physiological meaning, one possible interpretation would be that  $\beta$ -GALC in CSF is produced from two metabolic compartments. One compartment would represent myelin with a shorter half-life (413 days, as estimated by the model). The other compartment would turnover even more slowly, to the extent that the amount of deuterium enrichment present in its breakdown products after a 70-day labeling period is negligible. In this interpretation of the empirical model, the estimated fraction of  $\beta$ -GALC with a fast turnover then represents the fraction of  $\beta$ -GALC in the CSF that originates from the compartment with a 'fast' turnover. This combination of fast and slow turnover seems physiologically plausible, as it has been described for various myelin components in animals: cholesterol, galactosylceramide, sulfatide and phospholipids<sup>4,22</sup>.

One of several possible interpretations of these data is that there is a more stable metabolic pool consisting of inner layers of myelin that may be less accessible for metabolic turnover and that some of the newly formed myelin remains in outer layers and stays accessible for whatever mechanisms are involved in catabolism, thus accounting for the rapid turnover of this pool<sup>5</sup>.

The thickness of myelin sheath can be modified by oligodendrocytes, and oligodendrocyte turnover contributes to myelin remodeling. However, we expect the effect of oligodendrocyte turnover to be minimal as myelination has been shown to be considerably more dynamic than oligodendrocyte generation in human white matter<sup>7</sup>. Different myelin dynamics in different parts of the brain are not taken into account in our study as we estimated the average  $\beta$ -GALC turnover.

It is important to realize that the turnover of  $\beta$ -GALC does not necessarily represent the turnover of myelin. Two scenarios are possible: either the myelin turnover is slower than the  $\beta$ -GALC turnover and therefore rate limiting, or the  $\beta$ -GALC turnover is slower than myelin turnover and therefore rate-limiting.  $\beta$ -GALC kinetics would only be a suitable marker of myelin turnover if the myelin turnover is slower and therefore the rate limiting step. If  $\beta$ -GALC kinetics are rate limiting, it would be not suitable as a marker of myelin kinetics. We believe it is far more likely, however, that myelin turnover is rate limiting. First of all, a previous study in mice demonstrated that labeling of  $\beta$ -GALC with  $D_2O$  provided a good proxy marker for myelin turnover.<sup>6</sup> Secondly, most metabolic processes in the human body have a much faster turnover than 413 days<sup>22-24</sup> and it is therefore far more probable that the  $\beta$ -GALC turnover that we measure is this slow because  $\beta$ -GALC is attached to the myelin surrounding nerves, and nerves are known to have an extremely slow turnover<sup>23</sup>. Conversely is unlikely that  $\beta$ -GALC removal from the CSF compartment would be rate limiting and therefore influence the slow turnover of  $\beta$ -GALC that we report here. CSF proteins in general have a residence time in the CSF of hours to days, maybe some of weeks, but not of months to years<sup>6,24-26</sup>. An average adult human produces approximately 500 mL of CSF per day, which, with an average CSF volume of 150 mL, will lead to replacement of all circulating CSF more than three times daily. It would be hard to imagine how any molecule could reside in the CSF for months without being removed. It is therefore far more likely that if we measure deuterated  $\beta$ -GALC in the CSF over a very long period of up to 1.5 years, that there is a continuous source of shedding of  $\beta$ -GALC into the CSF from a reservoir, which we know from the literature to be myelin in the CNS<sup>27</sup>. In conclusion, although the turnover of  $\beta$ -GALC does not necessarily represent the turnover of myelin<sup>6</sup>,  $\beta$ -GALC found in the CSF is most likely produced by the breakdown of myelin in the central nervous system, and  $\beta$ -GALC CSF kinetics therefore likely reflect myelin turnover.

A measurement of the turnover rate of myelin in mice of various ages revealed that the turnover rate ranged from 94 to 250 days<sup>21</sup>. This rate differs considerably from the rate that we observed in healthy human subjects. However, such a difference in the rate of a metabolic process between humans and mice is not unexpected<sup>28-30</sup>. For example, previous studies reported that the overall turnover rate for proteins in mice is nearly ten-fold higher in mice than in humans<sup>23</sup>. The rate of cholic acid synthesis is 9.3-fold higher in mice than in humans, and the rate of cholesterol synthesis is 16-fold higher in mice. These differences are consistent with our observed difference between mice and humans with respect to the apparent turnover rate of myelin. Although it is likely that the turnover of myelin is correlated with age, the relatively low number of subjects in our study precluded the possibility of drawing any meaningful conclusions with respect to the relationship between age and turnover rate.

Here, we used compartmental modeling to accurately describe deuterium enrichment in body water and labeling of  $\beta$ -GALC during and after chronic ingestion of deuterium. Our use of compartmental modeling enabled us to interpret the isotope labeling data in the absence of steady-state labeling of any precursor. This was an important feature of our study, as the deuterium fraction in body water did not reach steady-state levels for a significant part of the study duration. It is also important to note that the model and its estimated parameters are empirical. As body water is not an immediate precursor of  $\beta$ -GALC, the apparent myelin turnover rate constant should not be interpreted as a measure for  $\beta$ -GALC turnover. Instead, it is a single rate constant for the entire biochemical pathway between body water and  $\beta$ -GALC in CSF. As this pathway includes the synthesis and degradation of myelin, the estimated turnover rate constant of  $\beta$ -GALC may, however, be suitable as a biomarker for the kinetics of myelin. Interestingly, the model did not improve upon including inter-individual variability in the myelin kinetics; correcting for the individual differences in body water turnover appeared to explain most of the inter-individual variability seen in the deuterium enrichment of  $\beta$ -GALC as well. This suggests that the variability in myelin kinetics in healthy human subjects is modest, although confirmation of this would require a study with more than six subjects.

The method that we describe here, in which we measured the deuterium enrichment of  $\beta$ -GALC in CSF of healthy human subjects, may be used to test novel therapeutic interventions designed to enhance remyelination. Currently, the demyelination and remyelination process is measured with MRI. A recent review evaluated imaging modalities that may be better suited to measuring myelin content *in vivo*, including magnetization transfer ratio, restricted proton fraction *f* (from quantitative magnetization transfer measurements), myelin water fraction, diffusion tensor imaging, and positron emission tomography (PET) imaging<sup>3</sup>. Unfortunately, no individual modality provides sufficient sensitivity or specificity for myelin, nor can any individual method provide a suitable correlation with clinical features<sup>3</sup>. PET imaging using [<sup>11</sup>C]PIB and [<sup>11</sup>C]MEDAS are promising imaging modalities. However, further studies are needed in order to validate their use, particularly with respect to the study of multiple sclerosis in human patients<sup>3</sup>. We therefore suggest that stable isotope labeling using  $D_2O$  may be a more useful method for measuring demyelination and remyelination. Drugs that can increase remyelination are currently being developed. Therefore, a method for quantifying remyelination is essential in order to determine the efficacy of such drugs. In this respect, we suggest that our method for measuring myelin kinetics may provide superior results compared to the imaging modalities that are currently available.

In a proof-of-concept study with a compound that is expected to enhance remyelination, it may not be necessary to follow-up subjects for the same 1.5–2.0-year period of this study. This is because peak  $\beta$ -GALC enrichment is probably more indicative of myelination than the elimination phase of  $\beta$ -GALC. So, there would be no need to measure long-term elimination of deuterium from  $\beta$ -GALC. This could shorten the study duration to as little as 15 weeks: 10 weeks of deuterium labeling and 5 weeks of wash-out to allow  $\beta$ -GALC to reach peak enrichment. 5 weeks is approximately five times the calculated half-life of  $D_2O$  disappearance from body water. In the absence of ongoing  $D_2O$  labeling,



deuterium-enrichment of the  $\beta$ -GALC cannot further increase when  $D_2O$  has been washed-out from body water.

In this study, we developed a safe methodology to measure the turnover rate of the myelin component  $\beta$ -GALC in humans, which is likely indicative of myelination. Additional studies in patients with MS are needed to validate this method as an outcome measure in clinical trials with remyelination therapies.

The ability to accurately measure the rate of myelin formation and breakdown may be used to measure pharmacological effects of novel drugs designed to increase remyelination, thereby facilitating the development of a more effective treatment for patients with multiple sclerosis or other demyelinating diseases/disorders.

## SUPPLEMENTAL MATERIAL

### Compartmental model equations

The model describing body water enrichment after chronic administration of  $D_2O$  includes a single compartment that represents the deuterium fraction in the body water pool ( $A_1$ ). As the total body water pool is considered to be constant, water input and output are balanced. The rate constant for body water turnover ( $K_{bw}$ ) is based on the daily  $D_2O$  dose (DDD), daily water input/output (DWI), and total body water pool (BW), as shown in Equation 1. If no deuterium dose is given,  $K_{bw}$  simplifies to DWI divided by BW.

$$K_{bw}(\text{day}^{-1}) = \frac{DDD + DWI}{BW} \quad \text{Eq. 1}$$

Because the actual daily water intake of the subjects was not monitored, it was treated as an unknown parameter and estimated with the model. Inter-individual variability was identified for DWI. Total body water (TBW, calculated with Watson formula) was normalized by the mean of the study population (35.6 liters), and implemented as a linear covariate for DWI, as shown in Equation 2.

$$DWI_i = DWI_{TV} \times \frac{TBW}{35.6} \times e^{\eta_i} \quad \text{Eq. 2}$$

Where  $DWI_i$  is the estimated daily water intake of subject  $i$ ,  $DWI_{TV}$  is the typical daily water intake for a subject with total body water of 35.6 liters. The inter-individual variability of daily water intake (after taking TBW into account) is described with  $e^{\eta_i}$ , which represents a log-normal distribution with a median of 1 and a variance that is estimated by the model.

The fraction of the water input that is deuterated ( $D_f$ ) is based on DDD and DWI, as shown in Equation 3.

$$D_f = \frac{DDD}{DWI + DDD} \quad \text{Eq. 3}$$

The system is considered to be well mixed; thus, the deuterium fraction in the water output is equal to the deuterium fraction in the body water pool. Hence, the differential equation describing the change in fraction of  $D_2O$  ( $dA_1$ ) over time ( $dt$ ) is described using Equation 4.

$$\frac{dA_1}{dt} = K_{bw} \times D_f - K_{bw} \times A_1 \quad \text{Eq. 4}$$

The previous equations 1–4 describe the deuterium enrichment in body water ( $A_1$ ) over time. This is then used as input for Equation 5, which describes the deuterium enrichment of the fraction of  $\beta$ -GALC with a faster or non-negligible turnover.

$$\frac{dA_2}{dt} = K_{\beta\text{-galc}} \times A_1 - K_{\beta\text{-galc}} \times A_2 \quad \text{Eq. 5}$$

Where  $dA_2/dt$  is the change in deuterium enrichment over time,  $K_{\beta\text{-galc}}$  is the  $\beta$ -GALC turnover rate constant and  $A_1$  is the enrichment of body water. Considering that the deuterium enrichment of the  $\beta$ -GALC fraction with a slower turnover is negligible in the present study, the average deuterium enrichment of  $\beta$ -GALC can be obtained with Equation 6.

$$\text{Enrichment}_{\beta\text{galc}} = A_2 \times S_{\beta\text{-galc}} \quad \text{Eq. 6}$$

Where  $A_2$  is the deuterium enrichment of the  $\beta$ -GALC with a faster turnover and  $S_{\beta\text{-galc}}$  is the fraction  $\beta$ -GALC with a faster turnover.

- 1 Compston, Ebers, Lassmann. McAlpine's multiple sclerosis. third ed. London: Churchill Livingstone; 1998.
- 2 Hartley, Altowajri, Bourdette. Remyelination and multiple sclerosis: therapeutic approaches and challenges. *Curr Neurol Neurosci Rep* 14[10], 484. 2014.
- 3 Mallik, Samson, Wheeler-Kingshott, Miller. Imaging outcomes for trials of remyelination in multiple sclerosis. *J Neurol Neurosurg Psychiatry* 85, 1396-1404. 2014.
- 4 Ando S, Tanaka Y, Toyoda Y, Kon K. Turnover of myelin lipids in aging brain. *Neurochem Res* 2003 Jan;28(1):5-13.
- 5 Quarles, Macklin, Morell. Myelin Formation, Structure and Biochemistry. *Basic Neurochemistry: Molecular, Cellular and Medical aspects*. 2006. p. 51-71.
- 6 Muse, Jurevics, Toews, Matsushima, Morell. Parameters related to lipid metabolism as markers of myelination in mouse brain. *Journal of Neurochemistry* 76, 77-86. 2001.
- 7 Yeung MSY, Zdunek S, Bergmann O, Bernard S, Salehpour M, Alkass K, et al. Dynamics of Oligodendrocyte Generation and Myelination in the Human Brain. *Cell* 159, 766-774. 6-11-2014.
- 8 Busch, Kim, Neese, Schade-Serin, Collins, Awada, et al. Measurement of protein turnover rates by heavy water labeling of nonessential amino acids. *Biochimica et Biophysica Acta* 1760, 730-744. 1-24-2006.
- 9 Jones PJ, Leatherdale ST. Stable isotopes in clinical research: safety reaffirmed. *Clin Sci (Lond)* 80[4], 277-280. 1991.
- 10 Lindwall, Hsieh, Misell, Chai, Turner, Hellerstein. Heavy Water Labeling of Keratin as a Non-Invasive Biomarker of Skin Turnover In Vivo in Rodents and Humans. *Journal of Investigative Dermatology* 126, 841-848. 2006.
- 11 Strawford, Antelo, Christiansen, Hellerstein. Adipose tissue triglyceride turnover, de novo lipogenesis and cell proliferation in humans measured with  $2H_2O$ . *American Journal of Physiology-Endocrinology and Metabolism* 286, E577-E588. 11-4-2003.
- 12 Klein PD, Klein ER. Stable isotopes: origins and safety. *Journal of Clinical Pharmacology* 26[6], 378-382. 1986.
- 13 Neese, Misell, Turner. Measurement in vivo of proliferation rate of slow turnover cells by  $2H_2O$  labeling of the deoxyribose moiety of DNA. *Proc Natl Acad Sci USA* 99[24], 15345-15350. 11-26-2002.
- 14 Peng, Ho, Taylor. Biologic effects of prolonged exposure to deuterium oxide. A behavioural, metabolic and morphologic study. *Arch Pathol* 94[1], 81-89. 1972.
- 15 Guan, Price, Ghaemmaghami, Prusiner, Burlingame. Compartment Modeling for Mammalian Protein Turnover Studies by Stable Isotope Metabolic Labeling. *Anal.Chem.* 84[9], 4014-4021. 2012.
- 16 Berne L. *Physiology*. 2003.
- 17 van Marken Lichtenbelt WD, Westerterp KR, Wouters L. Deuterium dilution as a method for determining total body water: effect of test protocol and sampling time. *British Journal of Nutrition* 72[4], 491-497. 1994.
- 18 Diraison, Pachiaudi, Beylot. In vivo measurement of plasma cholesterol and fatty acid synthesis with deuterated water: determination of the average number of deuterium atoms incorporated. *Metabolism* 45[7], 817-821. 1996.
- 19 Beal, Sheiner, Boeckmann, Bauer. *NONMEM Users Guides*. Ellicott City, Maryland, USA.: Icon Development Solutions; 2011.
- 20 Watson PE, Watson ID, Batt RD. Total body water volumes for adult males and females estimated from simple anthropometric measurements. *Am J Clin Nutr* 33[1], 27-39. 1980.
- 21 Ando, Tanaka, Toyoda, Kon. Turnover of Myelin Lipids in Aging Brain. *Neurochemical Research* 28[1], 5-13. 6-12-2002.
- 22 Cuzner, Norton. *Biochemistry of Demyelination*. Brain Pathology 6, 231-242. 1996.
- 23 Waterlow. Protein turnover with special reference to man. *Journal of Experimental Physiology* 69, 409-438. 1984.
- 24 Francesco Nicotra. *Organic and Bio-molecular Chemistry*. EOLSS Publications; 2009.
- 25 Zalc B, Monge M, Dupouey P, Hauw JJ, Baumann N. Immunohistochemical localization of galactosyl- and sulfogalactosylceramide in the brain of the 30-day-old mouse. *Brain Res* 211, 341-354. 1981.
- 26 Thuillier, Lubetzki, Goujet-Zalc, Galli, Lhermitte, Zalc. Immunological Determination of Galactosylceramide Level in Blood as a Serum index of active Demyelination. *Journal of Neurochemistry* 51, 380-384. 2-8-1988.
- 27 Haghighi S, Lekman A, Nilsson S, Blomqvist M, Andersen O. Increased CSF sulfatide levels and serum glycosphingolipid antibody levels in healthy siblings of multiple sclerosis patients. *Journal of Neurological Sciences* 326[1-2], 35-39. 3-15-2013.
- 28 Boxenbaum. Interspecies scaling, allometry, physiological time, and the ground plan of pharmacokinetics. *J Pharmacokinetic Biopharm* 10, 201-227. 1982.
- 29 Dietschy, Turley. Control of cholesterol turnover in the mouse. *J Biol Chem* 277[6], 3801-3804. 8-2-2002.
- 30 Hulzebos, Renfum, Bandsma, Verkade, Boer, Boverhof, et al. Measurement of parameters of cholic acid kinetics in plasma using a microscale stable isotope dilution technique: application to rodents and humans. *J.Lipid Res.* 42, 1923-1929. 2001.

TABLE 1 – Subject characteristics

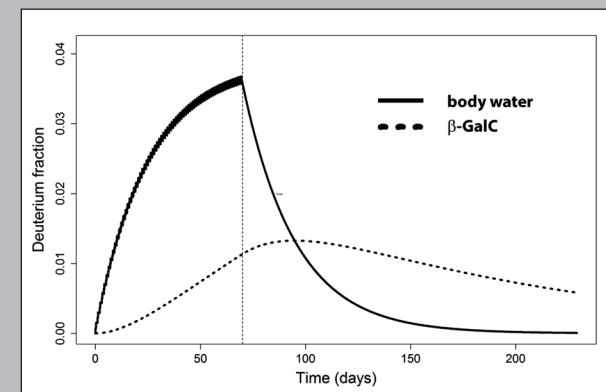
Characteristic	Mean (range) or number (%)
Age (years)	28.2 (19–67)
SEX	
Male	2 (33)
Female	4 (67)
Weight (kg)	67.5 (56.8–87.5)
Height (m)	1.75 (1.64–1.90)
BMI	21.9 (19.3–25.3)

BMI = Body Mass Index

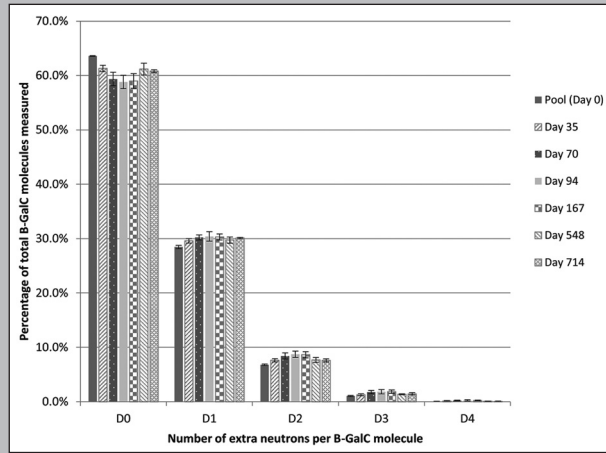
TABLE 2 – Parameter estimates derived from the final model

	Estimate	RSE (%) <sup>a</sup>	IIV <sup>b</sup>
DWI (L·day <sup>-1</sup> )	3.25	6.55	15.5
BW (L)	35.5	3.24	NE
K <sub>β-GALC</sub> (day <sup>-1</sup> )	0.00168	8.81	NE
S <sub>β-GALC</sub>	0.379	9.66	NE
Additive error <sub>body water</sub> <sup>2</sup>	0.00130	20.5	NA
Additive error <sub>β-GALC</sub> <sup>2 c</sup>	0.000116	19.7	NA

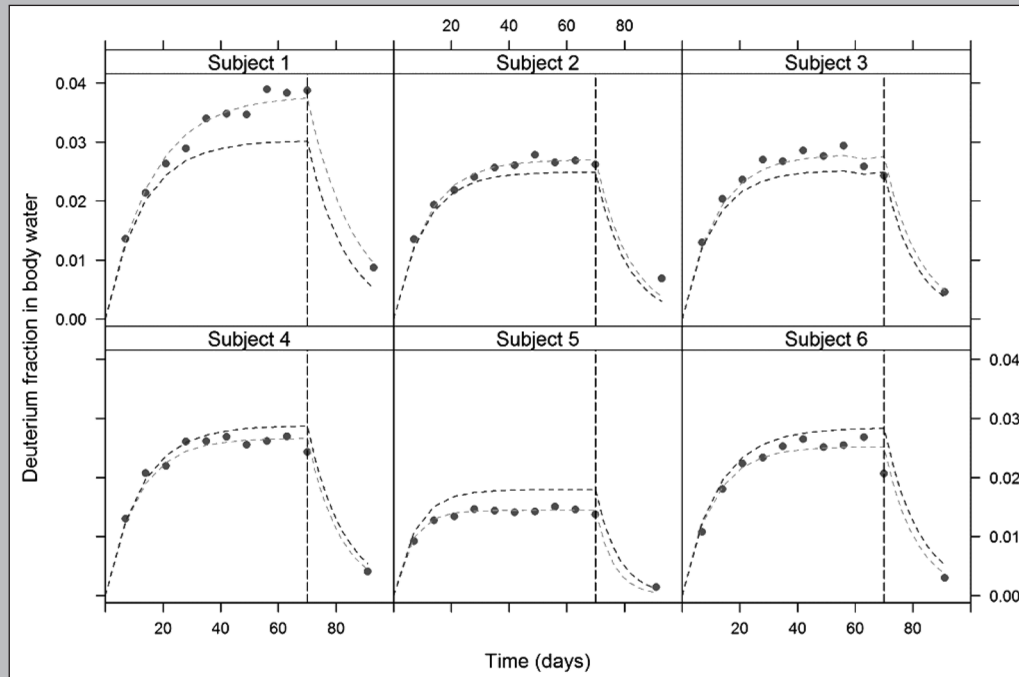
RSE=Relative standard error; NA=not applicable, NE=not estimated; a=Relative standard error, calculated from NONMEM's reported standard error; b=Coefficient of variation (%) of interindividual variability (IIV); c=Residual variability expressed as standard deviation

FIGURE 1 – Pre-study simulation of the deuterium enrichment of total body water and β-GALC after 70 days of consuming a daily dose of 120 mL of 70% D<sub>2</sub>O. The vertical dashed line indicates day 70.

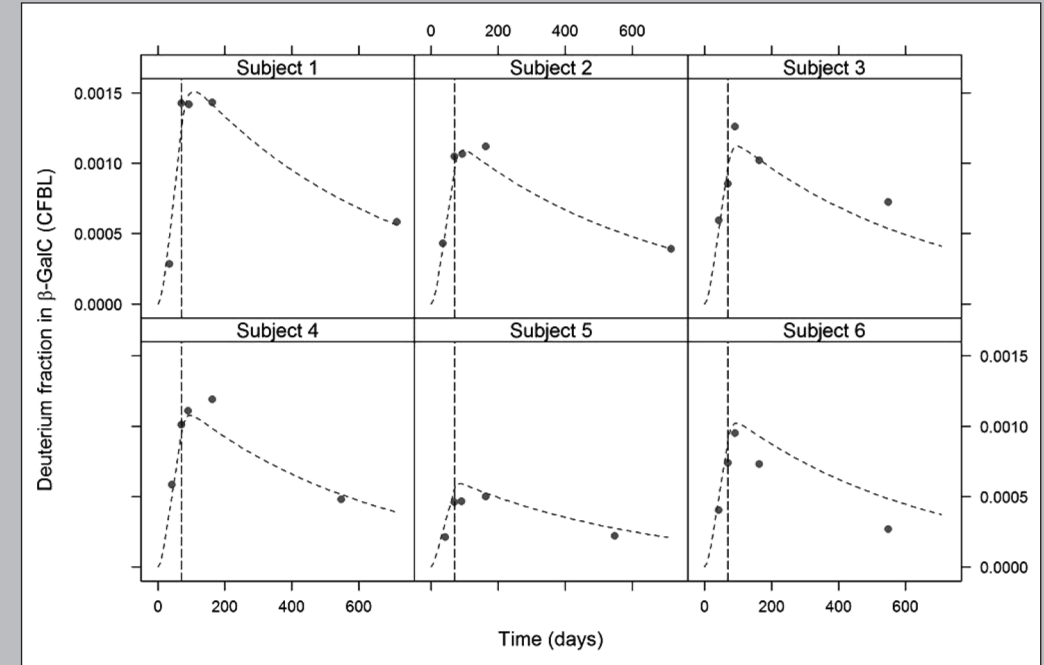
**FIGURE 2** – The isotopomers of  $\beta$ -GALC and how the relative quantity of each isotopomer changes over time during and after 10 weeks of  $D_2O$  labeling. D0 implies that the  $\beta$ -GALC molecule has no extra neutron, while D1, D2, D3, D4 means that the  $\beta$ -GALC molecule has 1, 2, 3 and 4 extra neutrons as determined by mass spectrometry. In the baseline sample (pool, day 0) the D1, D2, D3, and D4 isotopomers are also present, which is due to natural occurrence of stable radioisotopes in food substances (primarily  $C^{13}$ ).



**FIGURE 3** – Individual body water deuterium enrichment profiles and model predictions over time during and following 70 days of oral  $D_2O$  administration. In each panel, the individual observations are represented as dots, the population predictions are represented as a dashed dark grey line, and the individual prediction is represented as a dashed light grey line. The vertical dashed line indicates day 70.



**FIGURE 4** – Individual baseline-corrected  $\beta$ -GALC deuterium enrichment profiles and model predictions during and following 70 days of oral  $D_2O$  administration. In each panel, the observations are represented as dots, and the model prediction is shown as a dashed grey line. The vertical dashed line indicates day 70. Baseline samples were healthy volunteer CSF samples from a biobank.



CFBL = Change from baseline

**KINETICS OF MYELIN  
BREAKDOWN PRODUCTS:  
A LABELING STUDY IN PATIENTS  
WITH PROGRESSIVE MULTIPLE  
SCLEROSIS**

**Submitted to: MS and demyelinating disorders**

**K.M.S. Kanhai<sup>1,5</sup>, S.C. Goulooze<sup>1,2</sup>, J. van der Grond<sup>3</sup>, A. C. Harms<sup>2,4</sup>,  
T. Hankemeier<sup>2,4</sup>, A. Verma<sup>5</sup>, G. Dent<sup>6</sup>, J Chavez<sup>6</sup>, H. Meijering<sup>7</sup>,  
G.J. Groeneveld<sup>1</sup>**

<sup>1</sup> Centre for Human Drug Research (CHDR), Leiden, the Netherlands

<sup>2</sup> Department of Systems Biomedicine and Pharmacology, Leiden Academic Centre for Drug Research, Leiden University, Leiden, the Netherlands

<sup>3</sup> Radiology department Leiden University Medical Center, Leiden, the Netherlands

<sup>4</sup> Netherlands Metabolomics Centre, Leiden, the Netherlands

<sup>5</sup> United Neuroscience, Boston, United States

<sup>6</sup> Biogen, Cambridge, United States

<sup>7</sup> Ardena Bioanalytical Laboratory, Assen, the Netherlands

## ABSTRACT

**BACKGROUND** The majority of the available disease modifying therapies for Multiple Sclerosis (MS) reduce inflammation. These therapies do not yet target remyelination and neuronal degeneration, which is a major contributor to progressive disability in MS. The development of remyelinating therapies will benefit from a method to quantify myelin kinetics in patients with MS. In this study we labeled myelin *in vivo* with deuterium, which allowed us to model the kinetics of the myelin breakdown products  $\beta$ -galactosylceramide ( $\beta$ -GALC) and N-Octadecanoyl-sulfatide (NO-Sulf).

**METHODS** Five patients with MS, and six healthy subjects received 120 mL 70% D<sub>2</sub>O daily for 70 days to label  $\beta$ -GALC and NO-Sulf. Mass spectrometry and compartmental modeling were used to quantify the turnover rate of  $\beta$ -GALC and NO-Sulf in cerebrospinal fluid. The turnover rate of patients was compared to changes in MRI Magnetization Transfer-ratio of both normal appearing white matter and lesions.

**RESULTS** The turnover rate constants of the fractions of  $\beta$ -GALC and NO-Sulf with non-negligible turnover were 0.00186 and 0.00714 in MS patients, which corresponds to a turnover half-life of 373 days and 96.5 days, respectively. The effect of MS on the NO-Sulf (49.4% lower fraction with non-negligible turnover) was more pronounced compared to the effect on  $\beta$ -GALC turnover (18.3% lower fraction with non-negligible turnover).

**CONCLUSIONS** The kinetics of myelin breakdown products in the CSF are different in patients with MS compared with healthy subjects. This can be caused by slower myelin production in these patients, by a higher level of degradation of a more stable component of myelin, or, most likely, by a combination of these two processes.

Deuterium labelling in combination with lumbar punctures is a useful method for quantification of metabolic processes of the central nervous system. This method can be used to quantify myelin turnover in patients with progressive MS and can therefore be used in proof of concept studies with remyelination therapies.

## BACKGROUND

Multiple sclerosis (MS) affects millions of individuals worldwide and is the most common autoimmune disorder of the central nervous system (with estimated 2 million patients)<sup>1</sup>. Despite the fact that the disease has been known for more than 180 years, the exact pathophysiology of the disease is not clear<sup>2,3</sup>. MS is primarily an inflammatory disorder of the brain and spinal cord in which focal lymphocytic infiltration leads to damage of myelin (demyelination) and axons<sup>4</sup>. The majority of the available disease modifying therapies for MS reduce inflammation. However, these therapies do not enhance remyelination or inhibit neuronal degeneration, which is a major contributor to progressive disability in MS<sup>5</sup>.

Development of compounds that stimulate remyelination is seen as an important target for drug development. Examples of such compounds are anti-LINGO antibodies<sup>6</sup>, RHIGM22 antibodies<sup>7</sup>, Olesoxime<sup>8</sup>, and Quetiapine fumarate<sup>9</sup>. The most direct way to demonstrate pharmacological effects of these compounds in future proof-of-concept studies is the quantification of myelin formation or remyelination.

Currently, there are several methods to quantify remyelination in humans such as MRI magnetization transfer imaging (MTI) and diffusion-weighted imaging<sup>10</sup>. Also, non-MRI methods like Positron Emission Tomography using [<sup>11</sup>C]PIB<sup>11</sup>, or Visual Evoked Potential<sup>6</sup> can be used. Although these techniques are improving in accuracy, there is still a need to develop more sensitive and specific methods<sup>12</sup>, especially since the development of remyelinating and neuroprotective therapies is increasing<sup>13</sup>.

We recently demonstrated that myelin components could be labeled in healthy subjects using deuterium, which allowed us to model the kinetics of the myelin breakdown product  $\beta$ -galactosylceramide ( $\beta$ -GALC). This approach offered a method to quantify possible changes in myelin kinetics after treatment with a remyelinating compound<sup>14</sup>. In addition to  $\beta$ -GALC, N-Octadecanoyl-sulfatide (NO-Sulf) was also measured. Both lipids are present abundantly in the brain of vertebrates, comprising almost one-third of the lipid mass of myelin and can be regarded, when present in the CSF, as being specific for CNS myelin<sup>15</sup>. MRI scans were performed to compare our findings with imaging correlates of demyelination<sup>16</sup>.

In the current study we used the same method as in our previous study to measure and model kinetics of myelin breakdown products in patients with progressive multiple sclerosis. The kinetics of myelin formation and breakdown have so far never been measured *in vivo* in patients with MS.

## METHODS

### Subjects

Patients included had a diagnosis of primary progressive or secondary progressive MS according to the revised McDonald criteria<sup>17</sup> for at least 1 year. Patients had to be between 18 and 70 years old and have a body mass index of 18 to 30 kg/m<sup>2</sup> and had all given written informed consent. All subjects underwent a full medical screening, including medical

history, a physical examination, blood chemistry, hematology and virology (hepatitis B, C and HIV) urinalysis and electrocardiogram (ECG) to assess eligibility. Key exclusion criteria were: contraindications for lumbar puncture, contraindication of an MRI, clinically significant abnormalities during screening and a relapse in one month before start of the study.

### Study design

During the study, six patients with progressive multiple sclerosis were instructed to consume 120 mL of 70% D<sub>2</sub>O daily for 70 days. Weekly urine samples were collected and used to measure the percentage of D<sub>2</sub>O in the subject's total body water. All subjects underwent five lumbar punctures (LPS) for CSF collection on days 35, 70, 94, and 167, and a final LP 1-1.5 years after the start of the study. Blood was collected for safety measurements (routine hematology and chemistry). The patients had two MRIs: one between day 0 and 35 (before the first LP) and one on day 167 (fourth LP), to compare changes in imaging biomarkers related to myelination to the deuterium labeling results.

Published and unpublished data from our previous study in healthy subjects<sup>14</sup> were used not only to quantify the kinetics of myelin breakdown in patients, but also to compare them to healthy subjects through simultaneous modelling.

### Study approval

The study was approved by the Medical Ethics Committee of the BEBO Foundation (Assen, The Netherlands). The study was conducted according to the Dutch Act on Medical Research Involving Human Subjects (WMO) and in compliance with Good Clinical Practice (ICH-GCP) and the Declaration of Helsinki.

### Measurement of deuterium enrichment in the total body water

This method has been described previously<sup>14,18,19</sup>. D<sub>2</sub>O content in total body water was measured using a method which relies on the base-catalyzed exchange of hydrogen (deuterium) between water and acetone. <sup>2</sup>H-labeling of <sup>13</sup>C<sub>3</sub> acetone is then determined using gas chromatography/mass spectroscopy (GC-MS) analysis. The deuterium fraction in the urine sample was calculated using the ratio of singly deuterated to non-deuterated forms. Measuring D<sub>2</sub>O in urine has been established as reliable marker of body water D<sub>2</sub>O, and has been used in other studies<sup>20-22</sup>. Urine was used because its collection is least invasive for subjects participating.

### Measurement of deuterium enrichment of lipids in CSF

Isotopomer data of β-GALC and NO-Sulf were obtained using a tandem mass spectrometry method described previously<sup>14</sup>. The isotopomer data was used to calculate the change in average number of additional neutrons (the replacement of a hydrogen atom by a deuterium atom adds one neutron to the molecule). This was then divided by the total number

of measurable hydrogen atoms, which is 78 for β-GALC and 68 for the NO-Sulf. This yields the change from baseline of the average deuterium fraction of the hydrogen atoms of the lipids. N-Octadecanoyl-sulfatide results from the healthy subject cohort were not reported in the previous study but are reported in the current report.

### Compartmental model

A compartmental model that describes the turnover of body water (precursor) and the myelin lipid (product) was fitted to the enrichment data of β-GALC and NO-Sulf using the non-linear mixed effects modeling program NONMEM, version 7.3.0<sup>23</sup>. The first-order conditional estimation with interaction method was used to estimate typical parameter values and their inter-individual variability.

The body water turnover was characterized with two structural parameters: the daily water input/output, and the size of the total body water pool. A theoretical estimate of subjects' total body water—based on their sex, height, weight and age—was used as a covariate for daily water input/output<sup>24</sup>. This model described the deuterium enrichment of body water over time.

A schematic overview of the model is shown in figure 1. The production of the myelin lipids β-GALC and NO-Sulf from the (indirect) precursor body water was characterized with two structural parameters: fraction of the myelin lipid with a fast turnover, and the turnover rate of that fraction. The turnover rate of the remaining fraction of lipid (with a stable turnover) was assumed to have a negligible impact on the deuterium enrichment of the lipid in this study, and was therefore not estimated (i.e., assumed to be zero). The model parameters for β-GALC and NO-Sulf were estimated independent from each other.

With these models, data from both healthy subjects and patients with MS were analyzed in a pooled dataset. A potential effect of MS on the parameters of the lipid turnover model was explored in the model. An estimated effect of MS was included in the final model if it significantly ( $p < 0.05$ ) improved the model fit compared to a model in which the same parameter value was used for healthy subjects and patients. Minus two times the log likelihood was used to assess the model fit.

### MRI

To study changes in tissue integrity in the normal appearing white matter, high resolution structural MRI (3D-T1 and FLAIR) and magnetization transfer imaging (MTI) scans were performed. 3D-T1-w scans were made to segment white matter from CSF and from grey matter. FLAIR images were used to segment white matter lesions from the white matter. The MTI-ratio (MTR) was calculated in the remaining normal appearing white matter and lesions separately<sup>25</sup>. MRI was performed before the first LP, and a second one 167 days after start of the study. All imaging was performed on a whole-body MR system operating at 3 Tesla field strength (Philips Medical Systems, Best, The Netherlands). The following parameters were used: 3DT1-weighted images: TR = 9.7 ms, TE = 4.6 ms, FA = 8°, FOV = 224 × 177 × 168 mm, resulting in a nominal voxel size of 1.17 × 1.17 × 1.4 mm, covering the entire

brain with no gap between slices, acquisition time was approximately 5 minutes. FLAIR: TR = 11000 ms, TE = 125 ms, FA = 90°, FOV = 220 × 176 × 137 mm, matrix size 320 × 240, 25 transverse slices with a slice thickness of 5 mm with no gap between slices. MTI imaging: TR = 100 ms, TE = 11 ms, FA = 9°, FOV = 224 × 180 × 144 mm, matrix size 224 × 169.

## RESULTS

### Clinical study in patients

Six patients with progressive MS were enrolled in the study, four of them completed the study. Both drop-outs were replaced, but only one of the replaced patients completed the study. Only data from patients who completed the study were analyzed. Demographics are summarized in table 1. Missing data in the analysis are the LP 4 for subject 7 (LP failed) and LP 5 for subject 8 (subject did not participate). Most of the reported adverse events were mild and transient. One Serious Adverse Event was reported: subject 8 was admitted to the hospital 4 months after start of the study, with a diagnosis of urinary tract infection that required intravenous antibiotic treatment. This was assessed as unlikely related to the administration of D<sub>2</sub>O. Most frequent reported adverse events were fatigue (60%) and dizziness (60%). Post-dural puncture headache was not reported.

### Body water enrichment

Both patients and the healthy subjects described in the previously published study<sup>14</sup> reached steady state deuterium enrichment in body water during the 70-day labeling period (see table 2 and figure 2). There was considerable inter-individual variability in the extent of body water enrichment, with maximum values ranging from 0.017 to 0.037. Body water enrichment decreased rapidly after the last D<sub>2</sub>O dose, as expected.

### β-GALC enrichment

The maximum deuterium enrichment of β-GALC in patients was about 27-fold lower than that of body water and ranged from 0.00047 to 0.0015. Comparable to what was observed in the healthy subject cohort, the enrichment of β-GALC decreased slowly in the patients with MS: at day 167, the β-GALC enrichment was still high (between 71% and 100% of maximum observed enrichment) and 1.5–2.0 years after the start of the study, a measurable β-GALC enrichment above baseline was still present in all subjects: between 24% and 60% of maximum observed enrichment (figure 3).

### NO-Sulf enrichment

The maximum enrichment of NO-Sulf was about 2-3-fold higher than β-GALC, and 10-fold lower than that of body water. Maximum enrichment ranged from 0.0010 to 0.0018 in healthy subjects, and from 0.0026 to 0.0041 in MS patients (see table 2 and figure 4).

## Compartmental model output

Inter-individual variability in the precursor model (body water) was only estimated for the parameter that represents daily water input/output; for the other structural parameters it did not result in a significantly improved model fit. The kinetics of the deuterium enrichment were then used as input for the models describing the turnover of β-GALC and the NO-Sulf. The parameter estimates of the model are given in table 2. The final model resulted in an adequate characterization of the observed deuterium enrichment data in body water β-GALC and the NO-Sulf (figure 2, figure 3 and figure 4).

The typical values for the daily water input/output (3.39 L) and the size of the total body water pool (38.9 L) correspond to a turnover rate constant of 0.087 or a body water half-life of 8.0 days. The turnover rate constants of the fractions of β-GALC and NO-Sulf with non-negligible turnover were much lower: 0.00186 and 0.00714, which corresponds to a turnover half-life of 373 days and 96.5 days, respectively. The fraction of β-GALC that originates from the fast or non-negligible turnover rate, was estimated at 34.4%. Limited variability between individuals was observed in the value of this parameter, for which a coefficient of variation of 7.4% was estimated with poor precision (relative standard error of estimate of 93%). The fraction of the NO-Sulf with a non-negligible or fast turnover was estimated to a similar value of 36.6%, although a higher degree of unexplained variability between individuals was observed there (CV=24.3%).

We observed a significant difference in the turnover of both myelin lipids between the healthy subjects and the MS patients: for β-GALC 0.817 (95% confidence interval of 0.71 to 0.93, p-value: <0.01) and for NO-Sulf 0.506 (95% confidence interval of 0.35 to 0.66, p-value: <0.005). The effect of MS on the myelin lipid turnover was included in the model as an effect on the parameter that represents the estimated fraction with a non-negligible turnover. This resulted in a slightly better statistical fit of the data, when compared to model where the effect was included on the turnover rate of the fast fraction. The effect of MS on the NO-Sulf (49.4% lower fraction with non-negligible turnover) was more pronounced compared to the effect on β-GALC turnover (18.3% lower fraction with non-negligible turnover). Figure 5 shows model predictions for a typical healthy subject and a typical MS patient for β-GALC and NO-sulf, if they would participate in a study with the same design: 120 mL heavy water (70% D<sub>2</sub>O) daily, for 70 consecutive days. Without the administration of water, no deuterium would be incorporated, and the deuterium fraction would stay zero (same value as baseline).

## MRI

The normalized peak height (norPH) of the normal appearing white matter and of the white matter hyperintensity lesions was calculated for all patients at both time points. The MTI norPH in the normal appearing white matter decreased in 4 patients (with 16.6, 8.3, 9.1 and 10.8%) and increased in one patient (5.5%). For three subjects, the norPH of identified lesions increased in the period between the two scans (+8.7, +16 and +21%), the other two subjects had an decrease in norPH of the lesions (-12 and -14%) (table 3).

## DISCUSSION

This is the first study to measure the kinetics of deuterium-labelled myelin breakdown products beta-galactosylceramide and N-octadecanoyl-sulfatide in the CSF of patients with progressive MS. In a pooled compartmental analysis, we analysed data from these patients together with healthy subject data from a previous study<sup>14</sup>. This analysis showed that the level of deuterium incorporation in myelin breakdown products was lower in MS patients than in healthy subjects, which indicates that myelin formation was slower, or breakdown of a more stable myelin component was higher.

The lower levels of deuterium incorporation that we observed in patients with MS, were then described in a model, which estimated a lower fraction with non-negligible turnover in the MS patients compared to the healthy subjects: 49.9% lower for NO-sulf, and 18.3% lower for  $\beta$ -GALC. There are several possible physiological explanations for these model-based findings. First of all, the model for healthy subjects distinguishes a stable and a fast fraction in the turnover. It would be intuitively attractive to hypothesize that the fast fraction lies more on the outside of the myelin wrapping, and the stable fraction lies more closely to the axon, which is therefore harder to replace<sup>26</sup>. When considering myelin physiology, we expect that the extent of replacement of myelin close to the axon is low in healthy subjects and that the effect of labelling of this stable fraction is therefore very limited. Therefore, this may have only limited effect in the model for turnover in healthy subjects. In patients with progressive MS, this process is altered<sup>27</sup>. As demyelination exposes more of the stable fraction of myelin, we would expect that more of this stable fraction-myelin is broken down, which then contributes to the levels of  $\beta$ -GALC and NO-sulf present in the CSF. This part of myelin will have fewer deuterium-atoms incorporated due to its formation over a longer period of time, starting from before the onset of deuterium labelling, which could explain a lower labelling fraction in the breakdown products.

Secondly, evidence exists that remyelination in MS patients is ineffective<sup>27</sup>. This could slow down the formation of new myelin and thereby decrease the rate of incorporation of deuterium-atoms into myelin molecules. Either of these two pathophysiological processes could explain the lower level of labelling observed in patients with MS.

A third scenario, is that a combination of these processes, namely degradation of stable myelin and ineffective remyelination process, underlies our observations.

Deuterium fraction in body water results showed individual differences, which were comparable to the differences found in the healthy subjects cohort (figure 2). A maximum reported fraction in the MS cohort of 0.037 (table 2) the dosing of 120 mL for 70 days was considered safe<sup>28,29</sup>. From our previous study we know that these fractions should be high enough to label myelin breakdown products<sup>14</sup>. The individual differences in body water turnover seemed to explain most of the interindividual differences seen in the labelling enrichment of  $\beta$ -GALC, as the degree of interindividual variability in the  $\beta$ -GALC kinetics is limited (<10% CV, Table 3).

A limitation of the current study is its small sample size. As this was a proof-of-concept study, we only enrolled 6 healthy subjects and 5 patients completed the study. Exploring the effect of disease duration, and type of MS (primary of secondary progressive MS) would be very interesting but was not feasible due to the small sample size.

The model that describes the kinetics of body water and myelin breakdown products has several limitations. For example, because we had no deuterium enrichment data of intermediate biochemical product, the model directly links body water enrichment with the enrichment of the myelin breakdown products in the CSF with the single turnover rate constant. In this study, we interpreted this turnover rate constant as being representative of the myelin turnover rate, under the assumption that this is most likely the rate-limiting step. Additionally, the data did not allow the estimation of the turnover rate of the stable fraction of myelin, due to a negligible degree of deuterium labelling in this fraction.

In all patients we measured a difference in volume norPH of lesions between start of the study and after 6 months (table 3). The increase in three patients indicates an increase in the demyelinating process over time during the course of the study. However, we did not find a significant correlation between the kinetics of the myelin breakdown products and the change in volume norPH of lesions among the 5 patients ( $p > 0.05$ ).

## CONCLUSIONS

Myelin kinetics of myelin breakdown products in the CSF are significantly different in patients with MS compared to healthy subjects. This can be caused by slower myelin production in these patients, by a higher level of degradation of the stable component of myelin, or, most likely, by a combination of these two processes.

Deuterium labelling in combination with lumbar punctures is a useful method for quantification of metabolic processes of the central nervous system. This method in patients with MS can be used to quantify myelin turnover and can therefore be suitable for the use in proof of concept studies with remyelination compounds in patients with progressive MS.



- 1 Sospedra M, Martin R. Immunology of multiple sclerosis. *Annu Rev Immunol.* 2005;23:683-747.
- 2 Compston A. The 150th anniversary of the first depiction of the lesions of multiple sclerosis. *J Neurol Neurosurg Psychiatry.* 1988;51(10):1249-52.
- 3 Stys PK, Zamponi GW, van Minnen J, Geurts JJ. Will the real multiple sclerosis please stand up? *Nat Rev Neurosci.* 2012;13(7):507-14.
- 4 Compston A, Coles A. Multiple sclerosis. *Lancet (London, England).* 2008;372(9648):1502-17.
- 5 Hartley MD, Altowajiri G, Bourdette D. Remyelination and Multiple Sclerosis: Therapeutic Approaches and Challenges. *Current Neurology and Neuroscience Reports.* 2014;14(10):485.
- 6 Cadavid D, Balcer L, Galetta S, Aktas O, Ziemssen T, Vanopdenbosch L, et al. Safety and efficacy of placebo-controlled, phase 2 trial. *Lancet Neurol.* 2017;16(3):189-99.
- 7 Watzlawik JH, E, Edberg, DD; Marks, DL; Warrington, AE; Wright, BR; et al. Human remyelination promoting antibody inhibits apoptotic signaling and differentiation through Lyn kinase in primary rat oligodendrocytes. *Glia.* 2010;58:1782-93.
- 8 Magalon K, Zimmer C, Cayre M, Khalidi J, Bourbon C, Robles I, et al. Olesoxime accelerates myelination and promotes repair in models of demyelination. *Ann Neurol.* 2012;71(2):213-26.
- 9 Zhornitsky S, Wee Yong V, Koch MW, Mackie A, Potvin S, Patten SB, et al. Quetiapine fumarate for the treatment of multiple sclerosis: focus on myelin repair. *CNS Neurosci Ther.* 2013;19(10):737-44.
- 10 Schwartzbach CJ, Grove RA, Brown R, Tompson D, Then Bergh F, Arnold DL. Lesion remyelinating activity of GSK239512 versus placebo in patients with relapsing-remitting multiple sclerosis: a randomised, single-blind, phase II study. *J Neurol.* 2017;264(2):304-15.
- 11 Stankoff B, Freeman L, Aigrot MS, Chardain A, Dolle F, Williams A, et al. Imaging central nervous system myelin by positron emission tomography in multiple sclerosis using [methyl-(1)(1)C]-2-(4'-methylaminophenyl)-6-hydroxybenzothiazole. *Ann Neurol.* 2011;69(4):673-80.
- 12 Bove RM, Green AJ. Remyelinating Pharmacotherapies in Multiple Sclerosis. *Neurotherapeutics.* 2017;14(4):894-904.
- 13 Kremer D, Küry P, Dutta R. Promoting remyelination in multiple sclerosis: Current drugs and future prospects. *Multiple Sclerosis Journal.* 2015;21(5):541-9.
- 14 Kanhai KMS, Gouloze SC, Stevens J, Hay JL, Dent G, Verma A, et al. Quantifying Beta-Galactosylceramide Kinetics in Cerebrospinal Fluid of Healthy Subjects Using Deuterium Labeling. *Clin Transl Sci.* 2016;9(6):321-7.
- 15 Svennerholm L. Chromatographic separation of human brain gangliosides. *Journal of Neurochemistry.* 1963;10(9):613-23.
- 16 Zheng Y, Lee JC, Rudick R, Fisher E. Long-Term Magnetization Transfer Ratio Evolution in Multiple Sclerosis White Matter Lesions. *J Neuroimaging.* 2018;28(2):191-8.
- 17 Polman CH, Reingold SC, Banwell B, Clanet M, Cohen JA, Filippi M, et al. Diagnostic criteria for multiple sclerosis: 2010 Revisions to the McDonald criteria. *Annals of Neurology.* 2011;69(2):292-302.
- 18 Yang D, Diraison F, Beylot M, Brunengraber DZ, Samols MA, Anderson VE, et al. Assay of low deuterium enrichment of water by isotopic exchange with [U-13C3]acetone and gas chromatography-mass spectrometry. *Analytical biochemistry.* 1998;258(2):315-21.
- 19 Shah V, Herath K, Previs SF, Hubbard BK, Roddy TP. Headspace analyses of acetone: a rapid method for measuring the 2H-labeling of water. *Analytical biochemistry.* 2010;404(2):235-7.
- 20 Busch R, Kim YK, Neese RA, Schade-Serin V, Collins M, Awada M, et al. Measurement of protein turnover rates by heavy water labeling of nonessential amino acids. *Biochim Biophys Acta.* 2006;1760(5):730-44.
- 21 Strawford A, Antelo F, Christiansen M, Hellerstein MK. Adipose tissue triglyceride turnover, de novo lipogenesis, and cell proliferation in humans measured with 2H2O. *Am J Physiol Endocrinol Metab.* 2004;286(4):E577-88.
- 22 van Marken Lichtenbelt WD, Westerterp KR, Wouters L. Deuterium dilution as a method for determining total body water: effect of test protocol and sampling time. *Br J Nutr.* 1994;72(4):491-7.
- 23 Beal SL, Sheiner LB, Boeckmann AJ, Bauer RJ. *NONMEM Users Guides.* Ellicott City, Maryland, USA: Icon Development Solutions; 2011.
- 24 Watson PE, Watson ID, Batt RD. Total body water volumes for adult males and females estimated from simple anthropometric measurements. *Am J Clin Nutr.* 1980;33(1):27-39.
- 25 Sala M, de Roos A, van den Berg A, Altmann-Schneider I, Slagboom PE, Westendorp RG, et al. Microstructural brain tissue damage in metabolic syndrome. *Diabetes Care.* 2014;37(2):493-500.
- 26 Quarles RH, Macklin WB, Morell P. Myelin Formation, Structure and Biochemistry. In: *Neurochemistry ASf, editor. Basic Neurochemistry: Molecular, Cellular and Medical Aspects: Elsevier Inc.; 2006. p. 51-71.*
- 27 Koriem KMM. Multiple sclerosis: New insights and trends. *Asian Pacific Journal of Tropical Biomedicine.* 2016;6(5):429-40.
- 28 Jones PJ, Leatherdale ST. Stable isotopes in clinical research: safety reaffirmed. *Clin Sci (Lond).* 1991;80(4):277-80.
- 29 Klein PD, Klein ER. Stable isotopes: origins and safety. *J Clin Pharmacol.* 1986;26(6):378-82.
- 30 Thompson AJ, Baranzini SE, Geurts J, Hemmer B, Ciccarelli O. Multiple sclerosis. *Lancet (London, England).* 2018;391(10130):1622-36.

TABLE 1 – Subject characteristics (n=5)

Characteristic	Mean (range) or number (%)
Age (years)	54.6 (41–65)
Sex	
Male/female	4 (80) / 1 (20)
Weight (kg)	69.1 (55.3–79.6)
Height (m)	1.77 (1.65–1.84)
BMI	22.1 (18.3–24.1)
Years of MS	17.8 (10-32)

TABLE 2 – Parameters estimates of the precursor-product model describing deuterium enrichment data in body water,  $\beta$ -GALC and NO-sulf

Parameters	Parameter estimates (RSE%)	
<b>Body water (precursor) parameters</b>		
Water intake (L/day) <sup>1</sup>	3.39 (8.7%)	
Body water pool (L)	38.7 (4.9%)	
Interindividual variability of water intake (CV%)	28.8 (45%)	
Additive residual error	0.00163 (39%)	
<b>Myelin lipid (product) parameters</b>		
	<b><math>\beta</math>-GALC</b>	<b>NO-Sulf</b>
Fraction with non-negligible turnover in healthy subjects*	0.344 (12%)	0.366 (15%)
Relative fraction with non-negligible turnover in MS patients (compared to healthy subjects) *	0.817 (6.8%)	0.506 (16%)
Turnover rate of non-negligible fraction (day <sup>-1</sup> )	0.00186 (11%)	0.00714 (9.6)
Inter-individual variability of fraction with fast turnover (CV%)	7.4 (93.1%)	24.3 (32%)
Additive residual error	0.00011 (26%)	0.00044 (44%)

CV = coefficient of variation, RSE = relative standard error, HV = Healthy subjects

<sup>1</sup> = For an individual with a total body water of 35.6L predicted with the Watson Formula (24). For all parameters, a single parameter value is estimated for both healthy subjects and MS patients, except the fractions with non-negligible turnover (\*)

**FIGURE 1** – Schematic overview of the compartmental model describing the kinetics of the myelin breakdown product  $\beta$ -GALC and NO-sulf. The deuterium enrichment of the myelin breakdown products in CSF that originate from the stable fraction is assumed to be negligible.  $K_{fast, \beta-galc}$  = turnover rate of the fast fraction of  $\beta$ -GALC,  $F_{fast, \beta-galc}$  = fraction of  $\beta$ -GALC in CSF that originates from the fraction with fast turnover,  $K_{fast, NO-Sulf}$  = turnover rate of the fast fraction of NO-Sulf,  $F_{fast, NO-Sulf}$  = fraction of NO-sulf in CSF that originates from the fraction with fast turnover.

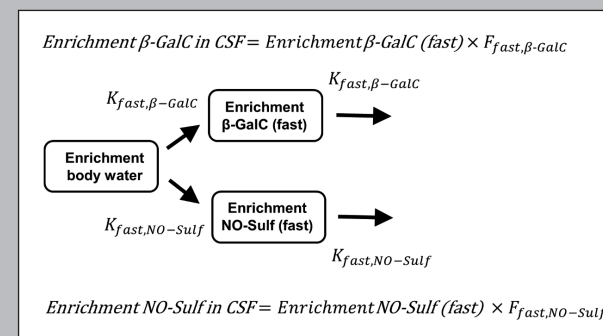


**FIGURE 2 – Deuterium fraction in body water:** Observation (dots), population prediction (dark grey dashed line), individual prediction (light grey dashed line). The vertical line at 70 days marks the end of the labeling period. Data from the previously published study in healthy subjects was adapted from the original publication (14) with permission.

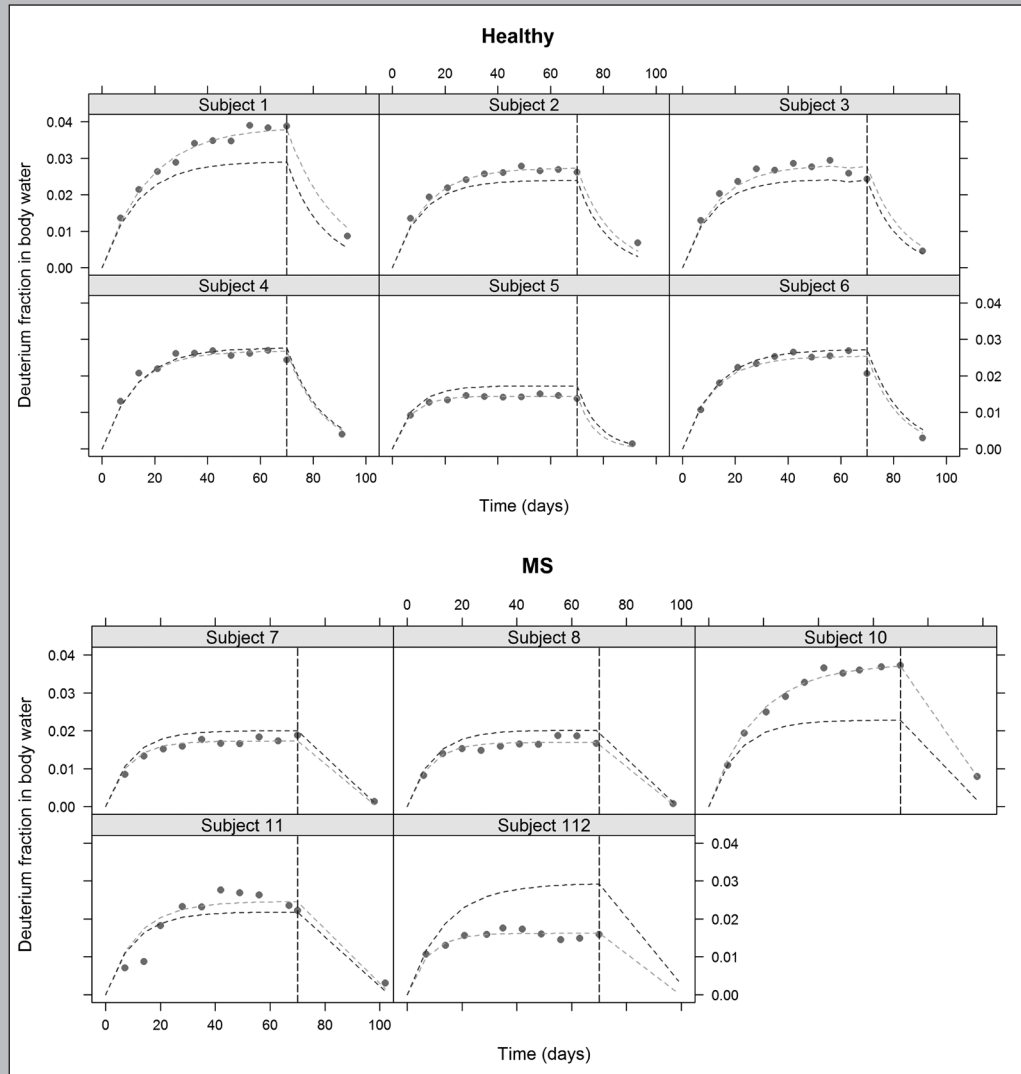


**FIGURE 3 – Deuterium fraction in  $\beta$ -GALC:** Observation (dots), population prediction (dark grey dashed line), individual prediction (light grey dashed line). The vertical line at 70 days marks the end of the labeling period. Data from the previously published study in healthy subjects was adapted from the original publication (14) with permission.

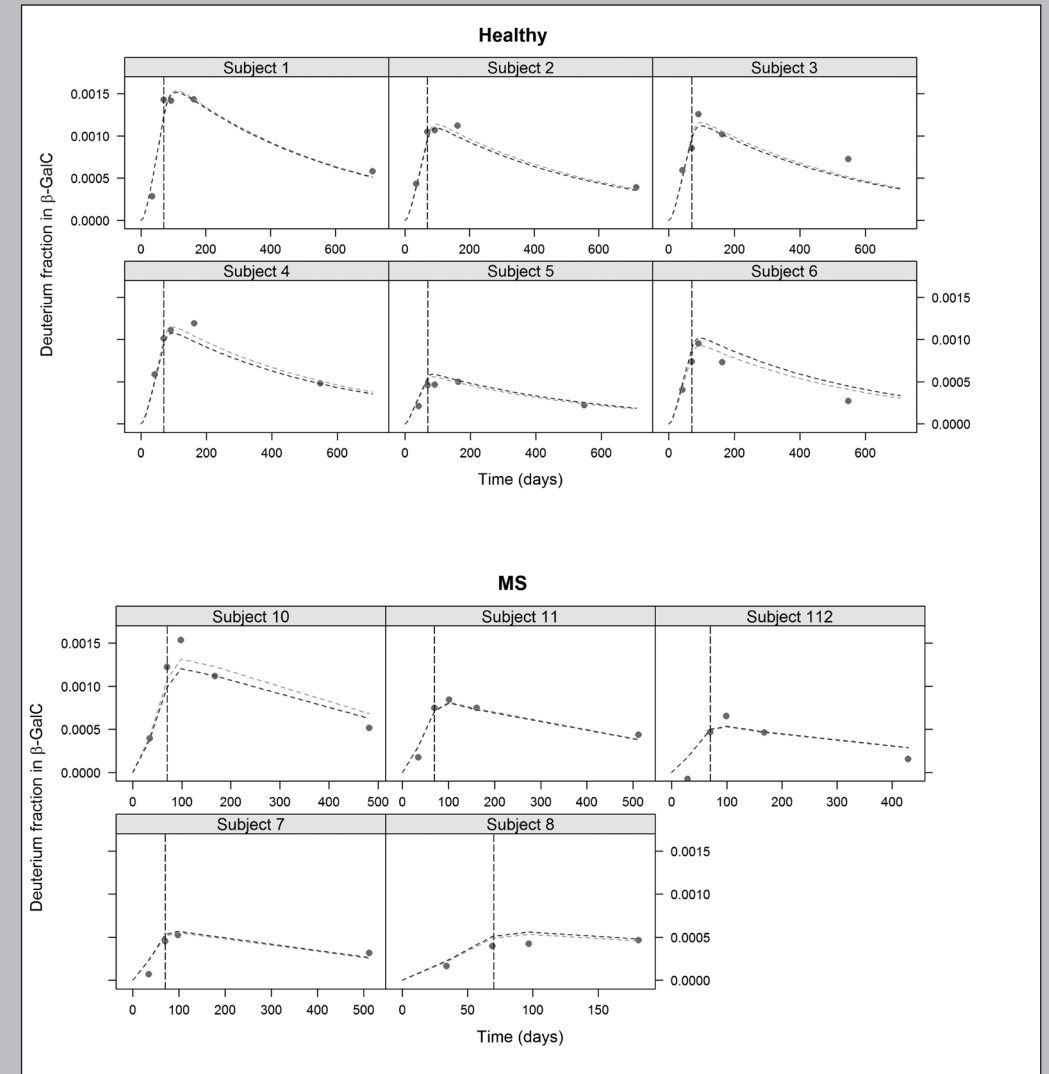


**FIGURE 4 – Deuterium fraction in NO-Sulf:** Observation (dots), population prediction (dark grey line), individual prediction (light grey line). The vertical line at 70 days marks the end of the labeling period.

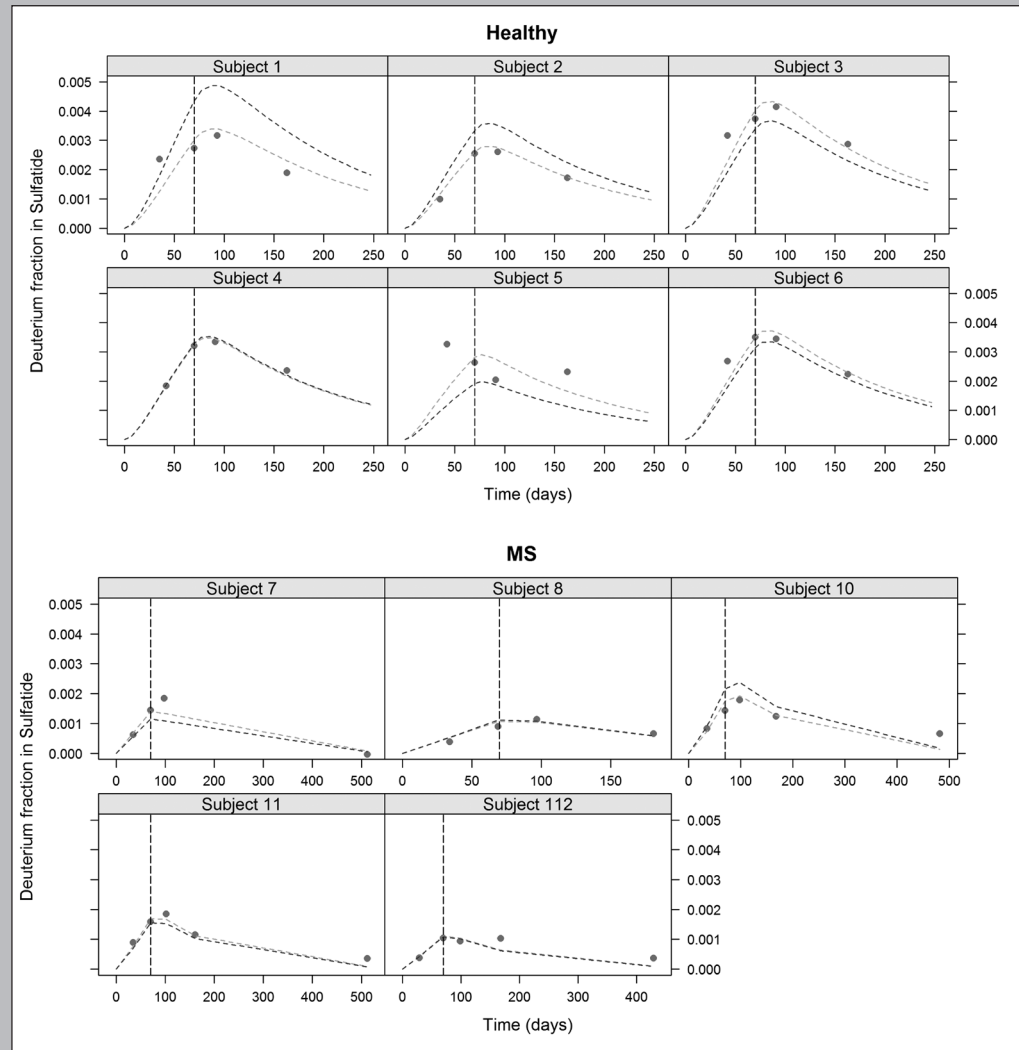
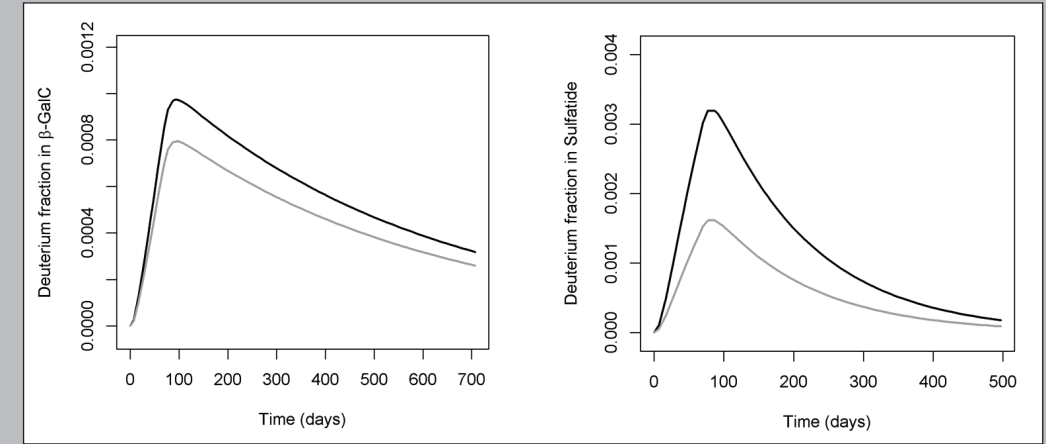


**FIGURE 5 – Model predictions for a typical healthy subject and a typical MS patient of deuterium fraction in  $\beta$ -GALC (left) and NO-sulf (right).** The simulation is based on the design described in this study: subject receive 120 mL heavy water 70%  $D_2O$  daily, for 70 consecutive days. It shows visually what the effect is of the parameter that estimates the difference between MS patients (grey) and healthy subjects (black) with respect to the fraction of non-negligible turnover.



**TREATMENT OF INTERNUCLEAR  
OPHTHALMOPARESIS IN  
MULTIPLE SCLEROSIS WITH  
FAMPRIDINE: A RANDOMIZED  
DOUBLE BLIND, PLACEBO-  
CONTROLLED CROSSOVER TRIAL**

Published in: *CNS Neuroscience & Therapeutics*, 2019 Jun;25(6):697-703

Kawita MS Kanhai,<sup>1</sup> Jenny A Nij Bijvank<sup>2,4</sup>, Yorick L Wagenaar<sup>1</sup>,  
Erica S Klaassen<sup>1</sup>, KyoungSoo Lim<sup>1,6</sup>, Sandrin C Bergheanu<sup>1</sup>,  
Axel Petzold<sup>2,4,9</sup>, Ajay Verma<sup>3</sup>, Jacob Hesterman<sup>7</sup>, Mike P Wattjes<sup>8</sup>,  
Bernard MJ Uitdehaag<sup>4</sup>, Laurentius J van Rijn<sup>2,4</sup>, Geert Jan Groeneveld<sup>1,4</sup>

<sup>1</sup> Centre for Human Drug Research (CHDR), Leiden, the Netherlands

<sup>2</sup> Department of Ophthalmology, Neuro-ophthalmology Expertise Center, Amsterdam UMC, Amsterdam, the Netherlands

<sup>3</sup> Experimental Medicine, Biogen, Cambridge, ma, usa

<sup>4</sup> Department of Neurology, MS Center and Neuro-ophthalmology Expertise Center, Amsterdam UMC, Amsterdam, the Netherlands

<sup>5</sup> Department of Ophthalmology, Onze Lieve Vrouwe Gasthuis, Amsterdam, the Netherlands

<sup>6</sup> KCRN Research, Germantown, MD, USA

<sup>7</sup> INVICRO, Boston, MA, USA

<sup>8</sup> Department of Radiology and Nuclear Medicine, Amsterdam University Medical Center, Amsterdam, the Netherlands

<sup>9</sup> The National Hospital for Neurology and Neurosurgery, Queen Square and Moorfields Eye Hospital, London, UK

## ABSTRACT

**AIM** Examine if the velocity of saccadic eye movements in internuclear ophthalmoparesis (INO) improves with fampridine treatment in patients with multiple sclerosis (MS).

**METHODS** Randomized, double-blind, placebo-controlled, cross-over trial with fampridine in patients with MS and INO. Horizontal saccades were recorded at baseline and at multiple time points post-dose. Main outcome measures were the change of peak velocity versional dysconjugacy index (PV-VDI) and first-pass amplitude VDI (FPA-VDI). Both parameters were compared between fampridine and placebo using a mixed model analysis of variance taking patients as their own control. Pharmacokinetics were determined by serial blood sampling.

**RESULTS** Thirteen patients had a bilateral and 10 a unilateral INO. One patient had an INO of abduction (posterior INO of Lutz) and was excluded. Fampridine significantly reduced both PV-VDI (-17.4%, 95% CI: -22.4%, -12.1%;  $p < 0.0001$ ) and FPA-VDI (-12.5%, 95% CI: -18.9%, -5.5%;  $p < 0.01$ ). Pharmacokinetics demonstrated that testing coincided with the average  $t_{max}$  at 2.08 hours (SD 45 minutes). The main adverse event reported after administration of fampridine was dizziness (61%).

**CONCLUSION** Fampridine improves saccadic eye movements due to INO in MS. Treatment response to fampridine may gauge patient selection for inclusion to remyelination strategies in MS using saccadic eye movements as primary outcome measure.

## INTRODUCTION

Successful remyelination remains the Holy Grail for treatment of multiple sclerosis (MS), a predominantly demyelinating disease. In a proof-of-principle study it has been shown that Clemastine fumarate has the potential to induce remyelination of the optic nerve<sup>1</sup>. Following treatment with clemastine, conduction velocities in patients with long standing optic neuritis improved compared to placebo. Optic neuritis has been the dominant model for testing remyelination strategies in MS<sup>2</sup>. In optic neuritis there is consistent evidence for substantial and irreversible axonal loss<sup>3</sup>. This had been recognized to limit the chance for successful remyelination and severe retinal nerve fiber loss ( $> 70 \mu\text{m}$ ) was an exclusion criterion in the REBUILD trial<sup>1</sup>. Other limitations of optic neuritis for testing remyelination encompass that recovery of high contrast visual acuities is typically excellent even without treatment, the need for combined assessment of electroretinogram (ERG) and visual evoked potential (VEP) in order to be compliant with international standards, which not all patients tolerate<sup>4</sup>. Finally, results from an optic neuritis treatment trial may require to be cross-validated by another model for remyelination in MS which has different, validated outcome measures.

Demyelination in MS does affect a functionally relevant single axon pathway, the medial longitudinal fasciculus (MLF)<sup>5</sup>. A MS lesion in the MLF causes an internuclear ophthalmoparesis which can be aggravated through Uhthoff's phenomenon indicating functioning axons with alterable conduction velocities<sup>6,7</sup>. Rapid (saccadic) horizontal adducting eye movements are impaired in an INO and patients report transient diplopia, visual confusion, the illusion of environmental movements during a saccade, vertigo, and a transient blur for example whilst reading<sup>8,9</sup>. The prevalence of clinically evident INO in MS ranges from 24-55% and are bilateral in most cases<sup>8,10-13</sup>. Anatomically the MLF is located close to the floor of the fourth ventricle and readily discernible on MRI. The MLF represents an efferent pathway which signals from the sixth nucleus to the third nucleus in order to enable coordinated horizontal eye movements<sup>9</sup>. These saccadic eye movements can be easily quantified by infrared oculography (eyetracking). We have developed and validated a novel protocol for assessment of horizontal saccadic eye movements suitable for a multi-centre setting with excellent parameter reproducibility<sup>14</sup>. For the most commonly used parameters for testing an INO the intra-class correlation coefficients (ICC) were  $> 0.9$  for the peak velocity versional dysconjugacy index (PV-VDI) and the first-pass amplitude VDI (FPA-VDI)<sup>14</sup>.

In this study we tested if a drug known to accelerate nerve conduction, fampridine (dal-fampridine), has an effect on saccadic eye movements in patients with MS who suffer from an INO. Previously fampridine, a voltage-gated potassium channel blocker was shown to improve walking speed in patients with MS<sup>15</sup>. A year later, fampridine was approved by the FDA for treating impaired walking in MS patients. Since, there is anecdotal evidence from in three cases that oral Fampridine (10 mg) improved horizontal saccades in INO<sup>16</sup>. This double-blind, placebo-controlled crossover study demonstrates that fampridine significantly improved our two carefully validated<sup>14</sup> primary outcome measures, the PV-VDI and FPA-VDI.

## METHODS

This single-center, double-blind, randomized placebo-controlled crossover study was conducted by the Centre for Human Drug Research (Leiden, the Netherlands) between April 2015 through August 2016. This study was approved by the Medical Ethics Committee of the BEBO Foundation (Assen, the Netherlands) and was conducted in accordance with the Dutch Act on Medical Research Involving Human Subjects (WMO) and in compliance with Good Clinical Practices (ICH-GCP) and the Declaration of Helsinki. This study was registered in the European Union Clinical Trials Register (protocol number 2015-000182-31) and in the Dutch Clinical Trial Registry ([www.toetsingonline.nl](http://www.toetsingonline.nl); dossier number NL52195.056.15). All patients were recruited and assessed at the Amsterdam UMC (Amsterdam, the Netherlands). All patients had to provide written consent prior to being considered for inclusion.

Patients were approached by their neurologists, through existing research projects and advertisements on the hospital website. Of 28 eligible patients two decided not to participate for personal reasons.

Twenty-four patients with MS who had a clinically evident or suspected INO participated in an initial screening visit and two further trial occasions. Each subject was randomly assigned to receive either fampridine (20 mg) on occasion 1 and placebo on occasion 2, or placebo on occasion 1 and fampridine on occasion 2. The interval between the occasions was at least 1 week, which is more than 5 half-lives of fampridine, thereby guaranteeing an adequate washout.

All patients had a diagnosis of clinical definite MS based on the 2010 revision of the McDonald criteria<sup>17</sup>. The disease duration had to be longer than one year and the time from last relapse at least 30 days. All patients were screened using a pro-saccadic task. The presence of INO (unilateral or bilateral) was determined by visual examination of the graphs depicting horizontal gaze position by two experienced observers (JANB, KMSK). The inter-rater agreement was 95.8% (23/24). The one patient in whom there was a disagreement had an INO of abduction and was excluded from this trial. This case has been published separately<sup>18</sup>. All patients were otherwise healthy, including normal ECG, hematology, and blood chemistry; all patients were also seronegative for HIV, hepatitis B, and hepatitis C, had no history of seizures, normal creatinine clearance, no contraindications for MRI, and no concomitant use either an inhibitor or substrate of organic cation transporter 2<sup>19</sup>.

The randomization was created by an independent statistician at the Centre for Human Drug Research using SAS version 9.4. Only independent staff members at the trial pharmacy of the Amsterdam University Medical Center were unblinded; all patients, investigators, and study coordinators were blinded with respect to treatment assignment.

The study medication was fampridine (Biogen). The most commonly prescribed daily dose of fampridine is 20 mg. To ensure optimal plasma levels through the day and reduce the risk of adverse events, fampridine is usually taken in two daily doses of 10 mg each. Because we were interested in studying the acute effects of a single dose of fampridine on INO, we administered a single 20 mg dose of fampridine in order to increase the likelihood of demonstrating a pharmacodynamic effect by achieving pharmacologically active yet

safe plasma concentrations. Based on published literature, the risk of adverse events following a single 20 mg dose of fampridine is acceptable<sup>20</sup>. Subjects were instructed not to eat within one hour before dosing and one hour after dosing.

Supplementary Table S1 summarizes the schedule and timing of all assessments. The safety evaluation included the recording of all adverse events and measurements of blood pressure and heart rate.

The pharmacokinetics of fampridine were assessed on serial blood plasma samples. Blood was collected prior to dosing and 1.5, 2, 2.5, 3, 3.75, 4.25, and 5.25 hours after dosing. Blood was drawn into 4-ml EDTA tubes and centrifuged at 2000xg for 10 min at 2-8°C; the plasma fractions were then transferred to 2-ml tubes and were stored at -20°C within 30 minutes of sampling. Plasma fampridine concentration was measured using ultra performance liquid chromatography tandem mass spectrometry (UPLC-MS/MS). Descriptive pharmacokinetics included the average time to reach maximum concentration ( $t_{max}$ ), the average maximum concentration ( $C_{max}$ ), and the average area under the curve from dosing until the final measurement ( $AUC_{K-last}$ ).

Eye movements were recorded by video-oculography using the EyeLink 1000 Plus eye-tracking system (SR Research, Ottawa, Canada). The set-up of the full protocol, including also fixation stability, anti-saccades and double step saccades in addition to a range of pro-saccadic tasks, has been described in detail<sup>14</sup>. For this study an abbreviated version was used. In brief, for testing the head was stabilized by a chin and forehead rest. The system uses the pupil and corneal reflection to determine the eye position at different eccentricities at 1000 Hz sampling frequency. A calibration procedure was performed prior to each assessment. The pro-saccade task consisted of 10 trials of 8 horizontal pro-saccades. Centrifugal saccades were analyzed from the center of the screen to an eccentric location either 6.25 or 12.5 degrees of visual angle to the left or right. The task lasted approximately 15 minutes and was performed prior to dosing and 1.5, 2.5, 3.75, and 5.5 hours after dosing.

The data were analyzed off-line using custom-made software written in MATLAB (MathWorks, Natick, MA). For each correct centrifugal saccade, peak velocity (PV) and the first-pass amplitude (FPA) were determined. The FPA was defined as the amplitude of the eye at the time point at which the abducting eye first reached the target position<sup>21,22</sup>. The versional dysconjugacy index (VDI) was then calculated for both PV and FPA by dividing the abducting eye's value by the adducting eye's value<sup>14,23</sup> (see Supplementary S5, S6 and S7 for additional explanation). The unity of the VDI is normal.

Brain imaging was performed by magnetic resonance imaging (MRI). We used a 3 Tesla machine (Discovery MR750 3.0T whole-body MR system, GE Healthcare). A multi-sequence MRI protocol was performed, including axial T1-weighted spin echo, axial proton density (PD), T2-weighted fast spin echo, 3D fluid-attenuated inversion recovery (FLAIR), coronal T2 short tau inversion recovery (STIR), 3D T1-weighted fast spoiled gradient echo (FSPGR), and axial diffusion tensor imaging (DTI) sequences. Data analysis included image pre-processing and segmentation steps to generate MLF and MS lesion masks, which comprised six unique regions of interest, including the entire left/right MLF, the lesioned left/right MLF, and the non-lesioned left/right MLF. Volume, length, and DTI-based scalars (median/axial/radial diffusivity and fractional anisotropy) were estimated for each of the

six regions of interest. The MLF lesion load was determined. The scans were reviewed by two researchers. An example MRI image is shown in Supplementary Figure S8.

All statistical analyses were performed in SAS version 9.4 (SAS Institute Inc., Cary, NC, USA). To determine whether significant treatment effects could be detected using the saccadic protocol, the PV-VDI and FPA-VDI were analyzed using a mixed model analysis of covariance (ANCOVA). Treatment, time, period, and treatment by time were used as fixed factors; subject, subject by treatment, and subject by time were used as random factors, and the average baseline measurement (pre-fampridine) per period was used as a covariate. Due to their log-normal distribution, the PV-VDI and FPA-VDI parameters were log-transformed prior to analysis. Any change relative to baseline value was analyzed using the same model for graphical purposes. We used the Spearman rank correlation test to measure the correlation between baseline characteristics and treatment conditions. For the eye-tracking tests, individual INOs were treated as individual subjects in both the ANCOVA and Spearman rank correlation test. The null hypothesis was rejected if  $p < 0.05$ . The alternative hypothesis was 2-sided.

## RESULTS

A total of 24 subjects participated and completed the study between April 2015 and August 2016 (see figure 1 for the CONSORT diagram). One patient was diagnosed with a rare posterior INO of Lutz and excluded from further analysis. We included 11 male and 12 female patients (table 1). The INO was bilateral in 13 and unilateral in ten.

The most commonly reported adverse event (AE) was dizziness 60.8% (14/23). This was followed by fatigue (3 fampridine, 5 placebo) and headache (2 fampridine, 2 placebo). Fampridine had no effect on blood pressure or heart rate. All reported AEs are listed in Supplementary table S9.

Descriptive pharmacokinetics revealed a mean ( $\pm$ SD)  $t_{\max}$  of 128 ( $\pm$  45) minutes, a mean  $C_{\max}$  of 65 ( $\pm$  15) ng/ml, and a mean  $AUC_{0-\text{last}}$  of 220 ( $\pm$  57) ng\*hr/ml. The plasma fampridine concentration over time is shown in figure 2.

Fampridine improved saccadic eye movements of the INO eyes in all 23 patients (figure 3a). This change was observed from the first measurement after dosing (1.5 hours after dosing) until the last measurement (5.5 hours after dosing). The effect of fampridine on the PV-VDI was significant if compared to placebo. The difference from baseline calculated to -17.4% (95% CI: -22.4%, -12.1%;  $p < 0.0001$ , table 2). Similar results were obtained for FPA-VDI (figure 3b), with an estimated difference of -12.1% (95% CI: -17.6%, -6.2%;  $p < 0.001$ , table 2).

There was no significant effect of fampridine on non-INO eyes ( $n=10$ ). The difference from baseline calculated to -4.6% (95% CI: -10.3%, 1.5%;  $p=0.105$ , table 2 and figure 3c).

The magnitude of improvement of saccadic eye movements in INO was directly correlated to the PV-VDI and FPA-VDI at baseline ( $Rho=0.35$ ,  $p=0.0345$ ; Supplementary figure S2). There was no such correlation with disease duration ( $Rho=0.02$ ,  $p=0.909$ ; Supplementary figure S3) or the MRI lesion load of the MLF ( $Rho=0.08$ ,  $p=0.658$ ; Supplementary figure S4).

## CONCLUSION

To our knowledge, this clinical trial together with prior pharmacological, pathological and clinical studies<sup>7-9,16,23,24</sup> provides evidence that fampridine significantly improves the PV-VDI and FPA-VDI with a single dose of 20 mg within 1.5 hours. The response is sustained for at least 5 hours which parallels the robust pharmacodynamic data over this period. The most common AE was dizziness in 60.8% of all patients.

The effect of fampridine appears to be selective for the demyelinated axons of the MLF, corroborated by MRI data, of INO eyes and absent in non-INO eyes. There appears also to exist a linear relationship between the degree of impairment of saccadic eye movements and the degree of improvement with treatment. These findings were independent to other covariates such as disease duration or MRI lesion load. The lack for a correlation of functional improvement with MRI metrics has been recognized before<sup>25</sup> and poses a challenge for clinical trials<sup>26</sup>. In this context present data provides a valuable, reproducible<sup>14</sup>, primary outcome measure suitable for testing remyelination strategies in INO in MS.

Our pharmacological data also suggest that the treatment effect of fampridine on eye movements already becomes significant prior to reaching  $t_{\max}$  after about 2 hours. Based on this and a prior trial on the effect of fampridine on walking speed<sup>15</sup> we suspect that a lower dose of 10 mg may be sufficient. A lower dose may also be better tolerated by patients, the majority of whom did suffer from drug related dizziness. The proportion of patients with dizziness in this study was higher than the 10%-20% expected from standard dosing. The prevalence of other AEs, including headache and fatigue, was similar between the placebo and fampridine occasions.

The findings of present trial are consistent with Serra's detailed study of the effect of 10 mg dalfampridine in three cases of INO<sup>16</sup>. Each, but one of the patients did show 'significant decrease of saccadic abduction/adducting eye peak velocities for the worst INO' after treatment with fampridine<sup>16</sup>. In other words, fampridine reduces on a patient level the pathological slowing of the adducting eye in an INO. Furthermore, the pharmacodynamic data excludes the possibility of a type II errors which could be caused by low/absent fampridine blood levels.

There is good preclinical data supportive of the observations reported in this trial. Waxman and others have clearly demonstrated that ion channels are redistributed along demyelinated axons during regeneration<sup>27,28</sup>. Of these, redistribution of potassium channels has the disadvantage of reducing the generation of axon potentials by accelerating membrane repolarization. Fampridine directly affects demyelinated nerves by blocking potassium channels and therefore promotes conduction in demyelinated axons<sup>29</sup>.

These experimental data also imply that there are other potassium channel drugs which may show similar effects. For example, the structure of fampridine (4-aminopyridine) is similar to the structure of 3,4-Diaminopyridine. The reasons for using fampridine for this trial was that it is FDA approved for treatment in MS. A limitation is that fampridine is not licensed for treatment of an INO and we would be hesitant to recommend it as a routine treatment. Least of all because of side effects.

Another limitation of this study is that we did not investigate the effect of fampridine on functional outcomes of vision in MS. One reason is that there is no validated questionnaire for the visual problems specifically caused by an INO. These symptoms can be difficult to be explained by patients. A further limitation is that we did not include a visual quality of life measure such as the National Eye Institute Visual Function Questionnaire (NEI-VFQ-25).

Taken together the main advantage of this trial is that it provides evidence that a chronic INO is helpful in expanding the number of patients to include in trials testing remyelinating strategies in MS. Testing of saccadic eye movements are a validated, highly reproducible primary outcome measures<sup>5,30</sup> and suitable for a multi-center setting. We believe this will be important to cross validate findings on remyelination in optic neuritis which rely on a range of visual evoked visual potential test paradigms and optical coherence tomography as an outcome measures<sup>1,31</sup>. The prevalence of INO in MS appears to be high enough, 24%-55% to ensure that there will sufficient patients suitable for trials<sup>14</sup>.

## REFERENCES

- Green AJ, Gelfand JM, Cree BA, Bevan C, Boscardin WJ, Mei F, et al. Clemastine fumarate as a remyelinating therapy for multiple sclerosis (REBUILD): a randomised, controlled, double-blind, crossover trial. *Lancet*. 2017;390(10111):2481-9.
- Scolding NJ, Pasquini M, Reingold SC, Cohen JA. Cell-based therapeutic strategies for multiple sclerosis. *Brain*. 2017;140(11):2776-96.
- Petzold A, Balcer LJ, Calabresi PA, Costello F, Frohman TC, Frohman EM, et al. Retinal layer segmentation in multiple sclerosis: a systematic review and meta-analysis. *Lancet Neurol*. 2017;16(10):797-812.
- Petzold A, Wattjes MP, Costello F, Flores-Rivera J, Fraser CL, Fujihara K, et al. The investigation of acute optic neuritis: a review and proposed protocol. *Nat Rev Neurol*. 2014;10(8):447-58.
- Frohman EM, Zhang H, Kramer PD, Fleckenstein J, Hawker K, Racke MK, et al. MRI characteristics of the ms in MLF patients with chronic internuclear ophthalmoparesis. *Neurology*. 2001;57(5):762-8.
- Davis SL, Frohman TC, Crandall CG, Brown MJ, Mills DA, Kramer PD, et al. Modeling Uhthoff's phenomenon in MS patients with internuclear ophthalmoparesis. *Neurology*. 2008;70(13 Pt 2):1098-106.
- Frohman TC, Davis SL, Frohman EM. Modeling the mechanisms of Uhthoff's phenomenon in MS patients with internuclear ophthalmoparesis. *Ann N Y Acad Sci*. 2011;1233:313-9.
- Muri R, Meienberg O. The clinical spectrum of internuclear ophthalmoplegia in multiple sclerosis. *ArchNeurol*. 1985 1985;851-5.
- Virgo JD, Plant GT. Internuclear ophthalmoplegia. *Pract Neurol*. 2017;17(2):149-53.
- Meienberg O, Muri R, Rabineau P. Clinical and oculographic examinations of saccadic eye movements in the diagnosis of multiple sclerosis. *Arch Neurol*. 1986 1986;438-43.
- Jozefowicz-Korczynska M, Lukomski M, Pajor A. Identification of internuclear ophthalmoplegia signs in multiple sclerosis patients. Saccade test analysis. *J Neurol* 2008;255(7):1006-11.
- Downey DL, Stahl JS, Bhidayasiri R, Derwenskus J, Adams NL, Ruff RL, et al. Saccadic and vestibular abnormalities in multiple sclerosis: sensitive clinical signs of brainstem and cerebellar involvement. *Ann N Y Acad Sci* 2002;956:438-40.
- Serra A, Derwenskus J, Downey DL, Leigh RJ. Role of eye movement examination and subjective visual vertical in clinical evaluation of multiple sclerosis. *J Neurol* 2003;250(5):569-75.
- Nij Bijvank JA, Petzold A, Balk LJ, Tan HS, Uitdehaag BMJ, Theodorou M, et al. A standardized protocol for quantification of saccadic eye movements: DEMONS. *PloS one*. 2018;13(7):e0200695.
- Goodman A, Brown T, Krupp L, Schapiro R, Schwid S, Cohen R, et al. Sustained-release oral fampridine in multiple sclerosis: a randomised, double-blind, controlled trial. *Lancet* 2009 2/28/2009:732-8.
- Serra A, Skelly M, Jacobs J, Walker M, Cohen JA. Improvement of internuclear ophthalmoparesis in multiple sclerosis with dalfampridine. *Neurology*. 2014 7/8/2014:192-4.
- Polman CH, Reingold SC, Banwell B, Clanet M, Cohen JA, Filippi M, et al. Diagnostic criteria for multiple sclerosis: 2010 Revisions to the McDonald criteria. *Ann Neurol*. 2011;69(2):292-302.
- Nij Bijvank JA, Balk LJ, Tan HS, Uitdehaag BMJ, van Rijn LJ, Petzold A. A rare cause for visual symptoms in multiple sclerosis: posterior internuclear ophthalmoplegia of Lutz, a historical misnomer. *J Neurol*. 2017;264(3):600-2.
- Xiao G, Rowbottom C, Boiselle C, Gan LS. Fampridine is a Substrate and Inhibitor of Human OCT2, but not of Human MATE1, or MATE2K. *Pharm Res* 2018;35(8):159.
- Weir S, Gao Y, Henney H. Population pharmacokinetics and pharmacodynamics of dalfampridine-ER in healthy volunteers and in patients with multiple sclerosis. *Curr Med Res Opin* 2013 9/25/2013:1637-45.
- Frohman E, O'Suilleabhain P, Dewey R, Frohman T, Kramer P. A new measure of dysconjugacy in INO: the first-pass amplitude. *J Neurol Sci*. 2003 2003:65-71.
- Frohman EM, Frohman TC. Horizontal monocular saccadic failure: an unusual clinically isolated syndrome progressing to multiple sclerosis. *Mult Scler (Houndmills, Basingstoke, England)*. 2003;9(1):55-8.
- Ventre J, Vighetto A, Bailly G, Prablanc C. Saccade metrics in multiple sclerosis: versional velocity dysconjugacy as the best clue? *J Neurol Sci*. 1991;102(2):144-9.
- Fielding J, Clough M, Beh S, Millist L, Sears D, Frohman AN, et al. Ocular motor signatures of cognitive dysfunction in multiple sclerosis. *Nat Rev Neurol*. 2015;11(11):637-45.
- Kappos L, Moeri D, Radue EW, Schoetzau A, Schweikert K, Barkhof F, et al. Predictive value of gadolinium-enhanced magnetic resonance imaging for relapse rate and changes in disability or impairment in multiple sclerosis: a meta-analysis. *Gadolinium MRI Meta-analysis Group*. *Lancet* 1999;353(9157):964-9.
- Andorra M, Nakamura K, Lampert EJ, Pulido-Valdeolivas I, Zubizarreta I, Llufrui S, et al. Assessing Biological and Methodological Aspects of Brain Volume Loss in Multiple Sclerosis. *JAMA Neurol* 2018;75(10):1246-55.
- Waxman SG. Membranes, myelin, and the pathophysiology of multiple sclerosis. *New Engl J Med* 1982;306(25):1529-33.
- Waxman SG, Ritchie JM. Organization of ion channels in the myelinated nerve fiber. *Science* 1985;228(4707):1502-7.
- Kim Y, Goldner M, Sanders D. Facilitatory effects of 4-aminopyridine on neuromuscular transmission in disease states. *Muscle Nerve*. 1980;3(2):112-9.
- Frohman E, Frohman T, O'Suilleabhain P, Zhang H, Hawker K, Racke M, et al. Quantitative oculographic characterisation of internuclear ophthalmoparesis in multiple sclerosis: the versional dysconjugacy index Z score. *J Neurol Neurosurg Ps*. 2002 2002:51-5.
- Cadavid D, Balcer L, Galetta S, Aktas O, Ziemssen T, Vanopdenbosch L, et al. Safety and efficacy of opicinumab in acute optic neuritis (RENEW): a randomised, placebo-controlled, phase 2 trial. *Lancet Neurol* 2017;16(3):189-99.



TABLE 1 – Subject characteristics.

Characteristic	Patients (n=23)
Age, mean (min-max), years	49 (31-72)
No. (%) females	12 (52)
Disease duration, mean (min-max) years	12.6 (1-25)
Weight, mean (min-max) kg	71.9 (45.1-103)
Height, mean (min-max) cm	176 (157-188)
BMI, mean (min-max) kg/m <sup>2</sup>	23.1 (17.2-29.4)
No. (%) bilateral INO	13 (56)

TABLE 2 – Analysis results table video-oculography.

Pharmacodynamic measurement	Estimate of the difference	95% CI		p-value
		Lower	Upper	
VDI peak velocity (%), eyes with INO	-17.4%	-22.4%	-12.1%	<0.0001
VDI peak velocity (%), eyes without INO	-4.6%	-10.3%	1.5%	0.105
VDI first pass amplitude (%), eyes with INO	-12.1%	-17.6%	-6.2%	0.0003

FIGURE 1 – CONSORT flow diagram for the randomized controlled trial.

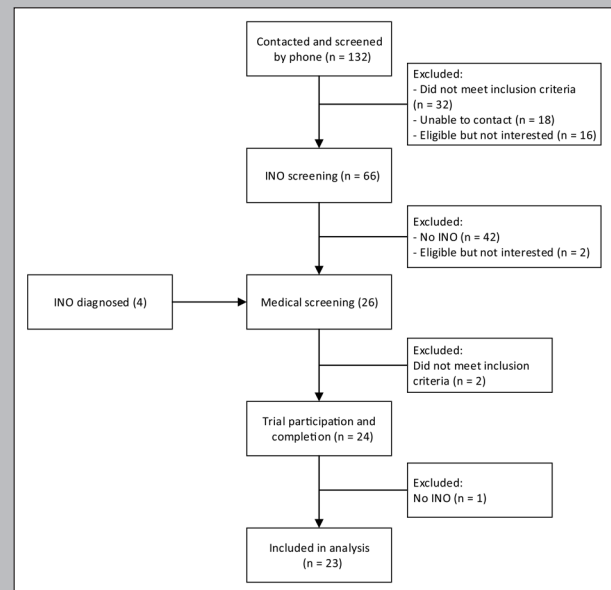


FIGURE 2 – Mean Fampridine serum concentrations with SD, measured in the subjects during the occasion.

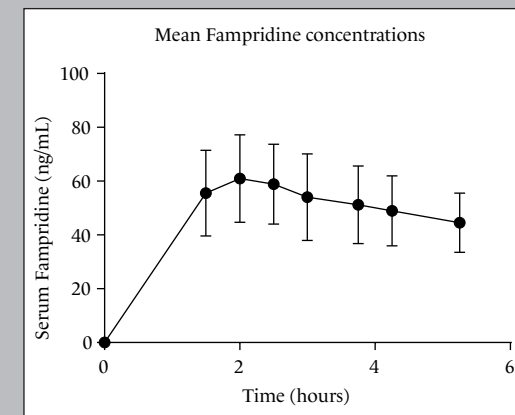


FIGURE 3 – Pharmacodynamic results. Figure 3A shows the VDI peak velocity change from baseline least square means with upper and lower limit, figure 3B the VDI first pass amplitude change from baseline least square means with upper and lower limit. Figure 3C shows the mean change from baseline least square means in VDI peak velocity for the non-INO eyes with upper and lower limit. Significant differences are indicated by an asterisk (\*).

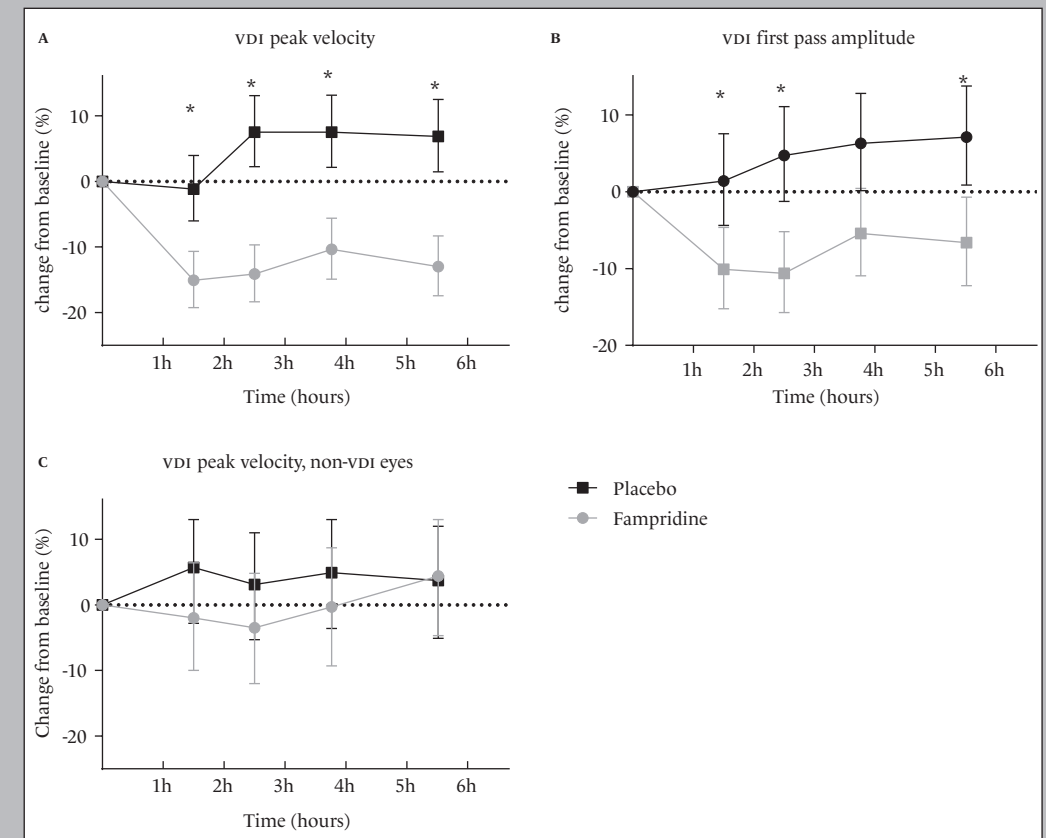


TABLE S1 – Visit and Assessment Schedule.

Timepoint Assessment	SCR	Treatment days 1, 8									
	Up to -21 d	-1h	0h	1.5h	2h	2.5h	3h	3.75h	4.25h	5.5h	
Informed consent	X										
Demography	X										
Inclusion and exclusion criteria	X										
Medical history	X										
Physical examination	X										
Concomitant medication	X	X									
Meals					X						
Virology	X										
BsHaem, BsChem, Urinalysis	X										
UrDrug, BrAlc	X										
ECG	X										
Vital Signs (BP, HR)	X	X		X		X		X		X	
Drug (-placebo) administration			X								
3T MRI	X										
PK sample		X		X	X	X	X	X	X	X	X
Eye Tracking Test	X	X <sup>1</sup>		X		X		X		X	
NeuroCart test battery	X <sup>2</sup>	X <sup>3</sup>						X		X	
Pharmac-EEG		X						X		X	
Simple reaction time task	X	X						X		X	
Adaptive tracking	X	X						X		X	
Rapid visual information processing	X	X						X		X	
Body sway	X	X						X		X	
Symbol digit substitution test	X	X						X		X	
National Eye Institute visual functioning questionnaire (VFQ-25)		X									
Discharge											X
(S)AE											<— continuous —>

SCR = Screening, BsHaem = Blood Sample Haematology, BsChem = Blood Sample Chemistry, UrDrug = Urine Drug Screen, ECG = Electrocardiogram, BP = Blood Pressure, HR = Heart Rate, MRI = Magnetic Resonance Imaging, (S)AE = (Serious) Adverse Event; 1 = Performed twice at baseline; 2 = Training session, except pharmac-EEG; 3 = Performed twice at baseline.

FIGURE S2 – Scatter plot showing the peak velocity vD1 at baseline versus peak velocity vD1 difference between fampridine and placebo (average difference over all time points). vD1 was calculated for every eye with INO (n=36; some patients have a bilateral INO).

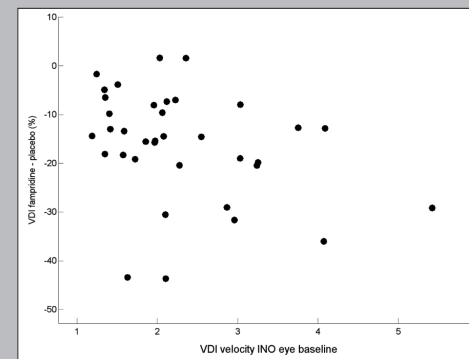


FIGURE S3 – Scatter plot showing the MRI lesion load (% of MLE) versus peak velocity vD1 difference between fampridine and placebo (average difference over all time points). vD1 was calculated for every eye with INO (n=36; some patients have a bilateral INO).

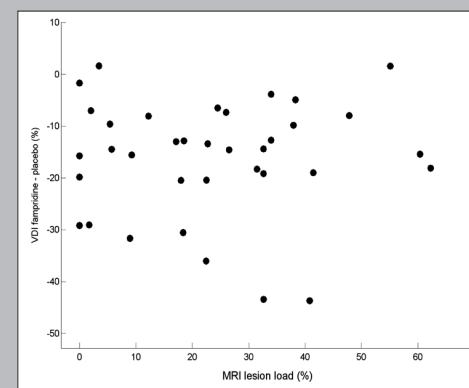
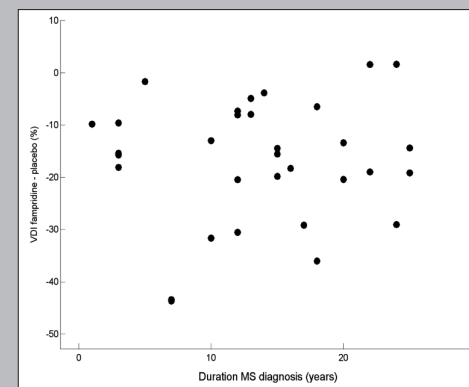


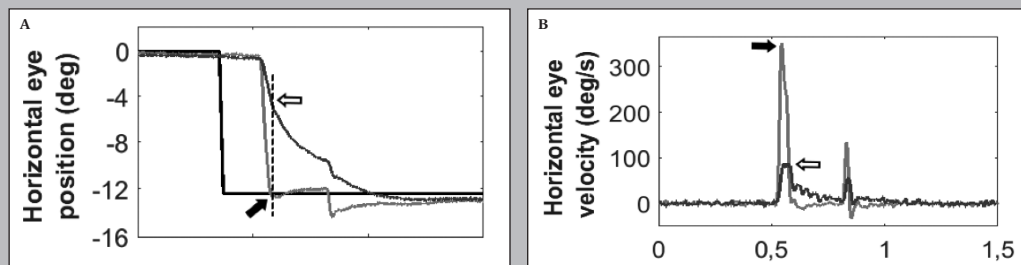
FIGURE S4 – Scatter plot showing the duration of disease (number of years since diagnosis) versus peak velocity vD1 difference between fampridine and placebo (average difference over all time points). vD1 was calculated for every eye with INO (n=36; some patients have a bilateral INO).



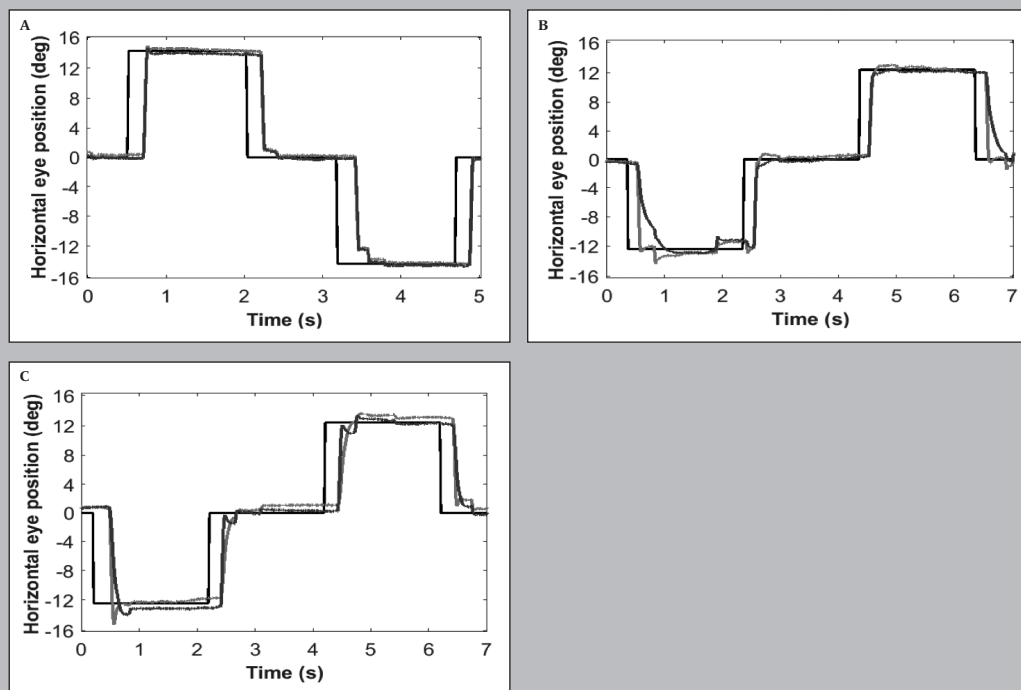
**FIGURE S5** – Horizontal eye position (left graph, degrees of visual angle) and eye velocity (right graph, degrees of visual angle per second) of a leftward saccade of a MS patient with INO, showing the FPA and peak velocity. In the left graph, the solid black line represents the target position. In both graphs, the dark grey line represents the right eye and the grey line represents the left eye.

A. The dashed line indicates the time point where the abducting eye first reaches the target position. The black arrow points out the eye position of the abducting eye at this time point, the black-lined arrow the eye position of the adducting eye. The FPA is the amplitude of an eye at this time point.

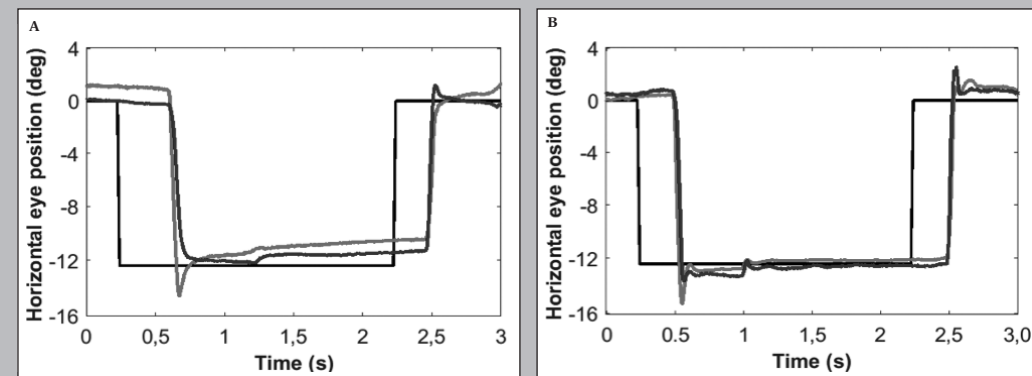
B. The black arrow points out the peak velocity of the abducting eye during the centripetal saccade, the black-lined arrow the peak velocity of the adducting eye.



**FIGURE S6** – Horizontal eye position (degrees of visual angle) of two centripetal saccades in a healthy volunteer (A), a MS patient with unilateral INO (B) and a MS patient with bilateral INO (C). The solid black line represents the target position, the dark grey line the right eye and the grey line the left eye. For the horizontal eye position, value zero corresponds to the center of the screen, a positive value to a position at the right side of the center and a negative value to a position at the left side of the center.



**FIGURE S7** – Horizontal eye position (degrees of visual angle) of a leftward centripetal saccades in a MS patients with a bilateral INO (subject 2), pre-dose (A) and 1.5 hours post-dose (B). The solid black line represents the target position, the dark grey line the right eye and the grey line the left eye.



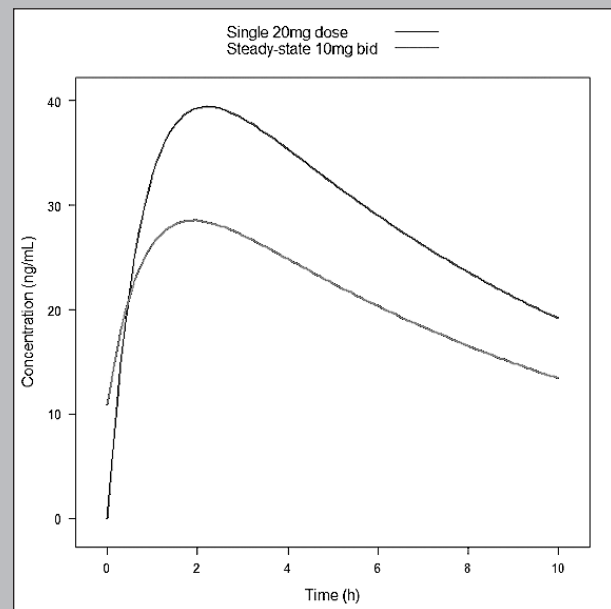
**FIGURE S8** – Axial T2-weighted image at the level of the pons showing a small periventricular lesion affecting the right MLF tract (arrow).



TABLE 59 – All reported adverse events (including those not related to the treatment).

Adverse event	Fampridine number of subjects with the AE (% of total number of subjects)	Placebo number of subjects with the AE (% of total number of subjects)
Dizziness	14 (61%)	
Fatigue	3 (13%)	5 (22%)
(Resting) tremor	2 (9%)	
Headache	2 (9%)	2 (9%)
Hyperhidrosis	2 (9%)	
Asthenia	1 (4%)	
Back pain	1 (4%)	
Chest discomfort	1 (4%)	
Diarrhoea	1 (4%)	
Nausea	1 (4%)	
Paraesthesia	1 (4%)	
Restless legs syndrome	1 (4%)	
Somnolence	1 (4%)	1 (4%)
Visual impairment	1 (4%)	
Nasopharyngitis		1 (4%)

FIGURE 510 – Fampridine concentrations (ng/mL) over time for a single 20mg dose (upper line) or a twice-daily 10mg dose at steady-state (lower line), predicted using the pharmacokinetic parameters from *Weir et al* (Curr Med Res Opin. 2013).



# VIII

## SUMMARY AND GENERAL DISCUSSION

This thesis describes six clinical studies: two studies that investigate new compounds to treat symptoms of multiple sclerosis (MS) (**chapters 2 and 3**), one study that investigates a new compound to treat MS (**chapter 4**) and three studies about the development of new methods to determine effects of a new class of compounds to treat MS (**chapters 5, 6 and 7**). When reflecting on the results of the studies, two major issues stand out: First, despite the range of treatments available (**chapter 1**), research into novel compounds is needed to improve the treatment and prognosis of patient with MS. Second, although we show it is feasible to integrate biomarker development into early phase clinical trials, it is not yet common practice.

## MAIN OUTCOMES

**Chapter 1** starts with a brief description of the disease multiple sclerosis (MS): the most common autoimmune disorder of the central nervous system, and primarily an inflammatory disorder of the brain and spinal cord in which focal lymphocytic infiltration leads to damage of myelin (demyelination) and axons. In the introduction, we divide current treatment of MS into disease-modifying treatments (DMTs) and symptomatic treatments. We indicate that – despite its increasing efficacy and discovery of these compounds over the years – most registered DMTs are associated with a high disease burden due to side effects. For that reason, there is still a need for an effective treatment to halt the progression of disability by developing remyelinating and neuroprotective therapies. As the current frequently used biomarkers in MS diagnosis and treatment management are not yet capable of accurately measuring treatment effects of this group of compounds, trials with potential neuroreparative or neuroregenerative agents will need improved and appropriate biomarkers.

**Chapter 2** describes a study to evaluate the efficacy of a novel oral formulation of  $\Delta^9$ -THC (ECP002A) in patients with progressive MS.  $\Delta^9$ -THC is one of the cannabinoids in the Cannabis sativa plant and a direct partial agonist of the cannabinoid receptors CB1 and CB2. Cannabinoids have previously shown to improve symptoms of MS including muscle spasticity and pain through the modulation of neuronal excitability via presynaptic cannabinoid receptors. The study described in chapter 2 was a proof-of-concept study with two phases: a crossover challenge (‘dose-finding’) phase and a 4-week parallel randomized, placebo-controlled treatment phase. Twenty-four patients with progressive MS and moderate spasticity were enrolled. Pain and spasticity were significantly reduced when measured directly after administration of ECP002A in the clinic, but not when measured in a daily diary. Nevertheless, despite the complex interplay of psycho-active effects and analgesia, the current oral formulation of  $\Delta^9$ -THC may play a role in the treatment of spasticity and pain associated with MS, as it was well-tolerated and showed a stable pharmacokinetic profile. Additionally, this study specifically underlined the potential added value of thorough investigation of PK/PD relationships in the target population.

In the study reported in **chapter 3** we tested a new formulation of methylprednisolone (MP), which is commonly used for the treatment of MS relapses. Both dose and dosing frequency might be reduced by incorporating free MP in glutathione (GSH) PEGylated

liposomes, creating a slow-release formulation with reduced toxicity and prolonged efficacy. This first-in-human study was designed to assess the safety, pharmacokinetics (PK) and pharmacodynamics (PD) of GSH-PEGylated liposomes containing MP (2B3-201). 2B3-201 led to a high occurrence of infusion related reactions (89%), but was otherwise considered safe, with no clinically relevant changes in (CNS) safety parameters and no serious adverse events. 2B3-201 was shown to have a long plasma half-life between 24 and 37 hours and led to prolonged immunosuppressive effects.

**Chapter 4** reports a first-in-human single ascending dose study (SAD), followed by a 21-days multiple ascending dose (MAD) study, performed to assess the safety and PK of CNM-AU8. CNM-AU8 is a solution of clean-surface gold nanocrystals and being developed for its potentially immunomodulating and remyelinating effects, while leading to fewer side effects than registered gold-containing compounds. In vitro inflammatory challenge experiments were initiated to investigate possible PD effects. CNM-AU8 showed a good safety profile, which appeared to be more favorable than existing gold formulations, with the most frequently reported adverse event related to CNM-AU8 being abdominal pain (20%). CNM-AU8 had a plasma half-life between 11.5 to 26.2 days, and a first dose  $t_{max}$  between 3.3 and 3.5 hours. The low concentrations and unusual pharmacokinetic profile corresponded to the reported data on gold nanoparticles. No anti-inflammatory effects of CNM-AU8 were observed in the in vitro challenge, and therefore no ex vivo PD measurements were implemented in the clinical study. Next studies should determine whether CNM-AU8 possesses anti-inflammatory effects and remyelinating effects.

Therapeutics promoting myelin synthesis may enhance recovery in demyelinating diseases such as MS. However, no suitable method exists to quantify myelination. The turnover of  $\beta$ -galactosylceramide ( $\beta$ -GALC, a myelin component) is indicative of myelination in mice, but its turnover has not been determined in humans.

**Chapter 5** describes a study in which six healthy subjects consumed 120 mL 70% D<sub>2</sub>O daily for 70 days to label  $\beta$ -GALC. We subsequently used mass spectrometry and compartmental modeling to quantify the turnover rate of  $\beta$ -GALC in cerebrospinal fluid. Maximum deuterium enrichment of body water ranged from 1.5 to 3.9%, while that of  $\beta$ -GALC was much lower: 0.05–0.14%. This suggested a slow turnover rate, which was confirmed by the model-estimated  $\beta$ -GALC turnover rate of 0.00168 day<sup>-1</sup>, corresponding with a half-life of 413 days. Based on the results, we suggested that additional studies in patients with MS are needed to investigate whether  $\beta$ -GALC turnover could be used as an outcome measure in clinical trials with remyelination therapies.

**Chapter 6** describes the follow-up study wherein we labeled myelin with deuterium in 5 MS patients, and besides  $\beta$ -GALC also modeled the myelin breakdown product N-Octadecanoyl-sulfatide (NO-Sulf). The turnover rate constants of  $\beta$ -GALC and NO-Sulf with non-negligible turnover were 0.00186 and 0.00714 day<sup>-1</sup> in MS patients, corresponding with a turnover half-life of 373 days and 96.5 days, respectively. The effect of MS on the NO-Sulf (49.4% lower fraction) was more pronounced compared to the effect on  $\beta$ -GALC turnover (18.3% lower fraction). The kinetics of myelin breakdown products in the CSF were different in patients with MS compared with healthy subjects. This could be caused by slower myelin production in these patients, a higher level of degradation of a more

stable component of myelin, or, most likely, by a combination of these two processes. Deuterium labelling in combination with lumbar punctures would be a useful method for the quantification of metabolic processes of the central nervous system and myelin turnover in patients with progressive MS and can therefore be used in proof of concept studies with remyelination therapies.

**Chapter 7** reports a randomized, double-blind, placebo-controlled, cross-over trial with fampridine in patients with MS and internuclear ophthalmoparesis (INO). We examined if the velocity of saccadic eye movements in INO improved with fampridine treatment in patients with MS. Main outcome measures were the change of peak velocity versional dysconjugacy index (PV-VDI) and first-pass amplitude VDI (FPA-VDI). Fampridine significantly reduced both PV-VDI (-17.4%, 95% CI: -22.4%, -12.1%;  $p < 0.0001$ ) and FPA-VDI (-12.5%, 95% CI: -18.9%, -5.5%;  $p < 0.01$ ) and therefore clearly improves saccadic eye movements due to INO in MS patients. According to the results of this study, treatment response to fampridine may be used in patient selection for enrolment in studies of compounds enhancing remyelination in MS using the velocity of saccadic eye movements as a primary outcome measure.

## EARLY IMPLEMENTATION OF BIOMARKERS IN CLINICAL STUDIES

When a new compound is tested in humans for the first time (First-in-Human studies, or FIH-studies), traditional study objectives concern the exploration of safety, tolerability and pharmacokinetics. This commonly used phased approach can accordingly support decisions to continue or discontinue with a new compound (go/no-go decision) and to plan dosage and dosage schedules<sup>1</sup>. Despite this phased approach, there is no reason to exclude the additional evaluation of the mechanism of action or efficacy of the compound in FIH studies<sup>2</sup>. This might save time, costs and it could support decisions in early stage of the development.

Saving costs and time during the developmental pipeline of new compounds is one of the largest challenges in early drug development. The current drug development time is over ten years<sup>3</sup>. Only one out of ten drug development projects make it all the way from FIH until approval, and this is even lower for neurological compounds, according to the industry lobby group BIO<sup>4</sup>. During drug development studies in large patient populations are often unsuccessful due to their inability to prove efficacy, as was shown by a study in four large pharmaceutical companies<sup>5</sup>. This report also showed that development programs that include a biomarker have increased chances of success. There is reason to believe that early implementation of biomarkers in clinical studies might shorten drug development timelines. Therefore, the early implementation of biomarkers in clinical studies is highly welcomed.

## HOW TO INTEGRATE BIOMARKERS IN EARLY CLINICAL TRIALS

There are several ways to integrate biomarkers in early clinical trials. This thesis shows examples of how to successfully plan and combine biomarker development with FIH-studies. In order to select appropriate biomarkers for a clinical development program, one should use knowledge of the pharmacology of the compound and the target patient population, and biomarkers should be fit-for-purpose, and capable of showing essential drug properties and effects<sup>6</sup>. The chapters of this thesis include studies that illustrate different ways of integrating biomarkers into early clinical trials:

- 1 a biomarker study prior to a FIH study,
- 2 a combination of a biomarker and FIH study, and
- 3 a biomarker study performed after a FIH study.

### A biomarker study prior to a FIH study

The studies performed to measure myelin kinetics (**chapters 5 and 6**) describe biomarker studies that were initiated before the start of a FIH study. We used animal data and literature to design a study aiming for the measurement of deuterium-labeled myelin breakdown products. The first part of this biomarker study was performed in healthy volunteers, as we were unconfident whether this biomarker would be measurable in humans. Including a cohort of healthy volunteers would enable us to observe how subjects adhered to the study protocol, e.g. drinking heavy water daily for a long period and 4 lumbar punctures within 6 months. Additionally, it would enable us to calculate kinetics of myelin breakdown products in healthy volunteers and to use this information for the development of future biomarker studies<sup>7</sup>. As this first study in healthy volunteers showed positive results, and the confirmation that myelin breakdown products were a measurable biomarker, a similar study with the same design in patients with MS was initiated<sup>8</sup>.

The testing of a biomarker in a study before the start of a FIH study has several advantages. It can be seen as proof-of-mechanism testing, before the FIH study has even started. In phase 1b or 2 studies, biomarkers can be useful to support clinical endpoints<sup>9</sup>. Biomarkers can be specifically present in the target patient group, for example MS patients with an internuclear ophthalmoplegia (INO)<sup>10,11</sup>, but can also be tested by the NeuroCart in healthy volunteers (**chapter 2**)<sup>12</sup>. Performing a biomarker study in patients prior to a FIH study allows us to have a subsequent patient cohort, but also investigational staff already in place for a phase 1 or 2 follow-up study. This can decrease timelines, while patient studies are generally more time (and therefore cost) consuming when it comes to the recruitment of patients and staff. Finally, biomarker studies provide novel insights into the (background of) diseases and pharmacological processes and therefore is a relevant field wherein scientists from industry and academia can interact.

**Chapter 7** illustrates how biomarker studies provide novel insights in the clinical pharmacology of diseases. We developed a biomarker that uses a pharmaceutical compound (fampridine) to show possible improvement in horizontal eye movements of patients

with MS and an INO (**chapter 7**). Fampridine is a potassium channel blocker that improves nerve conduction, and thereby function of demyelinated nerve fibers. It does not improve eye movements if demyelination of the medial longitudinal fasciculus (MLF) is absent. The fact that fampridine improved eye movements in these patients meant that the MLF was demyelinated, but also that axonal degeneration had not occurred yet. This population therefore appeared to be very useful to demonstrate effects of new compounds that are expected to accelerate (or improve) remyelination (**chapter 7**). For this reason, a subsequent study in healthy volunteers was not considered as INO is only present in a patient population. Because of the short half-life of fampridine, we chose a cross-over design to limit the duration of the study for patients (3-6 weeks). An additional advantage of this study design was that it yielded a database of INO patients who can be contacted as soon as this biomarker will be used in a study with a remyelinating compound. This study also added information about the efficacy of the compound used. Fampridine is not indicated for treatment of an INO yet, but this study showed that it might be worthwhile exploring fampridine as a treatment option for these patients. And if an INO patient would like to be treated with fampridine, an acute fampridine challenge (as described in **chapter 7**) could show if the patient is likely to respond to the treatment. Furthermore, the INO severity can be tracked with the same eye-tracking method to monitor long-term treatment response.

Prior to the FIH study with CNM-AU8 (**chapter 4**) we performed a small biomarker study. This was an in vitro study that was designed to show possible inflammatory effects of the compound that was being tested (gold nano-particles)<sup>13,14</sup>. Results of this in vitro biomarker study did not demonstrate inflammatory effects of gold nanoparticles. However, the specific inflammatory assay was based on previously reported animal studies<sup>14</sup>. One could speculate whether the use of other in vitro assays would have led to more insight into the role of gold in the immune system. In this specific example, the negative results from the biomarker study were a valid reason to not include the biomarker assay in the subsequent phase I clinical trial. Planning a biomarker study before start of the phase I clinical study did require higher initial costs, but eventually prevented the use of an unsuitable biomarker in the following phase I trials.

### A combination of a biomarker and FIH study

The use of biomarkers in a FIH study has several advantages. Treatment effects in such a combined study can easily be compared to the placebo arm, corrected for individual baseline levels. In **chapter 3** such a FIH study is described, wherein liposomal methylprednisolone was studied, and both blood biomarkers and cognitive testing were tested in the first three cohorts of healthy volunteers. In the subsequent three cohorts of the study, we decided to only measure the 'fit-for-purpose' biomarkers showing a clear effect. It should be noted that in this specific study the pharmacodynamics (PD) of the active part of the compound (methylprednisolone) had already been reported in previous studies: inhibition of the hypothalamic-pituitary-adrenal (HPA) axis<sup>15</sup>, glucose homeostasis disturbances, and depletion of osteocalcin<sup>16,17</sup> and lymphocytes<sup>18</sup>.

A proof-of-pharmacology study can be performed in healthy volunteers if the new compound affects the biomarker in healthy persons. If this is not feasible, it is a good option to do a FIH study in a patient population. A healthy volunteer study can generally be performed on a shorter term and is cheaper than a patient study, which is beneficial for planning purposes, i.e. early availability of safety and pharmacokinetic (PK) data allows for the timely adjustment of the development program. Nevertheless, PK and safety data can be different in patients and healthy subjects, which might cause modification of the existing drug development plan. Additionally, recruitment and enrollment of a specific patient population in this early stage can lead to increased awareness of patients as well as study sites, which can lead to a time and cost-effective planning of phase 2 studies. It should be noted though that patients in these studies are often less representative for the eventual target patient population: patients in such a study are usually less severely affected.

### A biomarker study after a FIH study.

Although the regulatory agencies encourage the use of efficacy parameters in early stage drug development<sup>1</sup>, it does have many advantages to wait for the first FIH-results. First of all, there will be more information available on safety, tolerability and the pharmacokinetic profile of the compound. Reported PK parameters of the compound be supportive when tracking and implementing the 'fit-for-purpose' biomarker in the most efficient way.

The phase 2 study with an oral formulation of  $\Delta 9$ -tetrahydrocannabinol described in **chapter 2** has an interesting design, being a hybrid between a typical multiple-dose study to investigate safety profiles, PK and PD parameters, and a FIH study to establish proof-of-pharmacology<sup>19</sup>. The study consisted of a challenge phase and treatment phase, and involved a variety of biomarkers: the objective measurement of spasticity (H/M ratio)<sup>20,21</sup>, postural instability, visual perception test, attention test and working-memory test. The challenge phase in the study design proved to be an elegant way to investigate individual PK and safety profiles, before continuing to the treatment phase, in which patients received the compound three times a day for four weeks. The cross-over design of this part of the study intended to support the interpretation of the different biomarkers tested, thereby reducing the risk of bias. The starting dose in the treatment phase was adjusted to the individual patient, reflecting clinical practice better than in other studies.

## THE INTEGRATION OF BIOMARKERS IN THE DEVELOPMENT OF TREATMENTS IN MS

This discussion summarizes the three approaches of how to integrate biomarker studies into early-phase clinical studies and its pros and cons. The studies performed and described in this thesis illustrate how these approaches can accordingly lead to a time and cost-efficient process of drug development. Looking back on the wide range of studies already performed to evaluate potential future treatments of MS, this knowledge allows us to reflect on the methodology used and the degree of biomarker integration in these studies.

The first clinical study with *opicinumab* (reported in 2014) consisted of two parts: single-dose administration in healthy volunteers and multiple dosing in participants with MS (both RRMS and SPMS). Although the main focus was safety, efficacy and pharmacokinetics, the study did contain exploratory efficacy markers: imaging biomarkers Magnetization Transfer Ratio (MTR) and Diffusion Tensor Imaging (DTI) of pre-existing lesions and non-lesional normal-appearing white matter (NAWM)<sup>22</sup>. These did not reveal any clear treatment effects, which may have been due to the small sample size (46 participants with MS). The addition of a patient cohort in this stage of development gave opportunities for the addition of proof-of-concept measurements. **Chapters 5, 6 and 7** describe methods that could have been of interest in a clinical study with a new, potentially remyelinating compound. Especially the method described in **chapter 7**, where we used video-oculography in 23 MS patients with an INO, showed significant results. This method will most likely not need a large cohort to show (significant) difference between treatment and placebo.

There was a second phase I study with *opicinumab* that evaluated whether the anti-LINGO-1 antibody had immunomodulatory effects<sup>23</sup>. Although this is worth evaluating in an auto-immune disease, the reason for this second phase I study was not clearly reported. And this did raise the question why to invest in a study evaluating immunomodulatory effects and not in a proof-of-concept study, or in the development of additional methods to measure possible remyelination? The first attempt to measure the efficacy of *opicinumab* was in a phase 2 study, wherein Visual Evoked Potential (VEP) latency was used as a measure of remyelination. VEP has shown to be a measure of remyelination in optic neuritis in a rat model<sup>24</sup>. It inferred remyelination and proved to be a practical but is an indirect measurement of remyelination<sup>25,26</sup>.

The phase I FIH study with *RHIGM22* was performed in patients with MS (72 in total) and included biomarkers comparable to the myelin turnover method described in **chapters 5 and 6**. In this study, 21 patients received 100 mL heavy water (70% D<sub>2</sub>O) daily for two periods: during two weeks prior to dosing (2 different doses and placebo) and between days 15 and 29. Fractional synthesis rates of specific myelin biomarkers were determined by mass spectroscopic methods from blood and CSF<sup>27</sup>. It is unclear why the researchers chose to give 100 mL daily in two separate periods of 14 days. Our labelling protocol, described in **Chapter 5** of this thesis, was based on animal data and the maximum amount of heavy water safely tested in previous clinical studies (120 mL, 10 weeks). Interim analyses allowed us to adapt the sampling period. Data in **chapters 5 and 6** of this thesis showed that labelling of myelin breakdown products was limited after 5 weeks of 120 mL daily heavy water administration. According to our analyses, the amount of D<sub>2</sub>O and period of exposure used in the *RHIGM22* study was probably too short to show difference in labelling. We also found that turnover of octadecanoyl-sulfatide is a useful biomarker. This molecule has not been reported as a useful biomarker to measure myelin turnover, and therefore not yet being used in studies like the phase I study with *RHIGM22*. Our data was not published at the time the researchers designed the study. However, the limited literature on human myelin turnover suggest that the turnover is multiple weeks to months<sup>28,29</sup>. This information did not support the decision to label for a limited time (2

weeks in the *RHIGM22* study). Since the turnover is much longer, labelled myelin in the post-dose sample might be due to labelling in the pre-dose period.

*Olesoxime* is already in development as a possible treatment agent for Amyotrophic Lateral Sclerosis (ALS)<sup>30</sup>, Spinal Muscular Atrophy (SMA)<sup>31</sup> and Huntington's disease<sup>32</sup> years before a trial in MS patients was initiated<sup>33</sup>. This means that FIH studies were already performed before *olesoxime* was explored as potential treatment for MS. Development of the compound was halted for ALS and SMA in a late phase: only after negative phase 3 results for ALS and after negative phase 2 results for SMA. Results from the study in MS patients have not been published yet. However, we know that the study enrolled 44 patients and aimed to measure potential remyelination with imaging biomarkers (secondary endpoint). The MRI scans were performed at baseline and after 12 and 24 weeks. Literature shows that a treatment response can only be observable between three to six months after the start of treatment and that a second MRI between six and twelve months is advisable<sup>34</sup>. Lack of a response or trend based on MRI data can therefore be due to this shorter period, especially since the use of quantitative MRI measures for the measurement of remyelination still limited in a lengthy process like the demyelination and remyelination of a MS lesion<sup>35,36</sup>.

*Amiloride* is a licenced diuretic with a proven safety record. The first study to explore the neuroprotective effect of *amiloride* was an open-label pilot study in 14 patients with PPMS, using MRI markers of neurodegeneration as outcome measures of neuroprotection<sup>37</sup>. A significant reduction in normalized annual rate of whole-brain volume was observed during the treatment phase compared with the pre-treatment phase. And although changes in whole-brain atrophy rate lack pathological specificity and are relatively indiscriminate with regard to effects of neuroaxonal and myelin loss on brain volume, the results suggest that *amiloride* may exert neuroprotective effects.

Next, a randomised, double blind, placebo-controlled phase 2 trial in 46 patients with optic neuritis was set up<sup>38</sup>. The main objectives of this study included biomarkers, like retinal nerve fibre thickness, imaging biomarkers, visual function, visual electrophysiology and quality of life questionnaires. Participants in this study received five months of treatment after optic neuritis, and biomarkers were measured at six and twelve months. Results could not show *amiloride* protected retinal nerve fibre layer thickness in optic neuritis<sup>39</sup>. One of the reasons the researchers reported is the possible lack of central nervous system (CNS) penetration of *amiloride*. The question regarding CNS penetration, however, could have already been answered in a healthy volunteer cohort with cerebrospinal fluid (CSF) sampling, or else by including lumbar punctures in the phase 2 trial.

Similar to *amiloride*, *quetiapine* is a registered drug, with psychosis as main treatment indication. Its potential neuroprotective and remyelinating properties have been well described<sup>40</sup>. Patients with MS are expected to benefit from *quetiapine* in multiple ways: besides possible remyelinating effects, *quetiapine* has shown to improve sleep<sup>41</sup> and might improve pain<sup>42</sup>, both common problems in patients with MS. But because patients with MS may be more susceptible to AES due to the brain injury that accompanies the disease, a safety, tolerability and dosing study was advised in this novel patient population.



Thirty-six RRMS patients were enrolled to find the appropriate dose for patients with MS<sup>43</sup>. This study unfortunately did not include biomarkers. The researchers did include clinical scales in the study, but these scales were no biomarkers related to remyelination. As quetiapine is expected to benefit patient in multiple ways, improvement in clinical scales is most likely due to multiple factors.

In an earlier article<sup>40</sup>, the researchers advised to add imaging biomarkers to examine if quetiapine could promote remyelination. However, quetiapine has shown to have an effect on multiple systems in the body, including the immune system<sup>44</sup>. Improvement on MRI might be due to remyelination, due to a less active immune system, or both. Ideally, a biomarker should measure the remyelination effect more directly. From the two methods described in this thesis, the measurement of changes in turnover of myelin breakdown products (**chapters 5 and 6**) and of improvements in horizontal eye movements in MS patients with INO (**chapter 7**), the first method is most suitable as a biomarker in a clinical study which quetiapine. Although both methods are probably able to measure remyelinating effects, the eye movements in MS patients with INO were sensitive to fatigue of the patient. Sleep improvement caused by quetiapine might improve these measurements, without even improving myelination.<sup>41</sup>

*Guanabenz* is a registered antihypertensive drug. A phase I study with oral guanabenz in patients with MS was performed<sup>45</sup> and supposedly has been completed, but no results have been reported yet. The main objective of the study was dose-finding; they planned to explore five different doses (28 days of treatment) in six patients with MS. The study design included MRI scans, and (although it was not specifically described) this probably included imaging biomarkers for remyelination as well.

It is not clear why they chose to use imaging biomarkers in a study with such a small sample size, and it follow the patients for a limited time period (3,5 months). Animal studies that tested guanabenz in the EAE model in mice showed the first difference with placebo ten days after the start, and this continued until day 30<sup>46</sup>. In **chapter 6** we describe a slower myelin turnover than reported in rodents<sup>28</sup>, which makes the measurement of an effect after 28 days of treatment unlikely. A small sample size can be a challenge in a pilot study like the study mentioned above. A sensitive method, like the method described in **chapter 7** (eye movements in MS patients with an INO), might be a suitable method. Such study could for example contain baseline measurements and monthly measurements. It does require a specific population, namely MS patients with an INO that responds to fampridine. Recruitment of these patients in a mono-centre study is achievable: we were able to recruit 23 patients in 16 months.

Lastly, we discuss the earlier-mentioned FIH study with *gold nanoparticles* (**chapter 4**). A compound that could enhance remyelination *and* influence the immune system at the same time would be ideal in the treatment of MS: a disease that is characterized by an autoimmune response against myelin, and possibly inefficient remyelination<sup>47</sup>. As registered gold-containing compounds are infamous for their side effects<sup>48,49</sup>, it was decided to perform the FIH study in healthy volunteers. However, improvement of remyelination in healthy volunteers cannot be measured, so the hypothesis that gold nanoparticles stimulate remyelination could not be tested in this study. The study did include in vitro

inflammatory challenge experiments to investigate possible pharmacodynamic effects, based on reports that gold nanoparticles influence inflammatory responses<sup>13</sup>. However, no anti-inflammatory effects of gold nanoparticles were observed in the in vitro challenge, and therefore the planned ex vivo PD measurements were not added to the clinical study. Currently, a phase 2 study in 150 MS patients with chronic optic neuropathy is ongoing<sup>50</sup>. Biomarkers planned in this study include a 24-week VEP measurement as a primary endpoint.

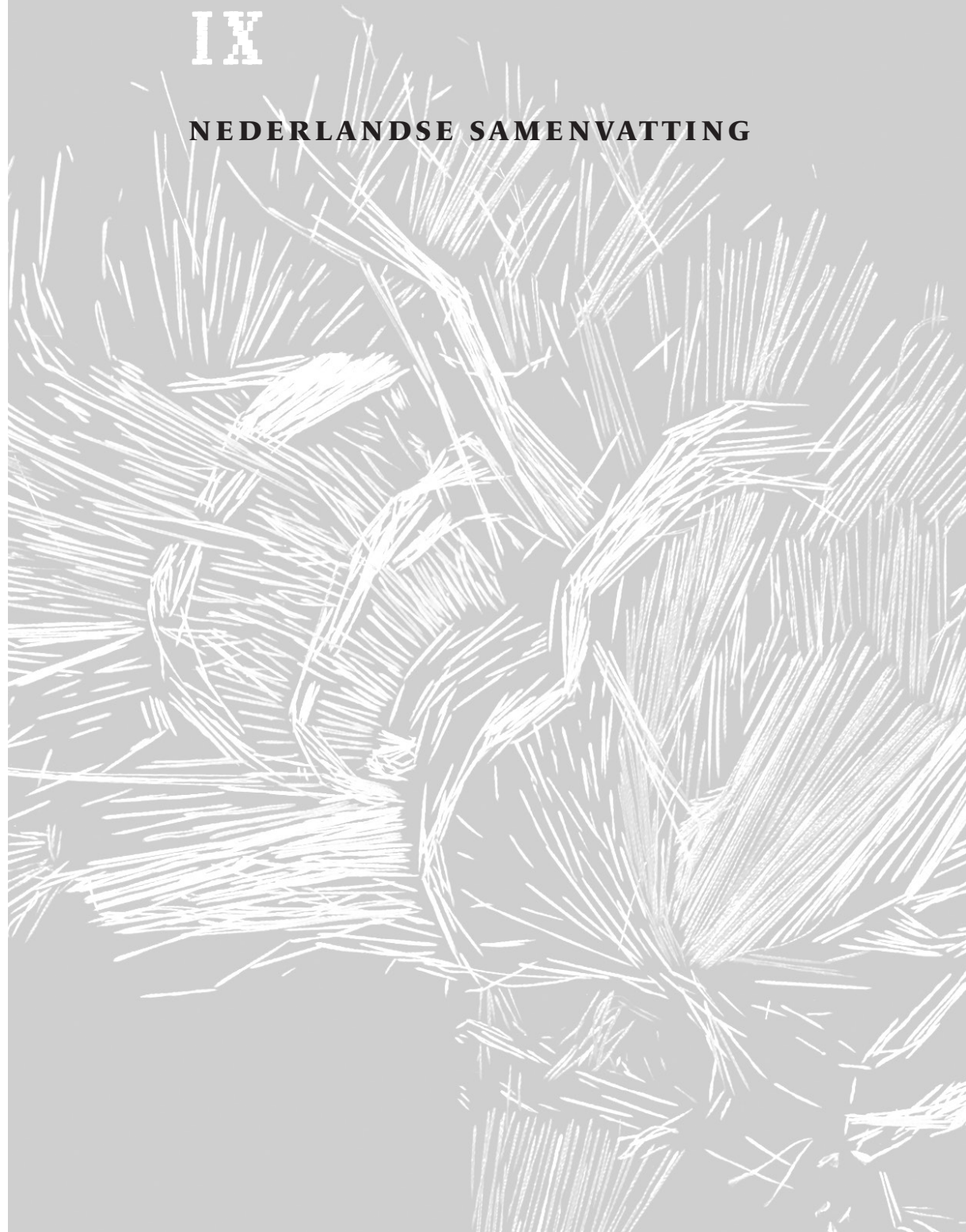
Just like in **chapter 2**, this example shows it might be necessary to wait for a study in patients to measure a specific effect (in this case: improvement in remyelination). However, the effect on the immune system probably could have been measured in healthy volunteers. In hindsight biomarker development well before start of the first study was needed, as it proved to be more difficult than expected.

In summary, early phase drug development could benefit from more and better biomarkers that can quantify pharmacological effects of treatments for MS.

## CONCLUSIONS AND FUTURE DIRECTIONS

Using biomarkers in early stage drug development should be the new standard. As long as new pharmacological treatments for MS are developed, there will be a need for more accurate biomarkers to demonstrate target engagement of the drug. There is a strong need for better biomarkers to study the effects of new drugs intended to enhance remyelination. This thesis provides examples of such biomarkers and how these can be easily integrated in early phase of drug development. Although a number of phase I studies have used exploratory efficacy objectives, it should be more common to use proof-of-pharmacology or proof-of-mechanism endpoints in these studies. Phase I studies can provide more information than safety and tolerability only.

- 1 EMA. Guideline on strategies to identify and mitigate risks for first-in-human and early clinical trials with investigational medicinal products. 2018.
- 2 Cohen AF. Developing drug prototypes: pharmacology replaces safety and tolerability? *Nature Reviews Drug Discovery*. 2010;9:856.
- 3 Paul SM, Mytelka DS, Dunwiddie CT, Persinger CC, Munos BH, Lindborg SR, et al. How to improve R & D productivity: the pharmaceutical industry's grand challenge. *Nature Reviews Drug Discovery*. 2010;9:203.
- 4 Mullard A. Parsing clinical success rates. *Nat Rev Drug Discov*. 2016;15(7):447-7.
- 5 Waring MJ, Arrowsmith J, Leach AR, Leeson PD, Mandrell S, Owen RM, et al. An analysis of the attrition of drug candidates from four major pharmaceutical companies. *Nat Rev Drug Discov*. 2015;14(7):475-86.
- 6 Cohen AF, Burggraaf J, van Gerven JMA, Moerland M, Groeneveld GJ. The Use of Biomarkers in Human Pharmacology (Phase I) Studies. *Annual Review of Pharmacology and Toxicology*. 2015;55(1):55-74.
- 7 Kanhai K, Goulooze SC, Stevens J, Hay JL, Dent G, Verma A, et al. Quantifying Beta-Galactosylceramide Kinetics in Cerebrospinal Fluid of Healthy Subjects Using Deuterium Labeling. *Clinical and translational science*. 2016;9(6):321-7.
- 8 Kanhai KMS, Goulooze SC, van der Grond J, Hankemeier T, Verma A, Chavez J, et al. Kinetics of myelin breakdown products: a labeling study in patients with progressive multiple sclerosis. *MS and demyelinating disorders*. 2019;submitted.
- 9 Strimbu K, Tavel JA. What are biomarkers? *Current opinion in HIV and AIDS*. 2010;5(6):463-6.
- 10 Kanhai KMS, Nij Bijvank JA, Wagenaar YL, Klaassen ES, Lim KS, Bergheanu SC, et al. Treatment of internuclear ophthalmoparesis in multiple sclerosis with fampridine: a randomized double blind, placebo-controlled crossover trial. *CNS Neuroscience & Therapeutics*. 2019.
- 11 Kanhai KMS, Nij Bijvank JA, Wagenaar YL, Klaassen ES, Lim K, Bergheanu SC, et al. Treatment of internuclear ophthalmoparesis in multiple sclerosis with fampridine: A randomized double-blind, placebo-controlled cross-over trial. *CNS neuroscience & therapeutics*. 2019.
- 12 Groeneveld GJ, Hay JL, Van Gerven JM. Measuring blood-brain barrier penetration using the NeuroCart, a CNS test battery. *Drug discovery today Technologies*. 2016;20:27-34.
- 13 Dykman LA, Khlebtsov NG. Immunological properties of gold nanoparticles. *Chemical science*. 2017;8(3):1719-35.
- 14 Tsai CY, Lu SL, Hu CW, Yeh CS, Lee GB, Lei HY. Size-dependent attenuation of TLR9 signaling by gold nanoparticles in macrophages. *Journal of immunology (Baltimore, Md. : 1950)*. 2012;188(1):68-76.
- 15 Russell GM, Henley DE, Leendertz J, Douthwaite JA, Wood SA, Stevens A, et al. Rapid glucocorticoid receptor-mediated inhibition of hypothalamic-pituitary-adrenal ultradian activity in healthy males. *The Journal of neuroscience: the official journal of the Society for Neuroscience*. 2010;30(17):6106-15.
- 16 Heuck C, Wolthers OD. A placebo-controlled study of three osteocalcin assays for assessment of prednisolone-induced suppression of bone turnover. *The Journal of endocrinology*. 1998;159(1):127-31.
- 17 Kuroki Y, Kaji H, Kawano S, Kanda F, Takai Y, Kajikawa M, et al. Short-term effects of glucocorticoid therapy on biochemical markers of bone metabolism in Japanese patients: a prospective study. *Journal of bone and mineral metabolism*. 2008;26(3):271-8.
- 18 Tornatore KM, Venuto RC, Logue G, Davis PJ. CD4+ and CD8+ lymphocyte and cortisol response patterns in elderly and young males after methylprednisolone exposure. *Journal of medicine*. 1998;29(3-4):159-83.
- 19 van Amerongen G, Kanhai KMS, Baakman AC, Heuberger J, Klaassen E, Beumer TL, et al. Effects on Spasticity and Neuropathic Pain of an Oral Formulation of Delta9-tetrahydrocannabinol in Patients With Progressive Multiple Sclerosis. *Clinical therapeutics*. 2017;40(9):1467-82.
- 20 Eisen A. Electromyography in disorders of muscle tone. *The Canadian journal of neurological sciences Le journal canadien des sciences neurologiques*. 1987;14(3 Suppl):501-5.
- 21 Matthews WB. Ratio of maximum H reflex to maximum M response as a measure of spasticity. *Journal of Neurology, Neurosurgery, and Psychiatry*. 1966;29(3):201-4.
- 22 Tran JQ, Rana J, Barkhof F, Melamed I, Gevorkyan H, Wattjes MP, et al. Randomized phase I trials of the safety/tolerability of anti-lingo-1 monoclonal antibody BliB033. *Neurology-Neuroimmunology Neuroinflammation*. 2014;1(2):e18.
- 23 Ranger A, Ray S, Szak S, Dearth A, Allaire N, Murray R, et al. Anti-LINGO-1 has no detectable immunomodulatory effects in preclinical and phase 1 studies. *Neurology-Neuroimmunology Neuroinflammation*. 2018;5(1):e417.
- 24 You Y, Klistorner A, Thie J, Graham SL. Latency delay of visual evoked potential is a real measurement of demyelination in a rat model of optic neuritis. *Investigative ophthalmology & visual science*. 2011;52(9):6911-8.
- 25 Leocani L, Guerrieri S, Comi G. Visual Evoked Potentials as a Biomarker in Multiple Sclerosis and Associated Optic Neuritis. *Journal of neuro-ophthalmology: the official journal of the North American Neuro-Ophthalmology Society*. 2018;38(3):350-7.
- 26 Mallik S, Samson RS, Wheeler-Kingshott CA, Miller DH. Imaging outcomes for trials of remyelination in multiple sclerosis. *Journal of Neurology, Neurosurgery, and Psychiatry*. 2014;85(12):1396-404.
- 27 Eisen A, Greenberg BM, Bowen JD, Arnold DL, Caggiano AO. A double-blind, placebo-controlled, single ascending-dose study of remyelinating antibody RH1GM22 in people with multiple sclerosis. *Multiple sclerosis journal-experimental, translational and clinical*. 2017;3(4):2055217317743097.
- 28 Ando S, Tanaka Y, Toyoda Y, Kon K. Turnover of myelin lipids in aging brain. *Neurochemical research*. 2003;28(1):5-13.
- 29 Morell P, H. QR. *Basic Neurochemistry: Molecular, Cellular and Medical Aspects*. In: Siegel GJ AB, Albers RW, et al, editor. 6th ed: Philadelphia: Lippincott-Raven; 1999.
- 30 Lenglet T, Lacomblez L, Abitbol JL, Ludolph A, Mora JS, Robberecht W, et al. A phase II-III trial of olesoxime in subjects with amyotrophic lateral sclerosis. *European journal of neurology*. 2014;21(3):529-36.
- 31 Bertini E, Dessaud E, Mercuri E, Muntoni F, Kirschner J, Reid C, et al. Safety and efficacy of olesoxime in patients with type 2 or non-ambulatory type 3 spinal muscular atrophy: a randomised, double-blind, placebo-controlled phase 2 trial. *The Lancet Neurology*. 2017;16(7):513-22.
- 32 Eckmann J, Clemens LE, Eckert SH, Hagl S, Yu-Taeger L, Bordet T, et al. Mitochondrial membrane fluidity is consistently increased in different models of Huntington disease: restorative effects of olesoxime. *Molecular neurobiology*. 2014;50(1):107-18.
- 33 NCT01808885 Cg. Safety Study of Olesoxime in Patients With Stable Relapsing Remitting Multiple Sclerosis Treated With Interferon Beta. (MSREPAIR) [Clinicaltrials.gov: u.s. National Library of Medicine; Available from: https://www.clinicaltrials.gov/ct2/show/record/NCT01808885?term=olesoxime&cond=Multiple+Sclerosis&rank=1](https://www.clinicaltrials.gov/ct2/show/record/NCT01808885?term=olesoxime&cond=Multiple+Sclerosis&rank=1).
- 34 Kaunzner UW, Gauthier SA. MRI in the assessment and monitoring of multiple sclerosis: an update on best practice. *Therapeutic advances in neurological disorders*. 2017;10(6):247-61.
- 35 Chen JT, Collins DL, Atkins HL, Freedman MS, Arnold DL. Magnetization transfer ratio evolution with demyelination and remyelination in multiple sclerosis lesions. *Annals of neurology*. 2008;63(2):254-62.
- 36 Wattjes MP, Steenwijk MD, Stangel M. MRI in the Diagnosis and Monitoring of Multiple Sclerosis: An Update. *Clinical Neuroradiology*. 2015;25(2):157-65.
- 37 Arun T, Tomassini V, Sbardella E, de Ruiter MB, Matthews L, Leite MI, et al. Targeting ASIC1 in primary progressive multiple sclerosis: evidence of neuroprotection with amiloride. *Brain: a journal of neurology*. 2013;136(Pt 1):106-15.
- 38 McKee JB, Elston J, Evangelou N, Gerry S, Fugger L, Kennard C, et al. Amiloride Clinical Trial In Optic Neuritis (ACTION) protocol: a randomised, double blind, placebo controlled trial. *BMJ open*. 2015;5(11):e009200.
- 39 McKee JB, Cottrill CL, Elston J, Epps S, Evangelou N, Gerry S, et al. Amiloride does not protect retinal nerve fibre layer thickness in optic neuritis in a phase 2 randomised controlled trial. *Multiple sclerosis (Houndmills, Basingstoke, England)*. 2019;25(2):246-55.



**Hoofdstuk 1** omvat de introductie van dit proefschrift en start met een korte beschrijving van de ziekte multiple sclerose (MS), de meest voorkomende auto-immuun ziekte van het centrale zenuwstelsel. MS is primair een ontstekingsziekte van de hersenen en het ruggenmerg waarin focale lymfocytinfiltratie leidt tot myelineschade (demyelinisatie) en beschadigde axonen. Bestaande behandelingen van MS kunnen worden gecategoriseerd als *disease-modifying* (ziekte-modificerende) behandelingen, die de ziekte beïnvloeden, en symptomatische behandelingen, die alleen de symptomen van de ziekte bestrijden. Ondanks de toename van nieuwe behandelingen en een verhoogde doeltreffendheid in de afgelopen jaren, zijn geregistreerde *disease-modifying* behandelingen vaak geassocieerd met een grote kans op bijwerkingen. Daarom is er behoefte aan de ontwikkeling van een nieuw soort behandelingen, die bijvoorbeeld remyelinisatie en neuroprotectie bevorderen. Nieuwe methodes zullen moeten worden ontwikkeld om de potentiële werkzaamheid van neuroreparatieve en neuroregeneratieve middelen te testen, aangezien huidige biomarkers daar nog niet of onvoldoende nauwkeurig toe in staat zijn.

**Hoofdstuk 2** beschrijft een studie naar de werkzaamheid van een nieuwe orale formulering van  $\Delta 9$ -THC (ECP002A) in patiënten met een progressieve vorm van MS.  $\Delta 9$ -THC is een van de cannabinoïden in de cannabis sativa plant en een directe partiële agonist van de cannabinoïd receptoren CB1 en CB2. Voorheen is aangetoond dat cannabinoïden symptomen, waaronder spasticiteit en pijn verbeterden door het moduleren van de neuronale reactiviteit via de presynaptische cannabinoïde receptoren in patiënten met MS. De studie beschreven in hoofdstuk 2 was een zogenaamde *proof-of-concept* studie, waarbinnen een methode wordt getest om te demonstreren dat het middel werkt zoals verwacht. Het bestond uit twee fases: een cross-over test om een geschikte dosis te vinden, en een parallelle, gerandomiseerde, placebogecontroleerde behandelingsfase van 4 weken. Vierentwintig patiënten met een progressieve vorm van MS en gematigde spasticiteit deden mee aan de studie. De resultaten lieten zien dat pijn en spasticiteit significant waren verminderd na een directe meting in de kliniek, maar dit werd niet als zodanig gerapporteerd in een dagboek. Ondanks de complexe wisselwerking van de psychoactieve effecten en analgesie werd de huidige orale formulering van  $\Delta 9$ -THC wel goed verdragen en had het een stabiel farmacokinetisch profiel. Deze studie benadrukt dat  $\Delta 9$ -THC een rol kan spelen bij de behandeling van spasticiteit en pijn in patiënten met MS en laat de toegevoegde waarde zien van een dergelijke *proof-of-concept* studie.

In het onderzoek beschreven in **hoofdstuk 3** is een nieuwe formulering van methylprednisolon (MP) getest in gezonde proefpersonen. MP wordt gebruikt bij de behandeling van een MS aanval (ook wel een *relaps*, *schub* of exacerbatie genoemd), die vaak voorkomt bij de *relapsing-remitting* vorm van MS. Zowel de dosis als de frequentie van MP zou kunnen worden verminderd door het verpakken van vrij MP in een glutathion (GSH)-gePEGyleerd liposoom. Dit kan zorgen voor een zogenaamde *slow-release* formulering met vertraagde afgifte, verminderde toxiciteit en een langere werkzaamheid. In deze studie werd een infusie met GSH-gePEGyleerde liposomen met MP (2B3-201) voor het eerst getest in mensen om de veiligheid, farmacokinetiek (PK) en farmacodynamiek (PD) van het middel te testen. Een veelvoorkomende bijwerking van 2B3-201 was de infusie-gerelateerde reactie (in 89% van alle proefpersonen), maar het was desondanks veilig, met geen

klinisch relevant veranderingen in alle veiligheidstesten, en geen serieuze bijwerkingen. 2B3-201 had een lange plasma-halfwaardetijd (tussen 24 en 37 uur) en zorgde voor langdurige immunosuppressieve effecten.

**Hoofdstuk 4** beschrijft een *first-in-human* studie naar de veiligheid en PK van CNM-Au8, een oplossing van goud nanopartikels met een zuiver oppervlak, dat is ontwikkeld vanwege de mogelijk immunomodulerende en remyeliniserende effecten met minder bijwerkingen dan bestaande medicatie met goud. De studie in gezonde proefpersonen bestond uit twee onderdelen bestaande uit 4 cohorten met per cohort oplopende doseringen van CNM-Au8. Tijdens het eerste onderdeel betrof het een enkele dosering, tijdens het tweede onderdeel betrof het dagelijkse inname van CNM-Au8 gedurende 21 dagen. Naast deze studie werden ontstekings-provocerende in vitro testen uitgevoerd om een mogelijk bruikbare ex vivo PD parameter te ontwikkelen. Resultaten lieten zien dat CNM-Au8 veilig was, met als meest voorkomende bijwerking buikklasten (in 20% van alle proefpersonen). De bijwerkingen waren gunstiger in vergelijking met bestaande medicatie met goud. CNM-Au8 had een plasma halfwaardetijd tussen de 11.5 en 26.2 dagen en de maximale concentratie na de eerste inname werd bereikt tussen de 3.3 en 3.5 uur. De lage concentraties die gerapporteerd werden en het ongebruikelijk farmacokinetische profiel komen overeen met de literatuur over goud nanopartikels in dierstudies. Omdat de in vitro testen geen ontstekingsremmende effecten zien, zijn deze testen niet gebruikt in de studie. Afgaande op deze resultaten zou vervolgonderzoek zich moeten richten op het bepalen of CNM-Au8 ontstekingsremmende en remyeliniserende werking heeft.

Middelen die myeline aanmaak bevorderen kunnen mogelijk een belangrijke rol spelen bij de behandeling van demyeliniserende ziektes zoals MS. Er is echter geen geschikte, nauwkeurige, methode om myeline vorming te kwantificeren. De turnover van  $\beta$ -galactosylceramide (een component van myeline, afgekort  $\beta$ -GALC), gemeten door middel van labeling met zwaar water, geeft een indicatie van myelinisering in muizen, maar dit werd nog nooit bepaald in mensen. **Hoofdstuk 5** beschrijft een studie waarin 6 gezonde proefpersonen gedurende 70 dagen dagelijks 120 mL zwaar water (70% D<sub>2</sub>O) dronken om  $\beta$ -GALC te labelen met deuterium. Vervolgens werden seriële lumbaal puncties verricht, werd met behulp van massaspectrometrie  $\beta$ -GALC in liquor bepaald en werd met behulp van een compartimenten-model de turnover van  $\beta$ -GALC in de liquor berekend. Resultaten lieten zien dat het maximale percentage deuterium gemeten in lichaamswater varieerde van 1.5 tot 3.9%, terwijl het percentage ingebouwde deuterium in  $\beta$ -GALC veel lager was: 0.05-0.14%. Dit wijst op een trage turnoversnelheid, wat werd bevestigd door het model, dat een schatting van deze snelheid gaf (0.00168 dag<sup>-1</sup>). Deze snelheid correspondeert met een halfwaardetijd van 413 dagen. Aan de hand van deze resultaten wordt duidelijk dat extra studies nodig zijn om te onderzoeken of de turnover van  $\beta$ -GALC gebruik kan worden als uitkomstmaat in klinisch onderzoek met remyeliniserende behandelingen in patiënten met MS.

**Hoofdstuk 6** beschrijft een vervolgstudie, waarin myeline ook werd gelabeld met deuterium in 5 patiënten met MS, en naast  $\beta$ -GALC ook een ander myeline afbraakproduct werd bepaald: N-Octadecanoyl-sulfatide (NO-Sulf). De turnoversnelheid van de  $\beta$ -GALC en NO-sulf fracties met niet-verwaarloosbare turnover waren 0.00186 en 0.00714 dag<sup>-1</sup>,

wat overeenkomt met turnover halfwaardetijden van respectievelijk 373 en 96.5 dagen. Het effect van MS op de NO-sulf turnover (49.5% lagere fractie) was meer uitgesproken dan het effect op de  $\beta$ -GALC turnover (18.3% lagere fractie). De resultaten laten zien dat de kinetiek van myeline afbraakproducten in liquor van gezonde proefpersonen blijkbaar anders is dan in patiënten met MS. Mogelijke oorzaken voor deze discrepantie zijn een tragere myeline synthese in de MS patiëntengroep, een grote afbraak van het stabielere component van myeline, of een combinatie van deze twee processen. Het labelen met deuterium in combinatie met lumbaalpuncties kan een zinvolle methode zijn voor het kwantificeren van metabole processen in het centrale zenuwstelsel en de myeline turnover in patiënten met MS, en zou kunnen worden gebruikt in *proof-of-concept* studies naar remyeliniserende behandelingen.

In **hoofdstuk 7** wordt een gerandomiseerde, dubbelblinde, placebogecontroleerde, cross-over studie beschreven met patiënten met MS en een internucleaire ophthalmoparese (INO). De onderzoeksvraag in deze studie was of de snelheid van saccadische oogbewegingen in deze patiënten zullen verbeteren na toediening van fampridine. Voornaamste uitkomstparameters in deze studie waren de verandering in *peak velocity versional dysconjugacy index (PV-VDI)* en de *first-pass amplitude VDI (FPA-VDI)*. Hogere VDI waarden worden vaak gezien bij een INO en impliceren een vertraging van de adductie van het oog ten opzichte van de abductie. Fampridine verlaagde zowel PV-VDI als FPA-VDI waarden en verbeterde de saccadische oogbewegingen veroorzaakt door de INO. Deze studie geeft handvatten voor de ontwikkeling van een methode die op basis van de respons op fampridine, op basis van de snelheid van de saccadische oogbewegingen, patiënten kan selecteren voor de toepassing van een remyeliniserende behandeling.

**Hoofdstuk 8** reflecteert op de voornaamste conclusies en bespreekt het gebruik van biomarkers in vroeg-stadium klinische onderzoekstudies. In dit hoofdstuk wordt nader toegelicht hoe biomarkers kunnen worden geïntegreerd in studies, en benadrukt hoe dit de nieuwe standaard zou moeten worden. Zolang de zoektocht naar nieuwe behandelingen van MS voortduurt, en zolang er geen succesvolle biomarker is van het effect van potentieel remyeliniserende middelen, zal er een sterke behoefte zijn naar meer accurate biomarkers.

## LIST OF PUBLICATIONS

Quantifying Beta-Galactosylceramide Kinetics in Cerebrospinal Fluid of Healthy Subjects Using Deuterium Labeling – **Kanhai KMS**, Goulooze SC, Stevens J, Hay JL, Dent G, Verma A, Hankemeier T, Boer T de, Meijering H, Chavez JC, Cohen AF, Groeneveld GJ – PUBLISHED (*Clin Transl Sci.* 2016 Dec;9(6):321-327)

Effects on Spasticity and Neuropathic Pain of an Oral Formulation of  $\Delta$ 9-Tetrahydrocannabinol in Patients With Progressive Multiple Sclerosis – van Amerongen G, **Kanhai KMS**, Baakman AC, Heuberger J, Klaassen E, Beumer TL, Strijers RLM, Killestein J, van Gerven J, Cohen A, Groeneveld GJ – PUBLISHED (*Clinical Therapeutics*, 2018 Sep;40(9):1467-1482)

Glutathione PEGylated liposomal methylprednisolone in comparison to free methylprednisolone: slow release characteristics and prolonged lymphocyte depression in a first in human study – **Kanhai KMS**, Zuiker RGJA, Stavrakaki I, Gladdines W, Gaillard PJ, Klaassen ES, Groeneveld GJ - PUBLISHED (*Br J Clin Pharmacol* (2018), 84: 1020–1028)

Treatment of internuclear ophthalmoparesis in multiple sclerosis with fampridine: a randomized, double-blind, placebo-controlled, crossover trial – **Kanhai KMS**, Nij Bijvank JA, Wagenaar YL, Klaassen ES, Lim KS, Bergheanu SC, Petzold A, Verma A, Hesterman J, Wattjes MP, Uitdehaag BMJ, van Rijn LJ, Groeneveld GJ – PUBLISHED (*CNS Neurosci Ther.* 2019 Feb 12.)

Kinetics of myelin breakdown products: a labeling study in patients with progressive multiple sclerosis – **Kanhai KMS**, Goulooze SC, van der Grond J<sup>1</sup>, Harms AC, Hankemeier T, Verma A, Dent G, Chavez J, Meijering H, Groeneveld GJ<sup>2</sup> – SUBMITTED (1. Radiology department LUMC, 2. Anaesthesiology department LUMC)

## CURRICULUM VITAE

Kawita Kanhai was born on 21 July 1984 in Leiden, the Netherlands, and has four sisters. She graduated in 2002 from secondary school, Da Vinci College in Leiden. After a gap year travelling Australia, New Zealand and Indonesia, she started medical school at the Leiden University Medical Centre (LUMC). In 2007 she started a pre-master in Biomedical Sciences at the LUMC. She obtained her medical degree in 2011, and her Master of Science (Biomedical Sciences) in 2012. She then started working as a research physician and PhD student at the Centre for Human Drug Research in Leiden in 2012, focusing on neurology clinical trials under the supervision of Geert Jan Groeneveld and Adam Cohen. In 2018 she joined United Neuroscience, a biotech company that develops vaccines to treat neurological diseases, where she currently holds a position as Associate Medical Director. Kawita Kanhai lives in Oegstgeest with her partner Melle Sieswerda and their two children: Varisha and Anil.

SEE INSIDE FOR ILLUSTRATIVE  
OVERVIEW OF CURRENT AND  
FUTURE TREATMENTS IN  
MULTIPLE SCLEROSIS.

FOR DETAILS, REFER  
TO TABLES 2 AND 3  
OF CHAPTER I

